Vector-boson production at hadron colliders — Lecture I

Radja Boughezal
Argonne National Laboratory

Lectures at the CTEQ School on QCD and Electroweak Phenomenology

Pittsburgh, July 6-16, 2022

Outline of the lectures

Lecture I:

- Drell-Yan like gauge boson production: overview of the basics and historical importance

- Underlying theory framework for W/Z production

- Importance of higher order corrections: QCD, electroweak, mixed QCD-EW

- Modern applications: W-mass, PDFs, BSM searches

- Drell-Yan in the future

Lecture II:

- W-production at NLO in QCD: calculation and lessons learned

- Vector boson production in association with jets: phenomenological importance

- Transverse momentum resummation for W/Z production

- The importance of multi-boson production and the special role of self-interactions — unitarity

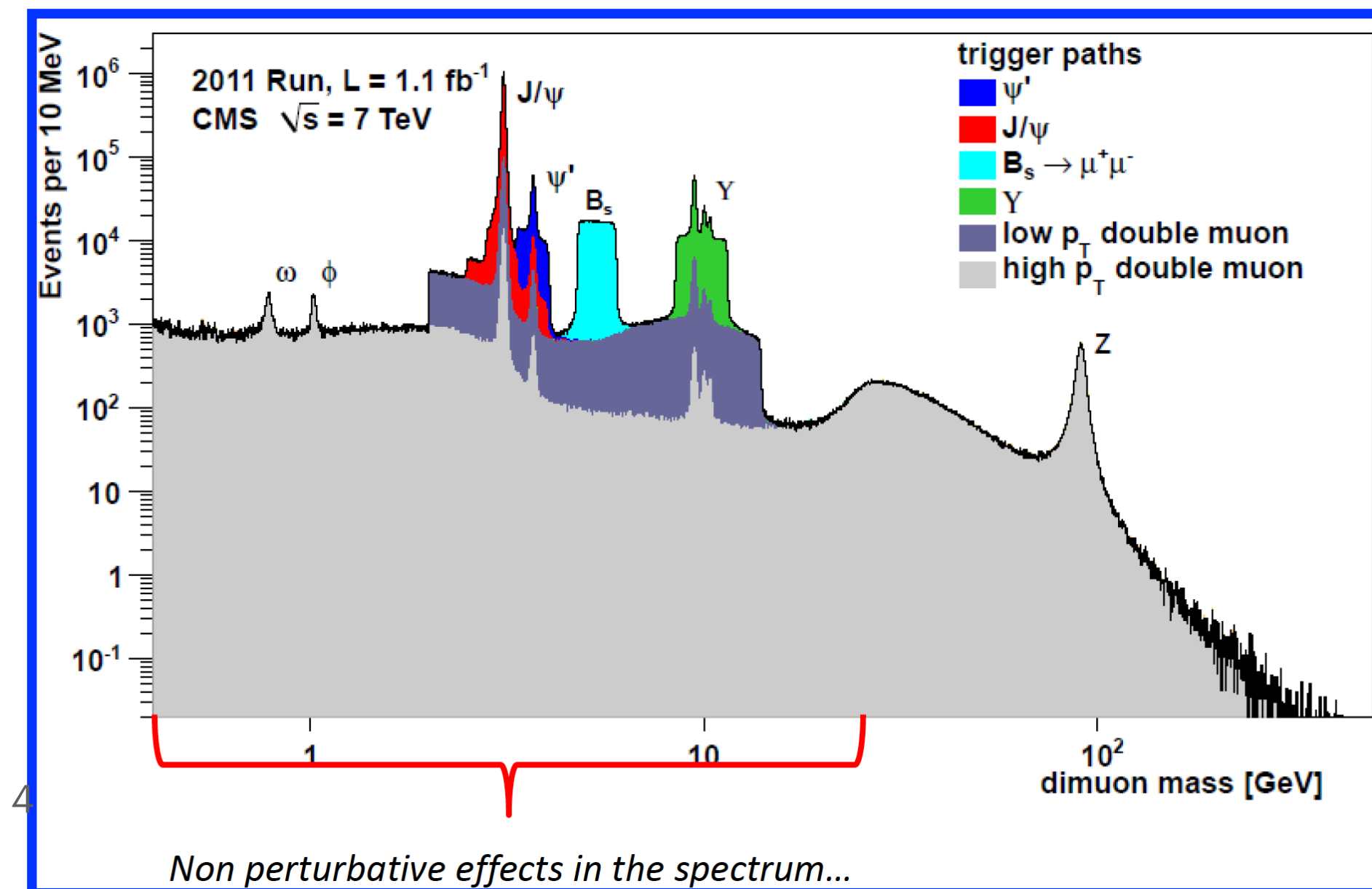# Lecture I

Drell-Yan-like gauge boson production
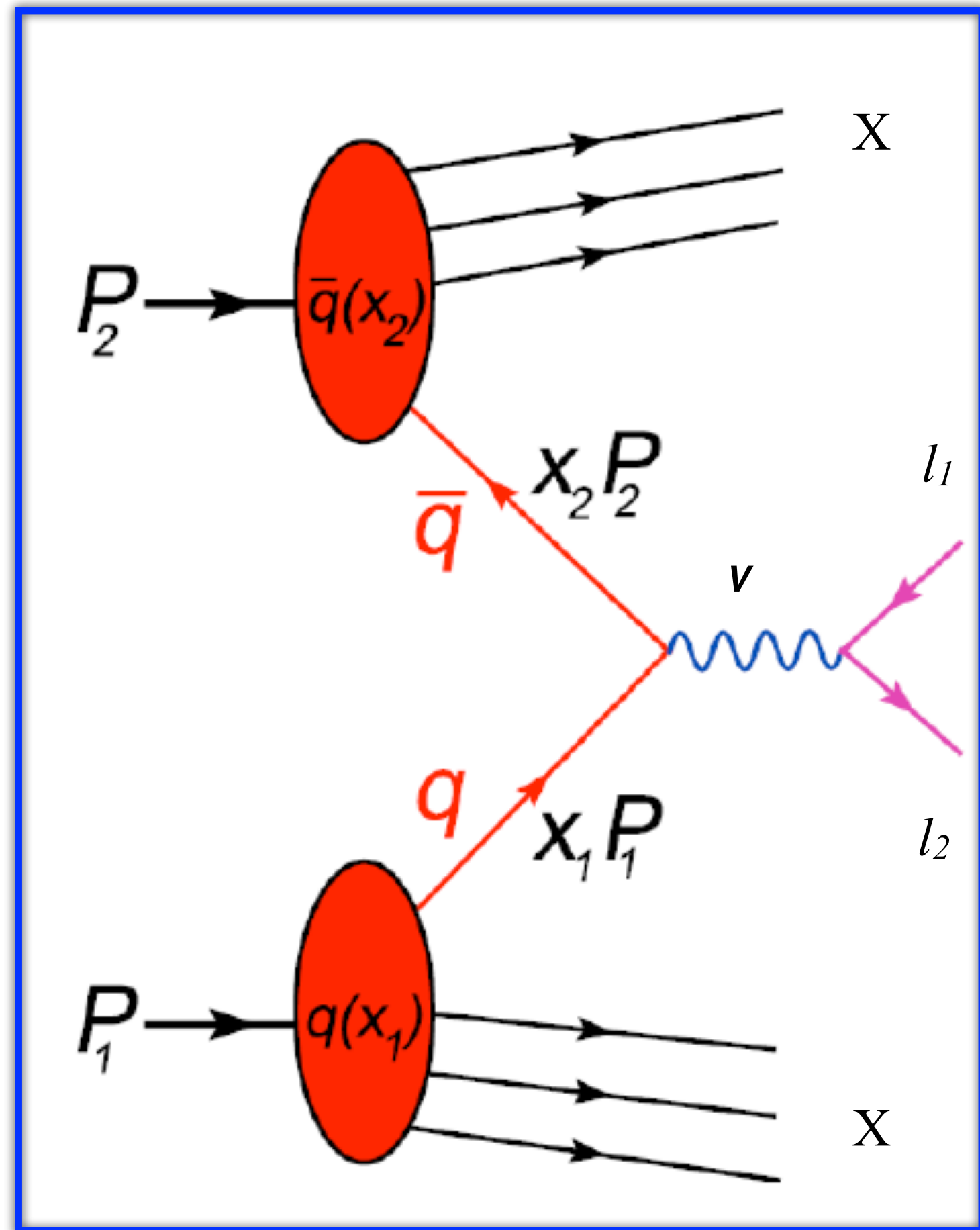
- Drell-Yan is the production of lepton pairs in the s-channel. Drell-Yan like processes include:

$$h(P_1) + h'(P_2) \rightarrow (\gamma^*, Z \rightarrow l^+ l^-)X \ \ \text{with} \ \ l = e, \mu$$

$$h(P_1) + h'(P_2) \rightarrow (W \rightarrow l\nu)X$$

$$h(P_1) + h'(P_2) \rightarrow V_{BSM}X; \quad V = Z', \dots$$

Non perturbative effects in the spectrum...

- Many resonances were discovered by studying the di-muon final state in Drell-Yan (J/Ψ, γ, Z, ...)

Facts about Drell-Yan

- Clean signal at hadron colliders, since the lepton pair does not interact strongly

- One of the best theoretically studied processes at a hadron collider with uncertainties at the few percent level

- factorization is proved to all orders in QCD perturbation theory (Collins-Soper-Sterman)

- Standard candle for detector calibration (eg. detector response to lepton energy)
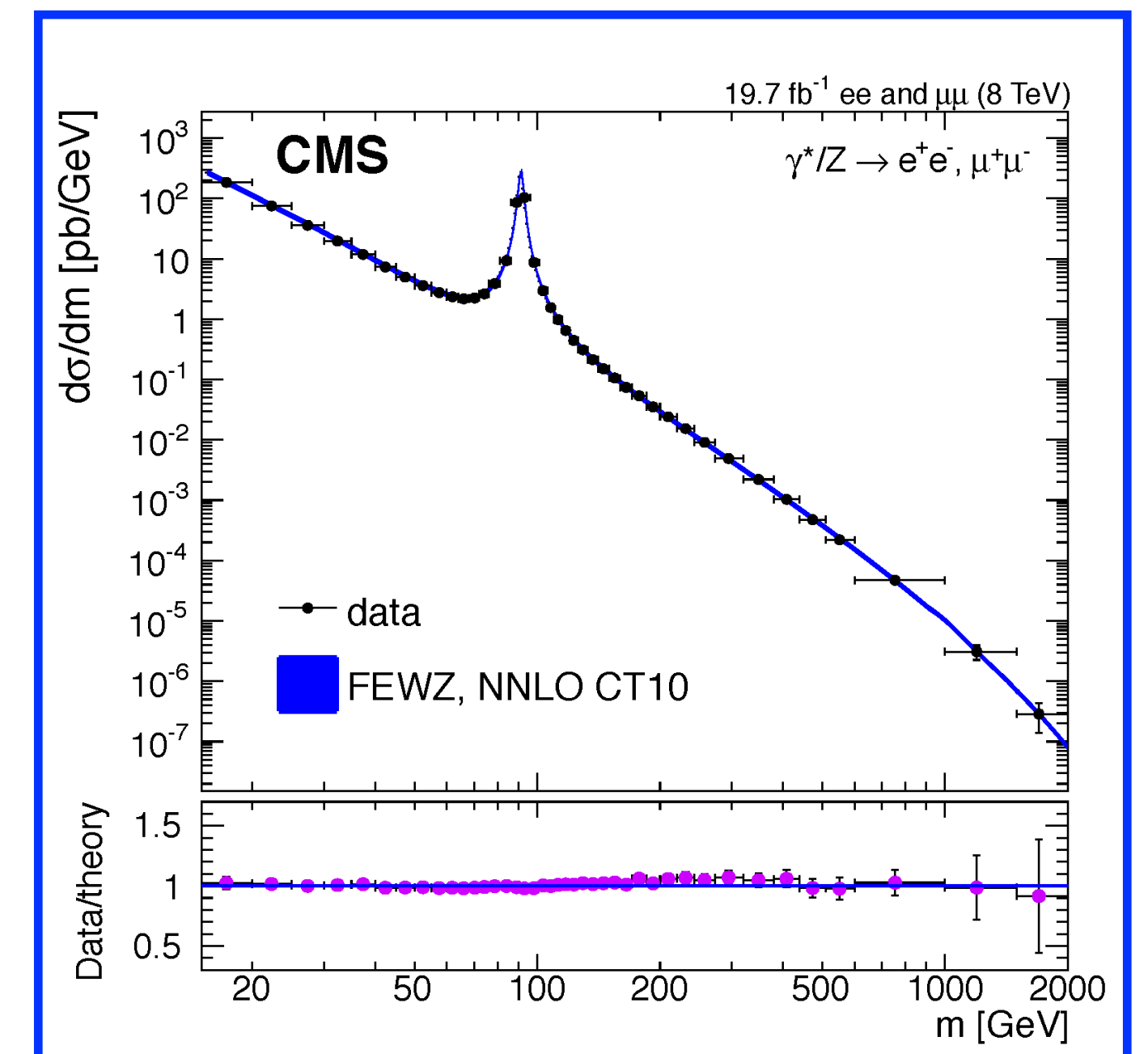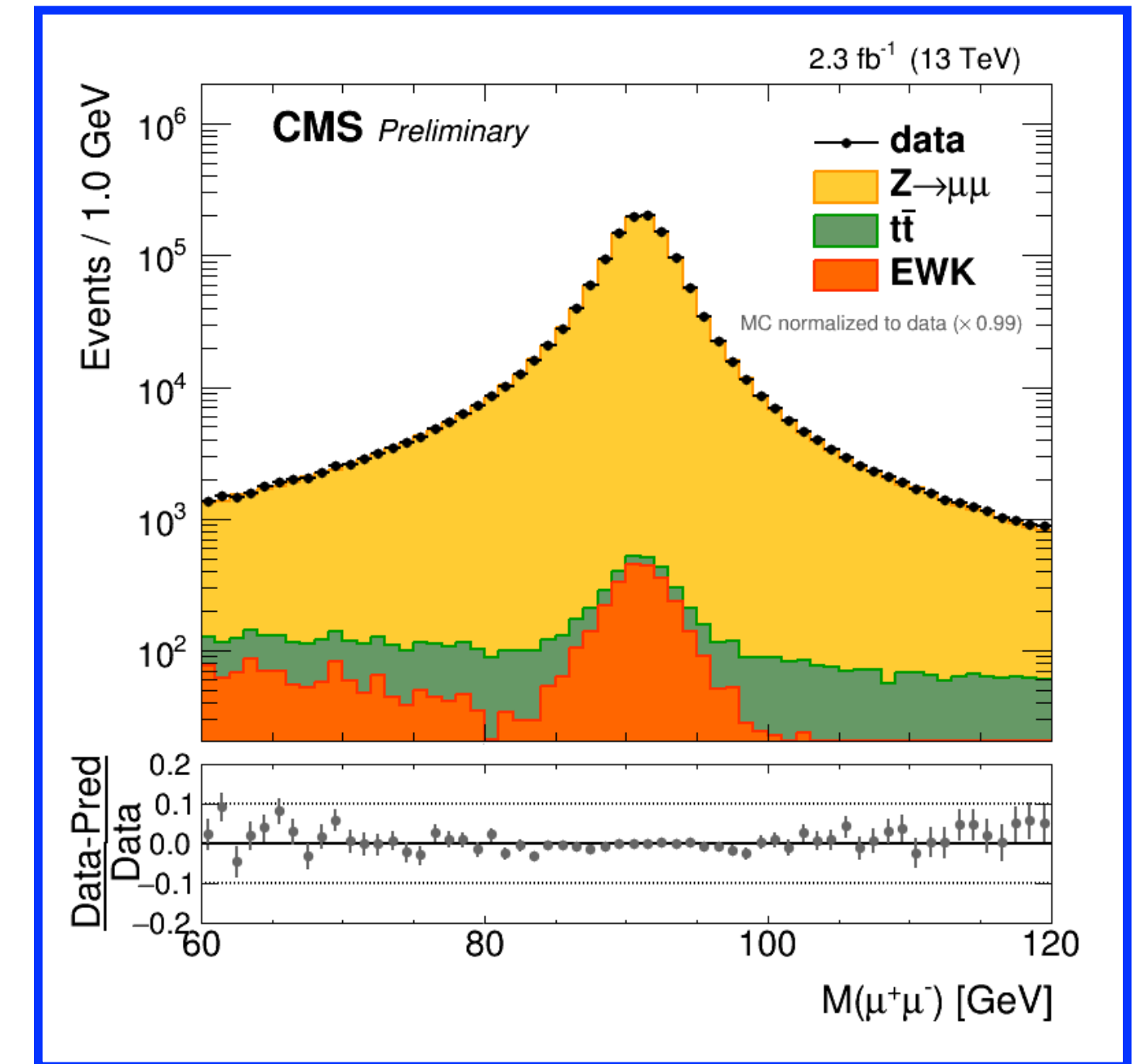
Feynman rules for electroweak interactions

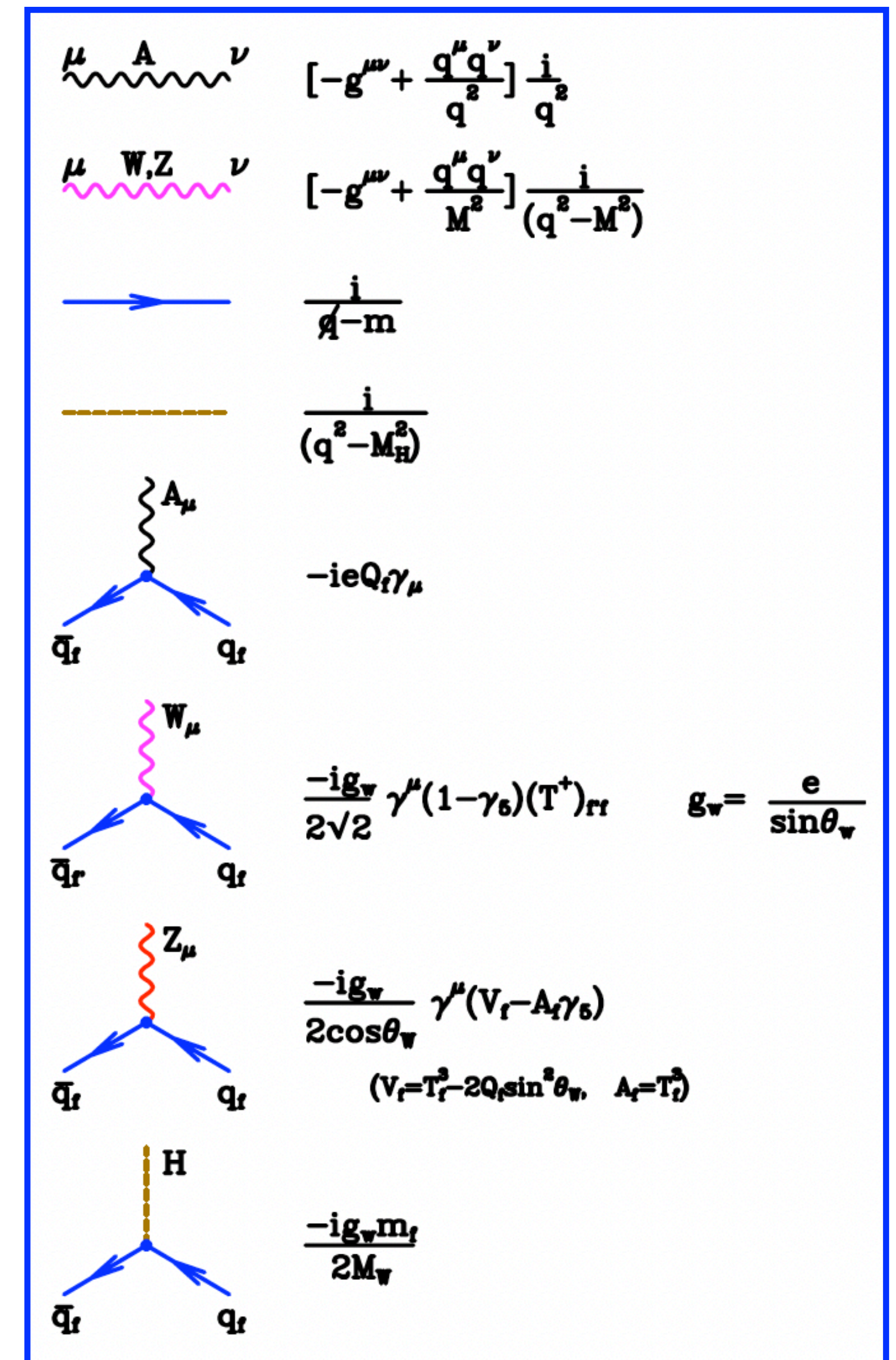- The Lagrangian for EW interactions:

$$\mathcal{L} = \sum_f \bar{\psi}_f \left(i\slashed{\partial} - m_f - g_W \frac{m_f H}{2M_W} \right) \psi_f$$

$$- \frac{g_W}{2\sqrt{2}} \sum_f \bar{\psi}_f (\gamma^\mu (1-\gamma_5) T^+ W^+_\mu + \gamma^\mu (1-\gamma_5) T^- W^-_\mu) \psi_f$$

$$- e \sum_f Q_f \bar{\psi}_f \slashed{A} \psi_f - \frac{g_W}{2\cos\theta_W} \sum_f \bar{\psi}_f \gamma^\mu (V_f - A_f \gamma_5) \psi_f Z_\mu$$

- W-boson couples to left-handed fermions, while the Z-boson couples to both with different strength:

$$V_f - A_f \gamma_5 = \frac{V_f + A_f}{2}(1-\gamma_5) + \frac{V_f - A_f}{2}(1+\gamma_5)$$

- Vector and Axial vector couplings in terms of weak isospin $T_{3\,f} = \pm 1/2$

$$V_f = T_f^3 - 2Q_f \sin^2\theta_W$$
$$A_f = T_f^3$$

$$V_u \approx 0.2, \ V_d \approx -0.35, \ V_\nu = \tfrac{1}{2}, \ V_e \approx -0.04$$
$$A_u = \tfrac{1}{2}, \ A_d = -\tfrac{1}{2}, \ A_\nu = \tfrac{1}{2}, \ A_e = -\tfrac{1}{2}$$

$$\mu \quad A \quad \nu \qquad [-g^{\mu\nu} + \frac{q^\mu q^\nu}{q^2}]\frac{i}{q^2}$$

$$\mu \quad W,Z \quad \nu \qquad [-g^{\mu\nu} + \frac{q^\mu q^\nu}{M^2}]\frac{i}{(q^2 - M^2)}$$

$$\frac{i}{\slashed{q} - m}$$

$$\frac{i}{(q^2 - M_H^2)}$$

$$A_\mu \qquad -ieQ_f\gamma_\mu$$

$$W_\mu \qquad \frac{-ig_W}{2\sqrt{2}} \gamma^\mu (1-\gamma_5)(T^+)_{rf} \qquad g_W = \frac{e}{\sin\theta_W}$$

$$Z_\mu \qquad \frac{-ig_W}{2\cos\theta_W} \gamma^\mu (V_f - A_f\gamma_5)$$
$$(V_f = T_f^3 - 2Q_f\sin^2\theta_W, \ A_f = T_f^3)$$

$$H \qquad \frac{-ig_W m_f}{2M_W}$$

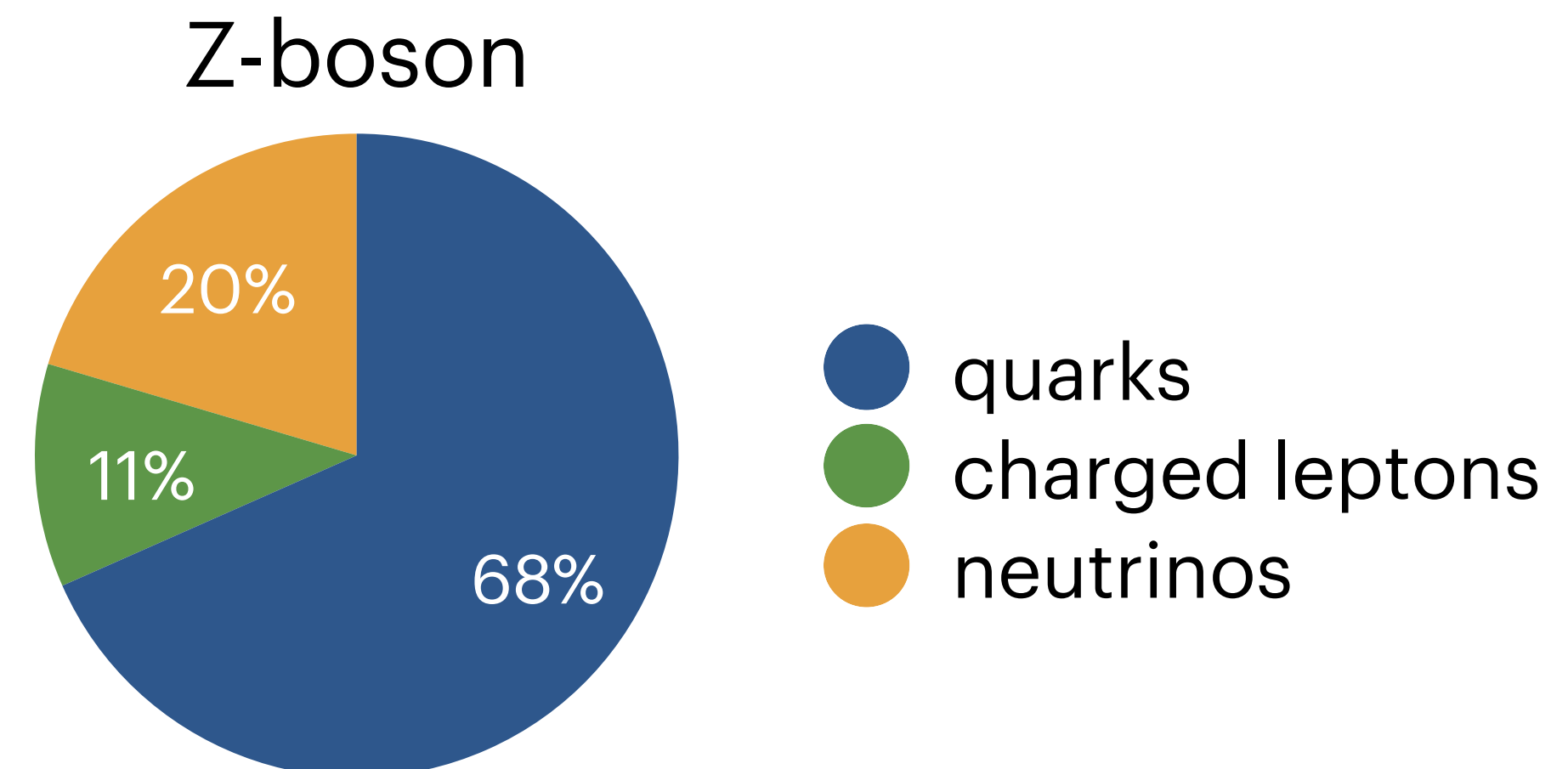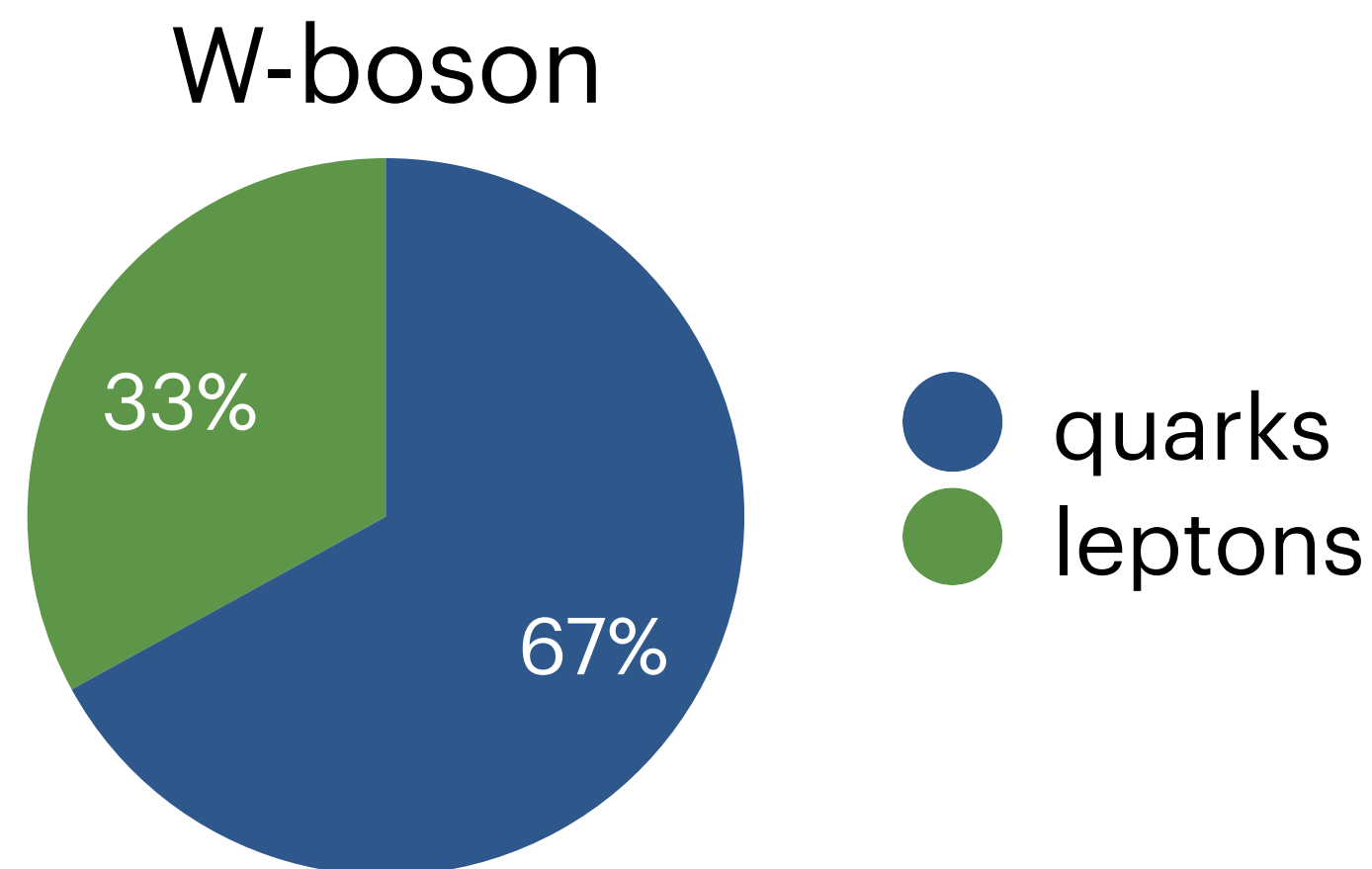# Decays of W- and Z-bosons

- At leading order (LO), the partial decay widths are given by:

$$\Gamma(W^+ \to f\bar{f}') = C\,\frac{G_F M_W^3}{6\sqrt{2}\pi} \qquad\qquad \Gamma(Z \to f\bar{f}) = C\,\frac{G_F M_Z^3}{6\sqrt{2}\pi}\left(V_f^2 + A_f^2\right)$$

C=1 leptons / C=3 quarks

- **W decays:** 3 charged leptons, and 2 light quark generations $\Rightarrow$ Br(W$^+$ → e$^+$ ν)=1/9

- **Z decays:**   Ve ≈ 0, |Ae|= |Aν|= |Vν| $\Rightarrow$ Br(Z → νν) ≈ **2 x** Br(Z → e+e-)

W-boson

- 33%
- 67%
- quarks
- leptons

Z-boson

- 20%
- 11%
- 68%
- quarks
- charged leptons
- neutrinos

- Large fraction of decays into difficult-to-measure modes.

Parton kinematics

- **Drell-Yan as an example:** lets look at lepton pair production via quark-antiquark annihilation

Lepton-pair four momentum (at LO):

$$\begin{cases} E = (x_1 + x_2)\sqrt{s}/2 \\ p_z = (x_1 - x_2)\sqrt{s}/2 \end{cases}$$
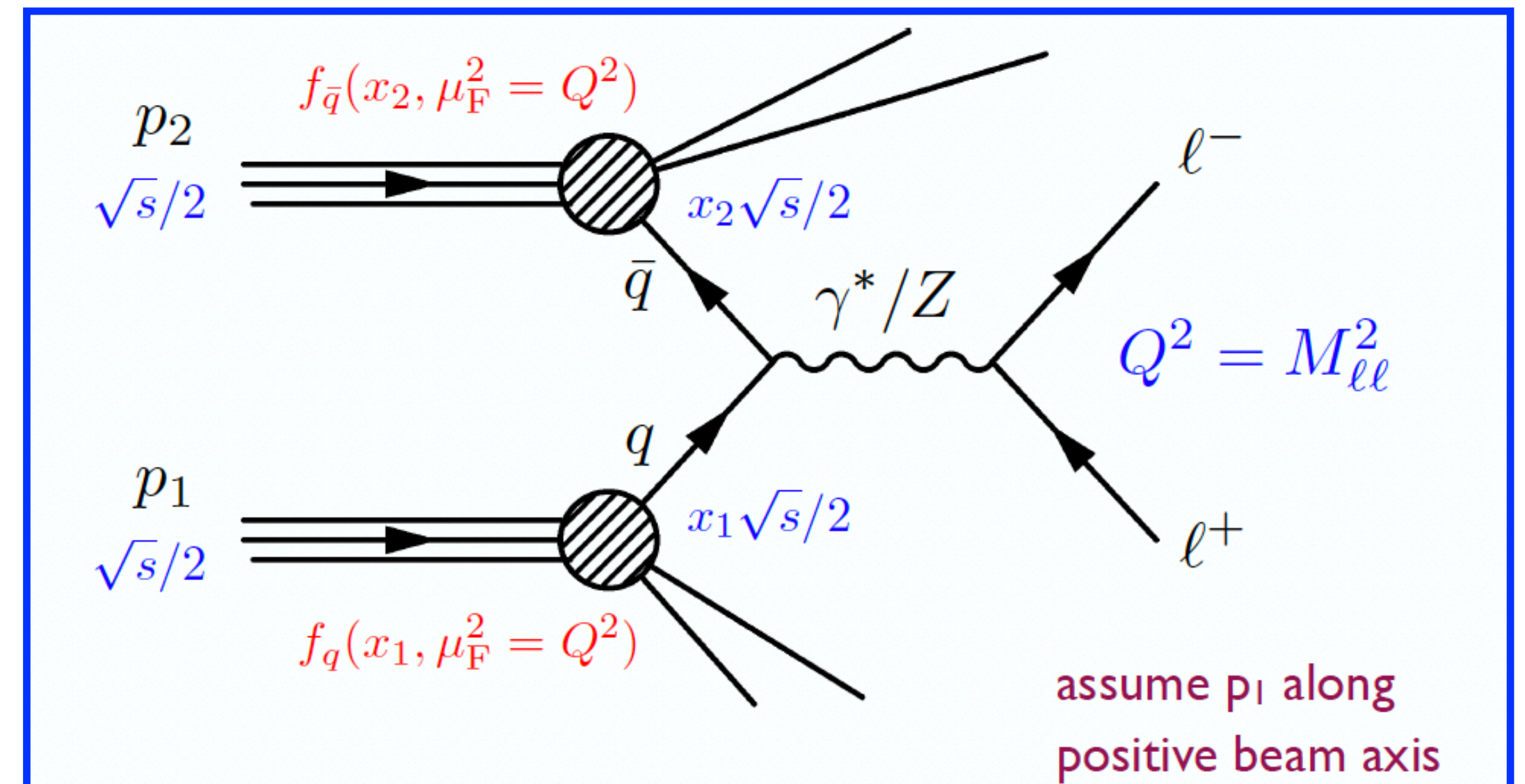
$$Q^2 = E^2 - p_z^2 = x_1 x_2 s$$

The rapidity ``y'' is defined as:

$$\frac{x_1}{x_2} = \frac{E + p_z}{E - p_z} \equiv e^{2y}$$

$$x_1 x_2 = Q^2/s$$
$$x_1/x_2 = e^{2y}$$

$$\Rightarrow \quad x_{1,2} = \frac{Q}{\sqrt{s}} e^{\pm y}$$

$$q(x_1) + \bar{q}\,(x_2) \rightarrow \gamma^*/Z \rightarrow l^+ l^-$$

For a given Q^2 the rapidity ``y'' of the lepton pair defines the x_1 and x_2 of the two partons

8

Parton kinematics

- Kinematic variables often studied at hadron colliders:

$$p_T \equiv \sqrt{p_x^2 + p_y^2}$$

Transverse momentum p_T

$$y \equiv \frac{1}{2} \ln \frac{E + p_z}{E - p_z}$$
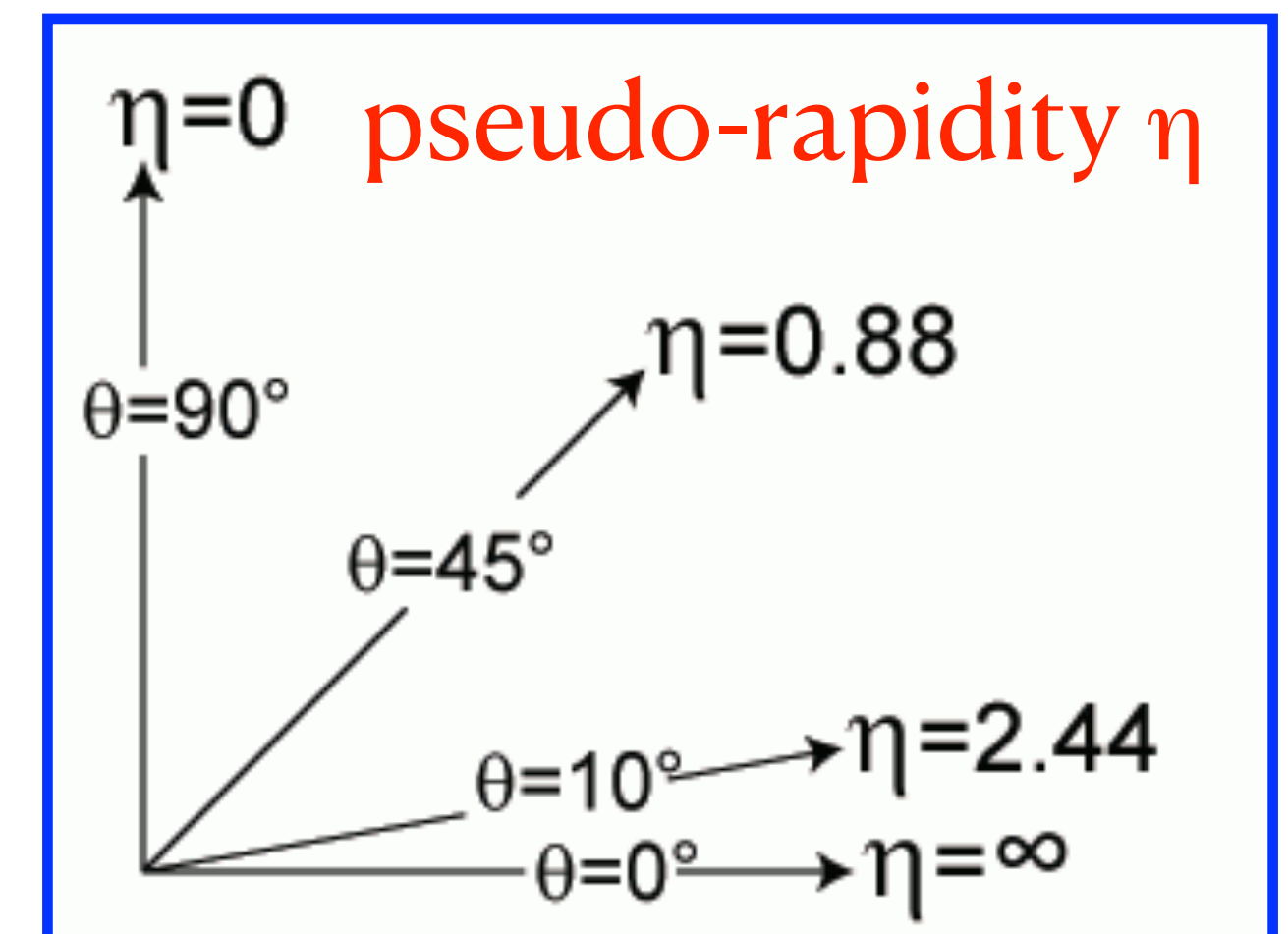
Rapidity y

The transverse momentum p_T is invariant under Lorentz boosts along z

- Sometimes we talk about the rapidity and other times we talk about the pseudo- rapidity. What is the difference?

For a massless particle (E>>M) :

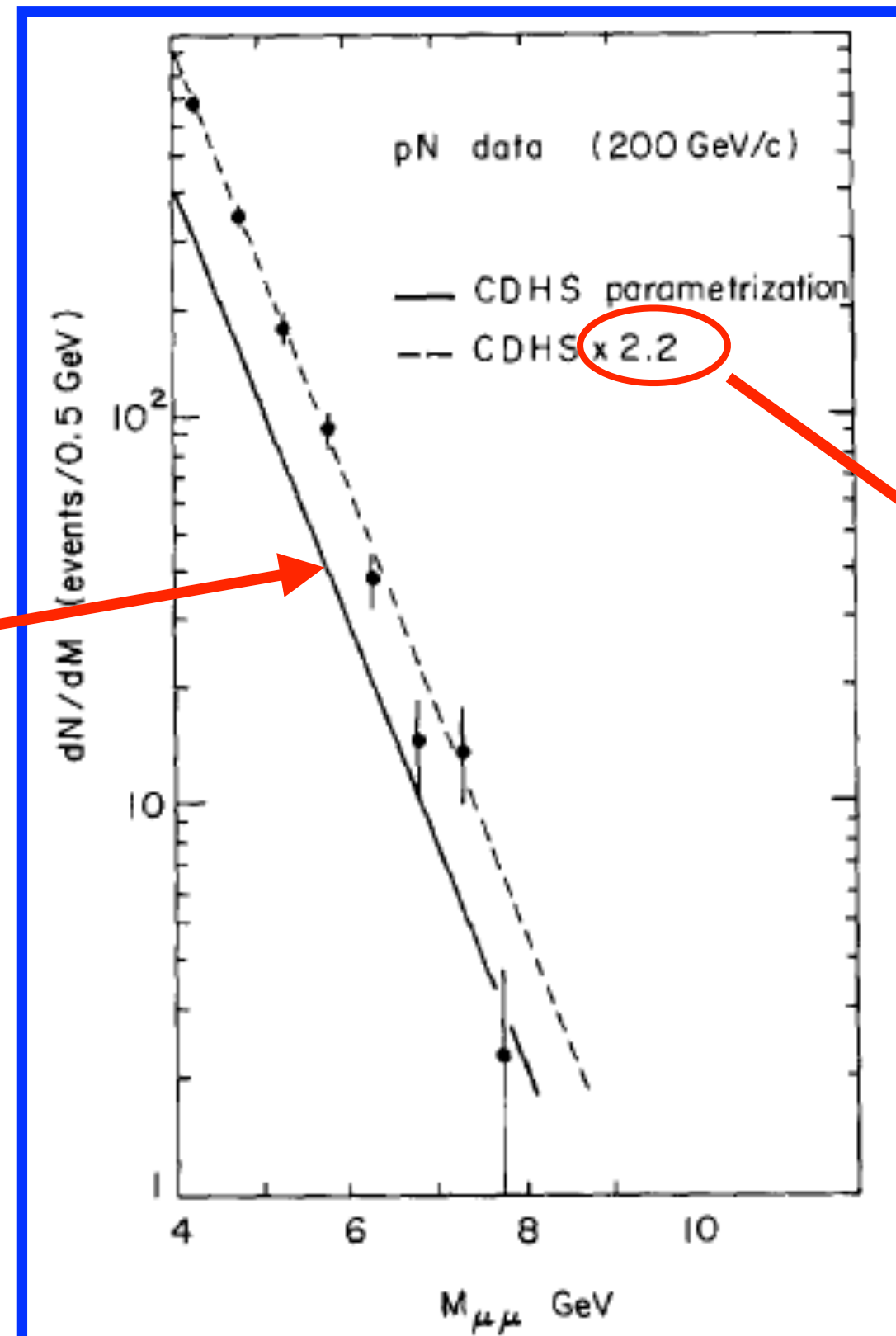$$y \rightarrow \frac{1}{2} \ln \frac{1 + \cos \theta}{1 - \cos \theta} = -\ln \tan \theta/2 \equiv \eta$$

pseudo-rapidity

pseudo-rapidity η

η=0

θ=90°

η=0.88

θ=45°

θ=10° η=2.44

θ=0° η=∞

θ: centre-of-mass scattering angle

Historical importance

- Study of the Drell-Yan process was critically important in establishing QCD as a quantitative theory

  - Comparison of di-muon invariant mass data from the NA3 experiment (proton-nucleon scattering) at CERN in 1979:

pN data (200 GeV/c)

— CDHS parametrization
-- CDHS x 2.2

dN/dM (events / 0.5 GeV)

10^2

10

1

4   6   8   10

$M_{\mu\mu}$ GeV

LO cross section obtained using old CDHS parametrization of PDFs

In all the channels studied the experimental cross section is significantly larger by a factor of 2.3 ± 0.5 than expected

The first introduction of a "K-factor" to explain discrepancies between theory and data

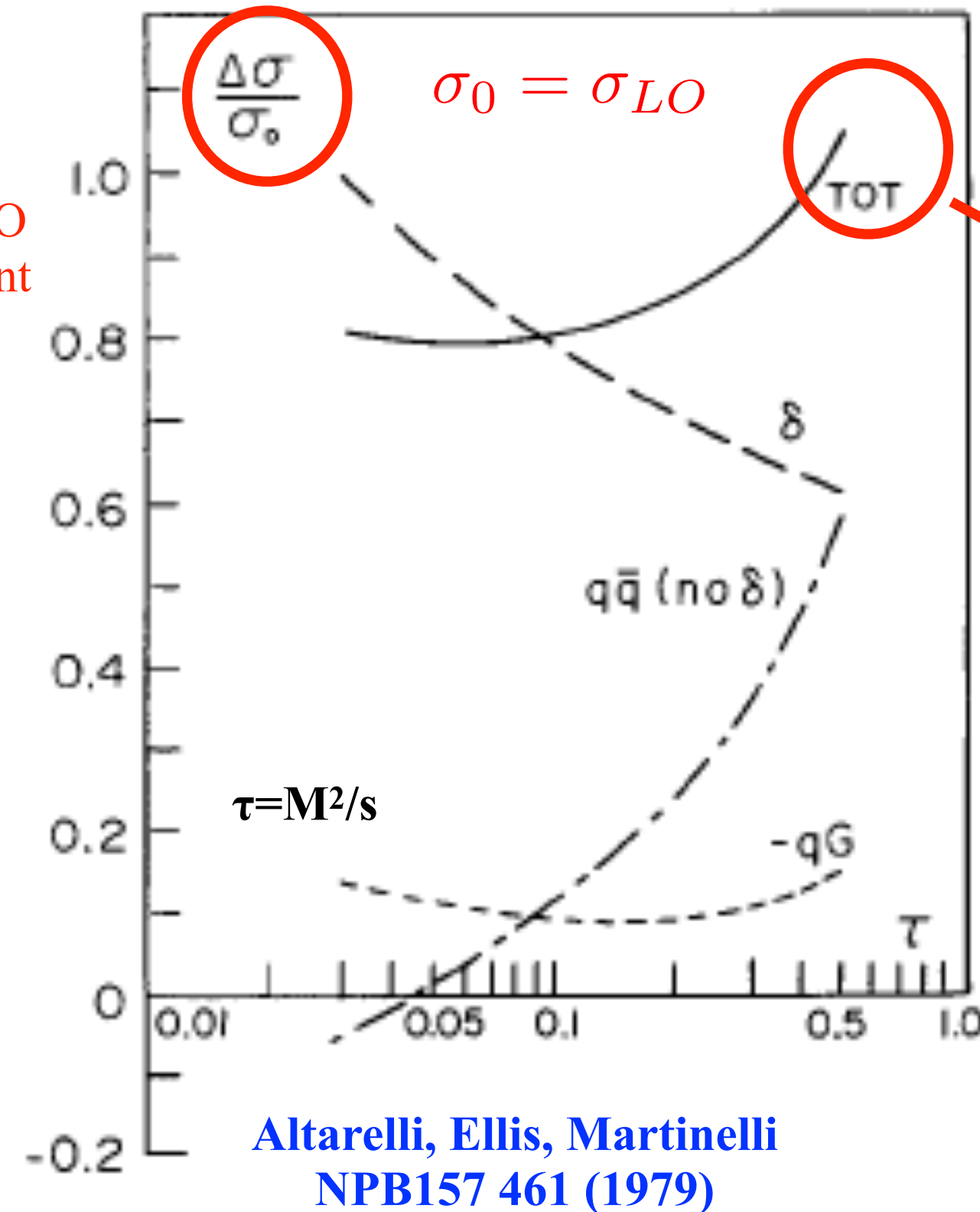$$K = (d^2\sigma/dx_1 dx_2)_{exp}/(d^2\sigma/dx_1 dx_2)_{DY \, model}.$$

Reaction	pN	p̄N
K	2.2 ± 0.4	2.4 ± 0.5

Historical importance

- Study of the Drell-Yan process was critically important in establishing QCD as a quantitative theory

TOT= sum of all partonic channels @ NLO

$\sigma_0 = \sigma_{LO}$

$\Delta\sigma =$ pure NLO coefficient

$\tau = M^2/s$

Altarelli, Ellis, Martinelli NPB157 461 (1979)

$$\Delta\sigma_{TOT}/\sigma_0 \sim 0.8 - 1.0$$

$$\sigma_{NLO} = \sigma_0 + \Delta\sigma_{TOT}$$

NLO QCD corrections reach nearly a factor of 2, greatly reducing tension between theory and experiment

Discrepancy resolved by next-to-leading order QCD!

Historical importance

- Understanding of vector boson production through the Drell-Yan process has required continued advances in our ability to understand QCD precisely, with data from the Tevatron and the LHC requiring NNLO predictions and beyond.
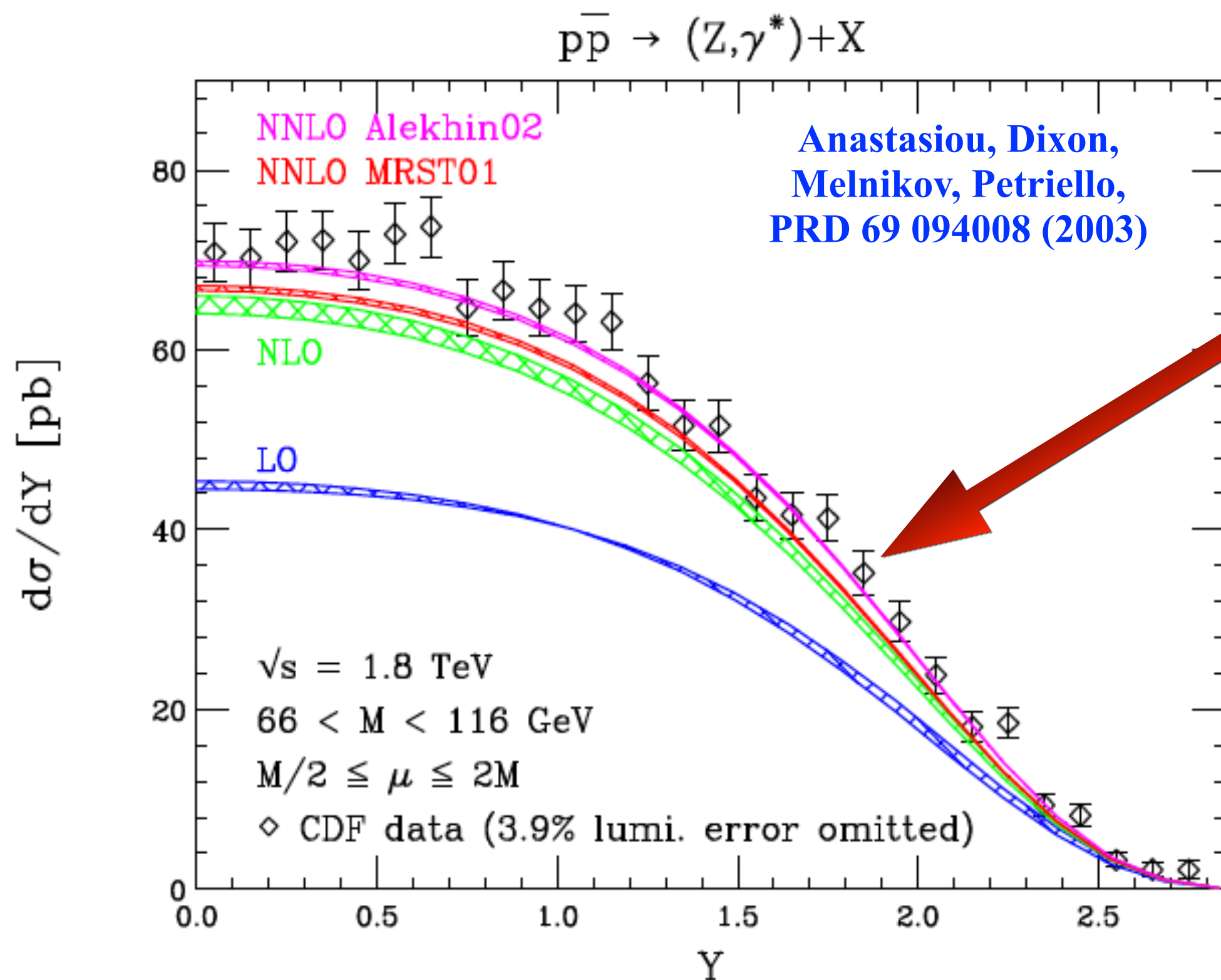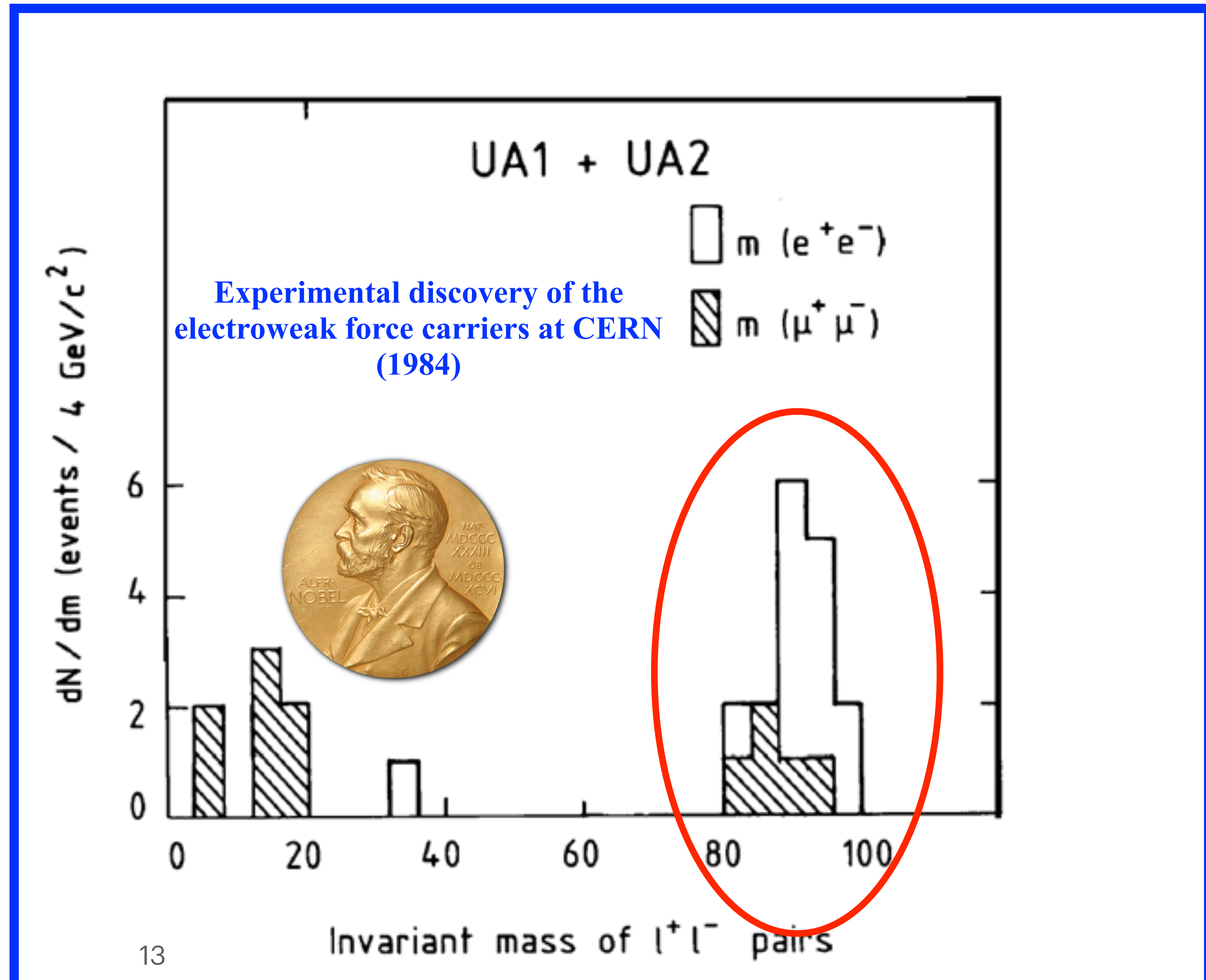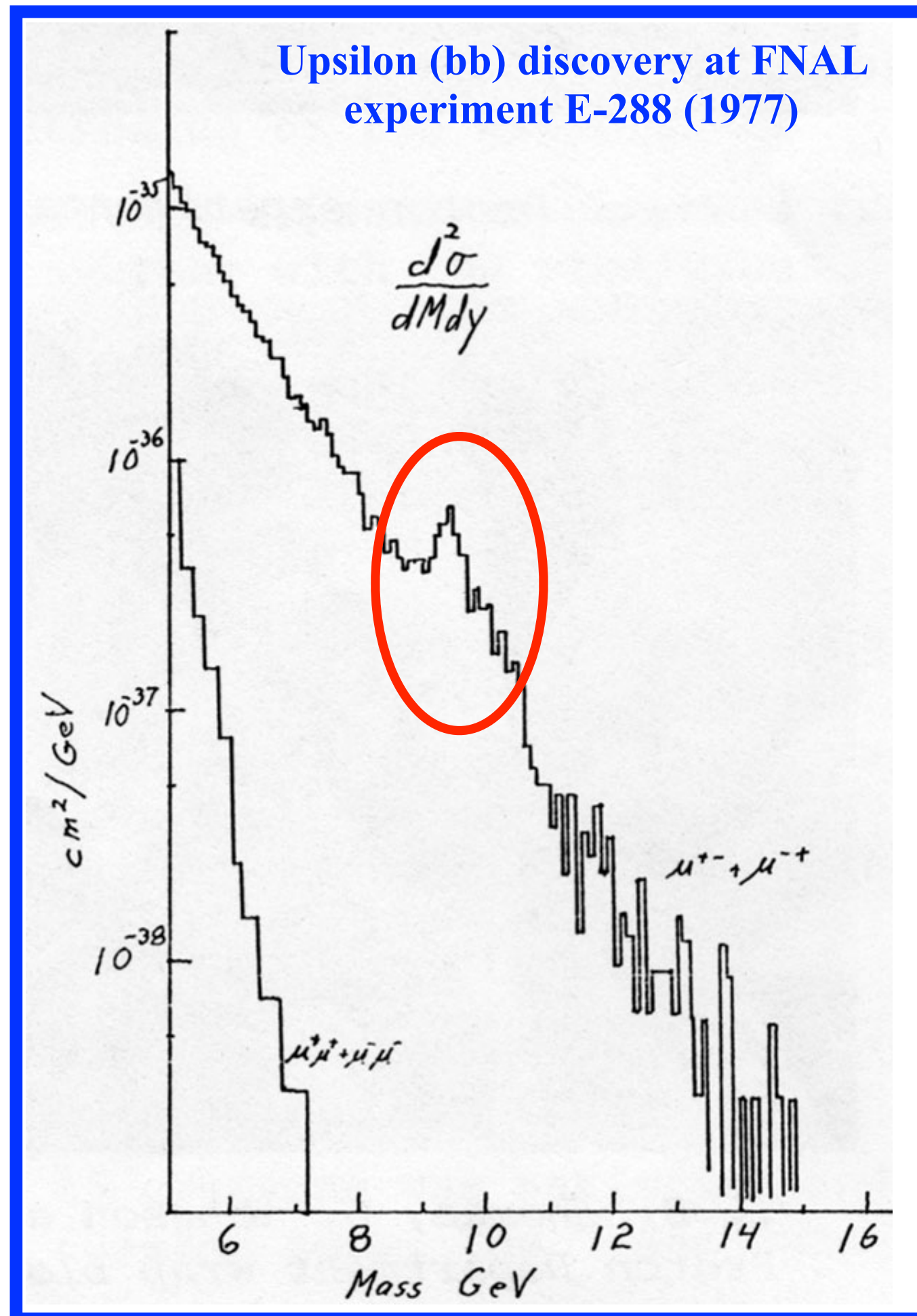

Drell-Yan data and predictions can be used to to improve our understanding of proton structure
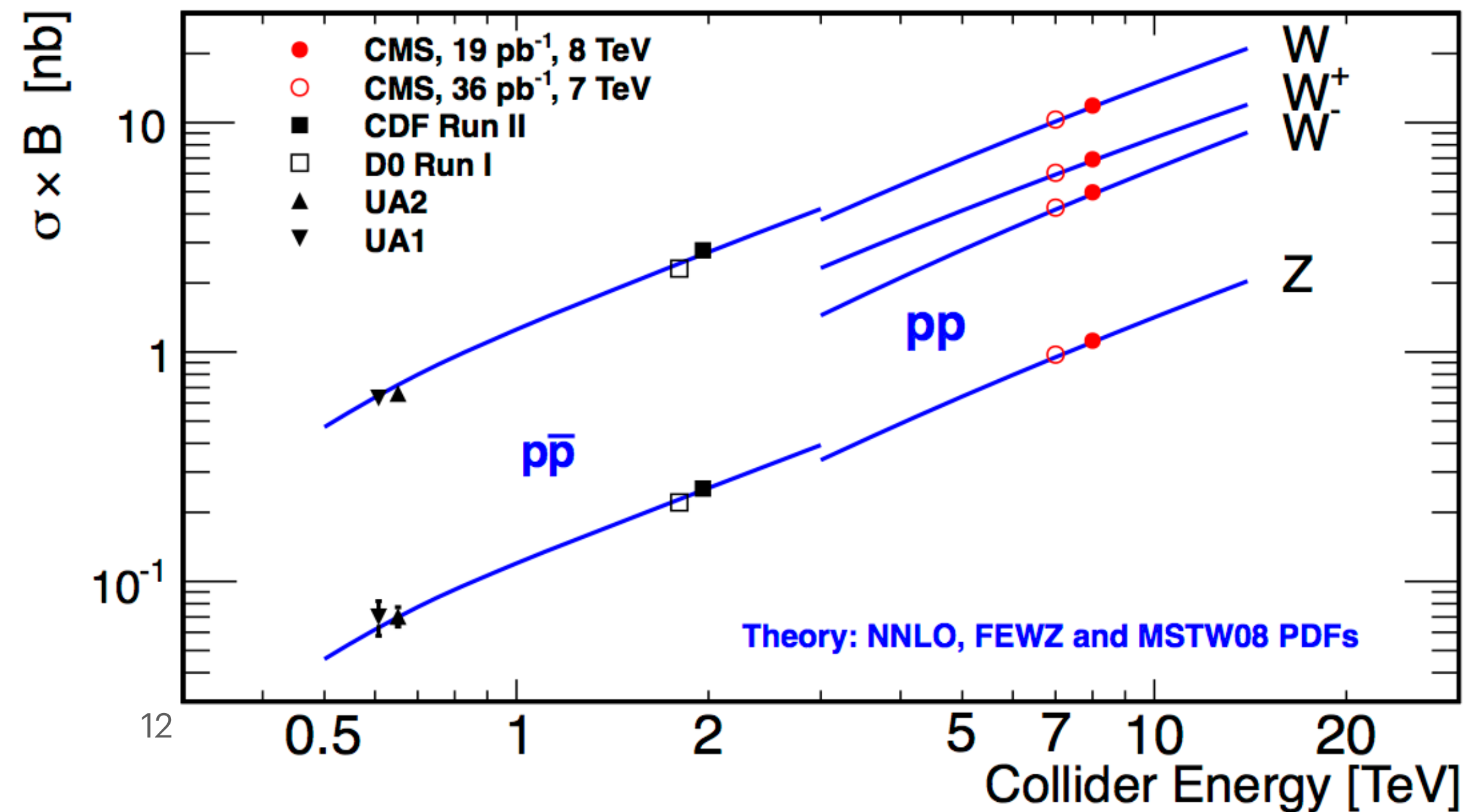
Historical importance
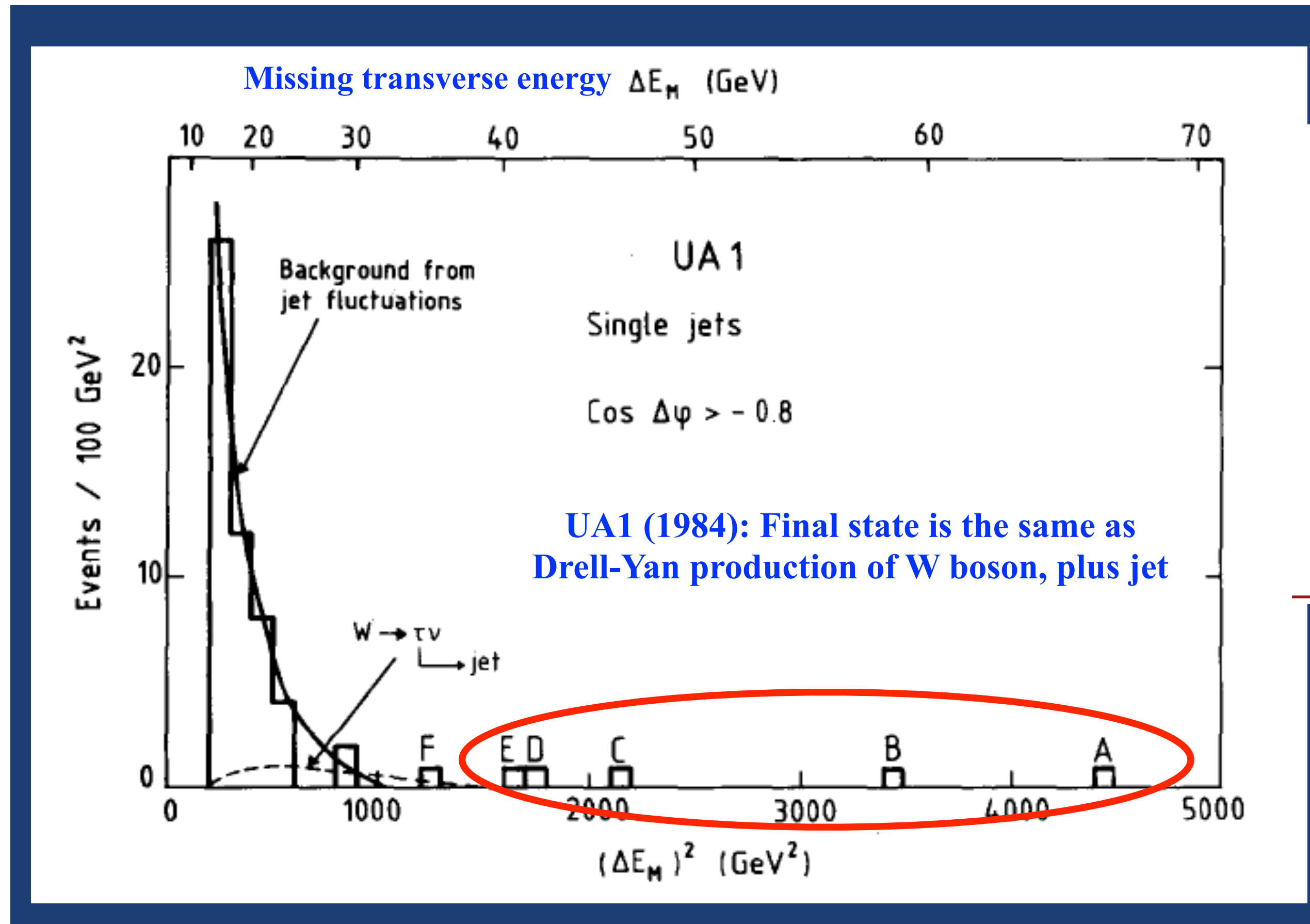
- The Drell-Yan process has been an important discovery mode throughout the modern history of high energy physics

Upsilon (bb) discovery at FNAL experiment E-288 (1977)

Experimental discovery of the electroweak force carriers at CERN (1984)

Historical importance

- The Drell-Yan production of vector bosons has also played a prominent role in famous non-discoveries in particle physics...

Missing transverse energy ΔE_M (GeV)

UA 1
Single jets

$\cos \Delta \varphi > - 0.8$

Background from jet fluctuations

$W \to \tau \nu$
$\quad \to$ jet

UA1 (1984): Final state is the same as Drell-Yan production of W boson, plus jet

Events / 100 GeV^2

$(\Delta E_M)^2$ (GeV^2)

4. *Conclusions.* We have presented a sample of five single-jet events and two "photon" events with $\Delta E_M > 40$ GeV. We have been unable to find a reasonable explanation in terms of background including W and Z^0 decays or within the expectation of the Standard Model. Therefore we believe they are due to some new physical phenomenon.
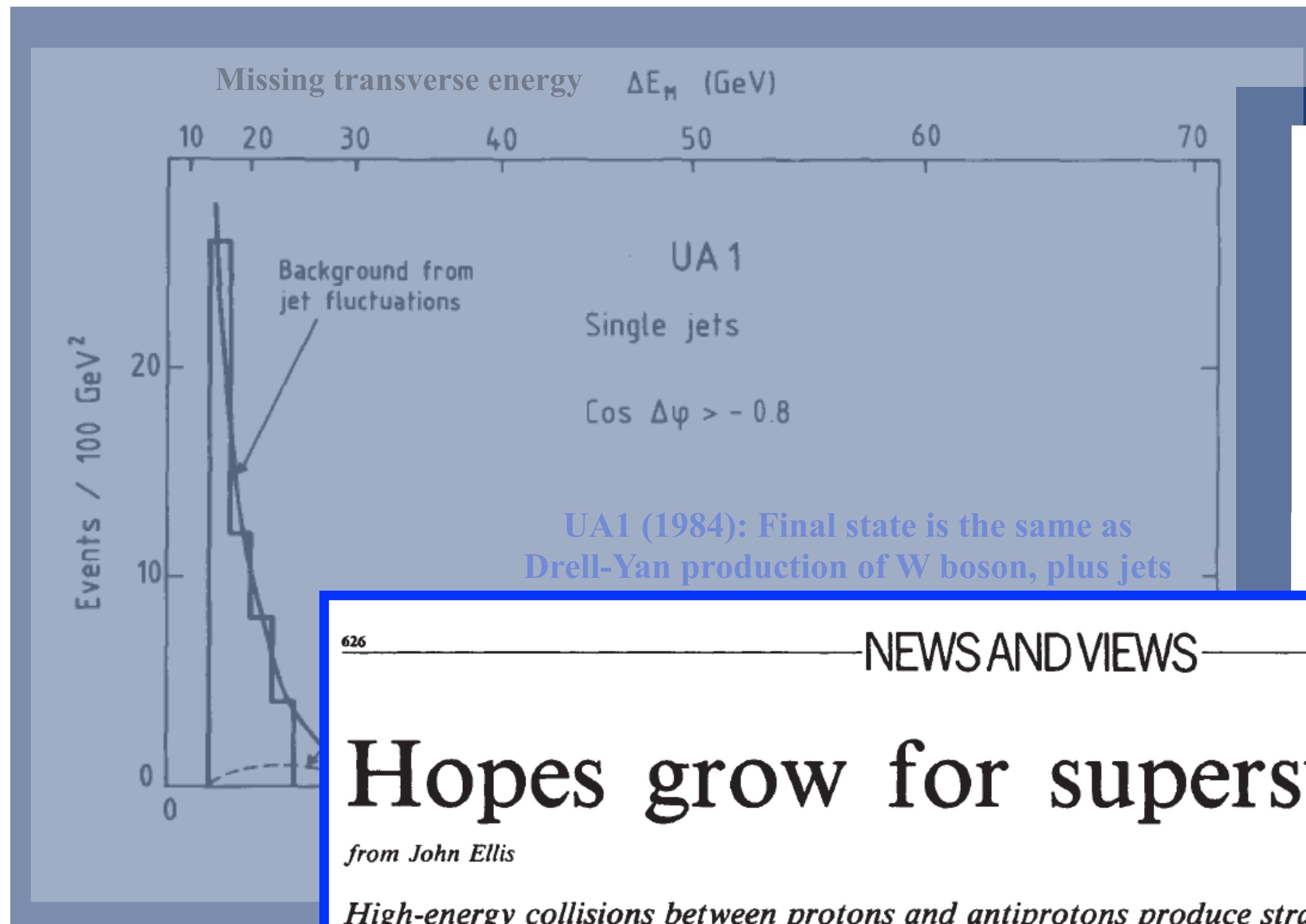
Physics Letters B
Volume 139, Issues 1–2, 3 May 1984, Pages 115-125

ELSEVIER

Experimental observation of events with large missing transverse energy accompanied by a jet or a photon (S) in pp collisions at s= 540GeV

UA1 Collaboration,, G. Arnison [m], O.C. Allkofer [g], A. Astbury [m, 1], B. Aubert [b], C. Bacci [l], G. Bauer [p], A. Bézaguet [d], R.K. Bock [d], T.J.V. Bowcock [h], M. Calvetti [d], P. Catz [b], P. Cennini [d], S. Centro [2], F. Ceradini [l], S. Cittolin [d], D. Cline [p], C. Cochet [n] ... M. Yvert [b]

Historical importance

- The Drell-Yan production of vector bosons has also played a prominent role in famous non-discoveries in particle physics…

Missing transverse energy ΔE_M (GeV)

UA1

Single jets

$\cos \Delta\varphi > -0.8$

Background from jet fluctuations

Events / 100 GeV²

UA1 (1984): Final state is the same as Drell-Yan production of W boson, plus jets

4. *Conclusions.* We have presented a sample of five single-jet events and two "photon" events with $\Delta E_M > 40$ GeV. We have been unable to find a reasonable explanation in terms of background including W and Z^0 decays or within the expectation of the Standard Model. Therefore we believe they are due to some new physical phenomenon.

NEWS AND VIEWS

626   NATURE VOL. 313 21 FEBRUARY 1985
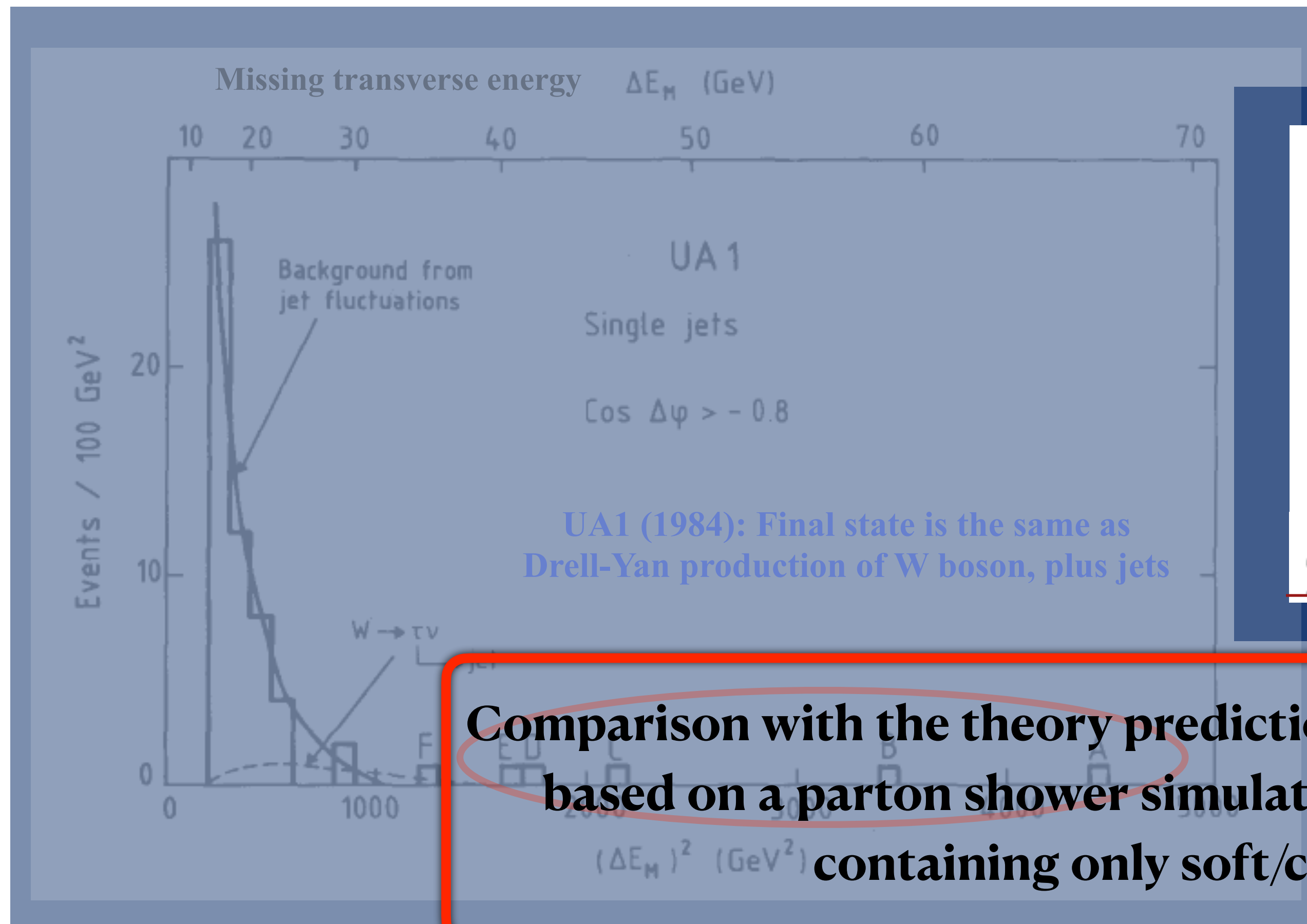
Hopes grow for supersymmetry

from John Ellis

High-energy collisions between protons and antiprotons produce strange events in which momentum fails to balance. Missing momentum may be carried by photinos, super-partners of the photon.
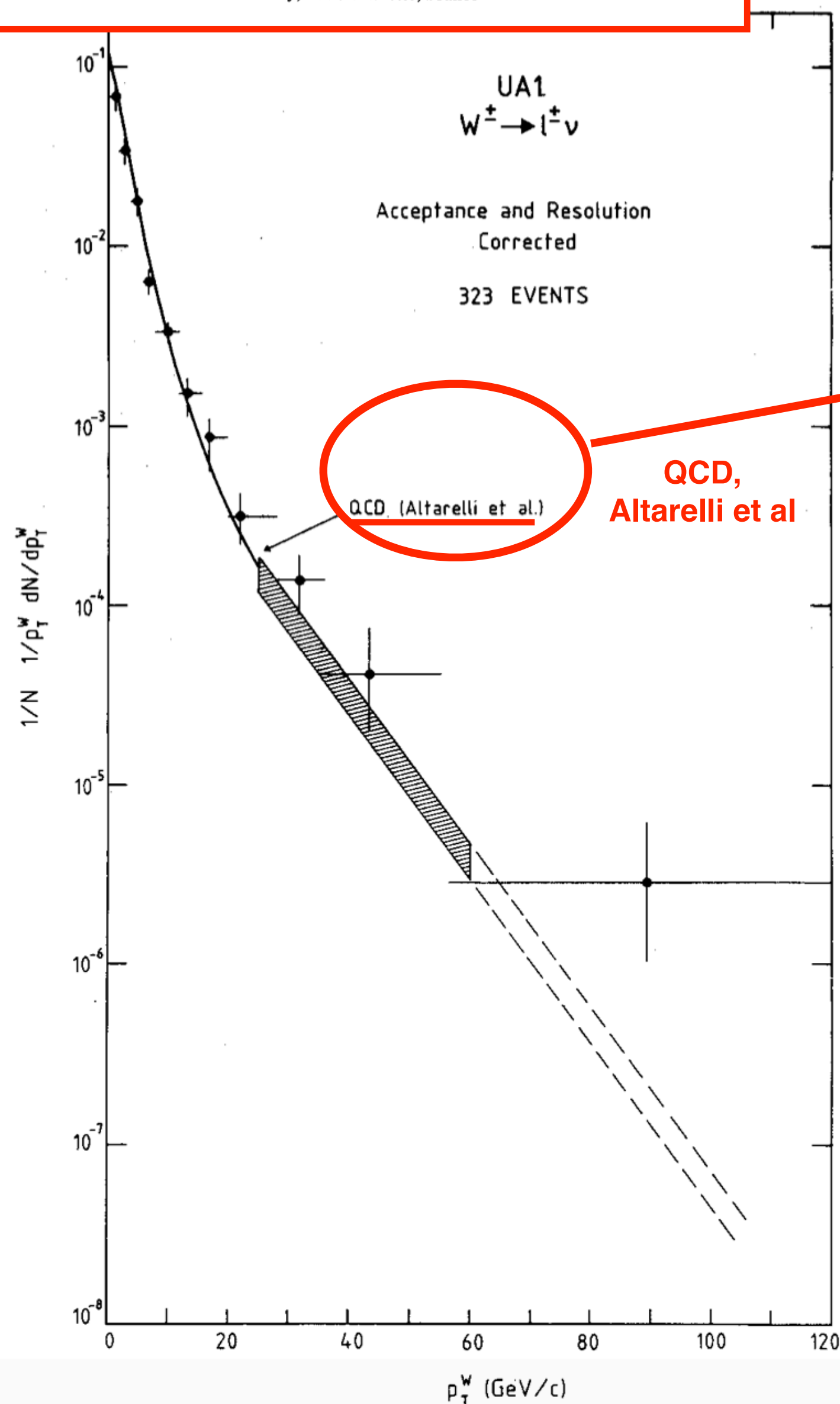
Historical importance

- The Drell-Yan production of vector bosons has also played a prominent role in famous non-discoveries in particle physics...

Missing transverse energy ΔE_M (GeV)

UA1

Single jets

$\cos \Delta\varphi > -0.8$

$W \to \tau\nu$

Background from jet fluctuations

Events / 100 GeV^2

$(\Delta E_M)^2$ (GeV^2)

UA1 (1984): Final state is the same as Drell-Yan production of W boson, plus jets

4. Conclusions. We have presented a sample of five single-jet events and two "photon" events with $\Delta E_M > 40$ GeV. We have been unable to find a reasonable explanation in terms of background including W and Z^0 decays or within the expectation of the Standard Model. Therefore we believe they are due to some new physical phenomenon.

Comparison with the theory prediction for the background was based on a parton shower simulation for W/Z-production containing only soft/collinear jets

16

Historical importance

W AND Z PHYSICS AND THE STANDARD MODEL

UA1 Collaboration

Aachen – Amsterdam (NIKHEF) – Annecy (LAPP) – Birmingham – CERN – Harvard – Helsinki –
Kiel – Imperial College, London – Queen Mary College, London – Madrid – MIT – Padua –
Paris (Collège de France) – Riverside – Rome – Rutherford Appleton Lab. – Saclay (CEN) –
Victoria – Vienna – Wisconsin

Presented by E. Locci
CEN Saclay, Gif-sur-Yvette, France

UA1
$W^{\pm} \rightarrow l^{\pm} \nu$

Acceptance and Resolution
Corrected

323 EVENTS

QCD (Altarelli et al.)

QCD,
Altarelli et al

$1/N \; 1/p_T^W \; dN/dp_T^W$

p_T^W (GeV/c)

A proper SM prediction for the background requires including W+hard jet emissions. This explained the discrepancy!

Parton showers without matching to exact tree level matrix elements do not explain hard emissions correctly.

UA1 CM energy = 540 GeV ⇒ 40 GeV missing energy is hard, not soft !

Predicting hadronic cross sections

- How does theory allow us to peer into the inner hard-scattering in a typical hadron collider process?
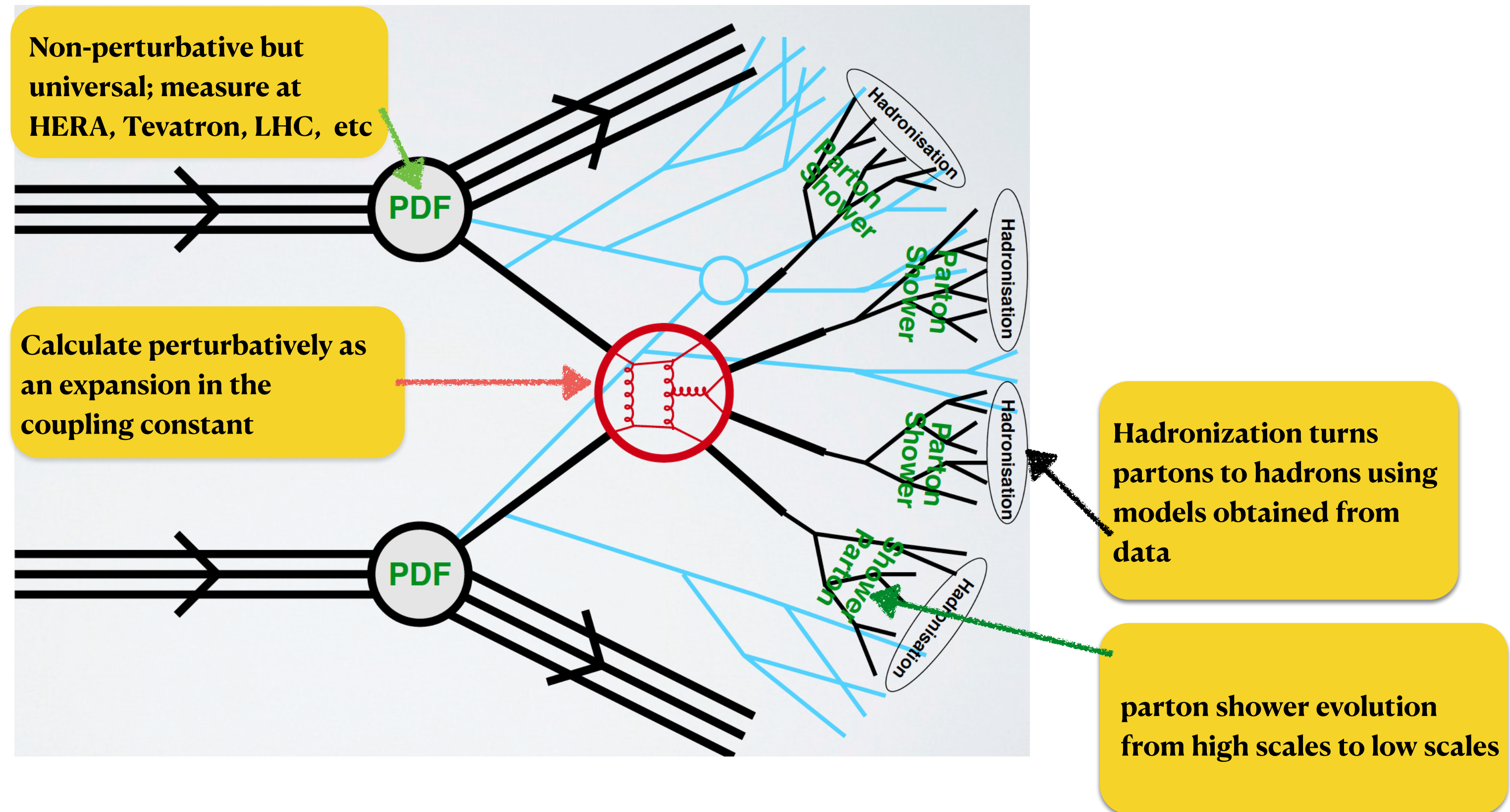
We rely on factorization: divide and conquer!

Predicting hadronic cross sections

- Our formalism for predicting hadronic cross sections:

factorization and renormalization scales

$$\sigma(P_1, P_2) = \sum_{i,j} \int dx_1 dx_2 f_{i/h_1}(x_1, \mu_F^2) f_{j/h_2}(x_2, \mu_F^2) \hat{\sigma}_{ij}(p_1, p_2, \alpha_S(\mu_R), Q^2; \mu_F^2, \mu_R^2) + \mathcal{O}\left(\frac{\Lambda_{QCD}}{Q}\right)$$

Parton density functions, universal, non-perturbative

Parton level cross sections, process dependent, perturbative

Power suppressed contributions

- The parton level cross sections are obtained from the matrix elements. They are model and process dependent.

- Parton density functions (PDFs) are universal, i.e process independent.

Predicting hadronic cross sections

$$\hat{\sigma}_{ab \to X}(\hat{s}, \mu_F, \mu_R) \quad \text{Parton-level cross section}$$

Computed perturbatively as an expansion in the coupling constant, for example the strong coupling:

$$\hat{\sigma} = \sigma^{\text{Born}}\left(1 + \frac{\alpha_s}{2\pi}\sigma^{(1)} + \left(\frac{\alpha_s}{2\pi}\right)^2 \sigma^{(2)} + \left(\frac{\alpha_s}{2\pi}\right)^3 \sigma^{(3)} + \dots \right)$$
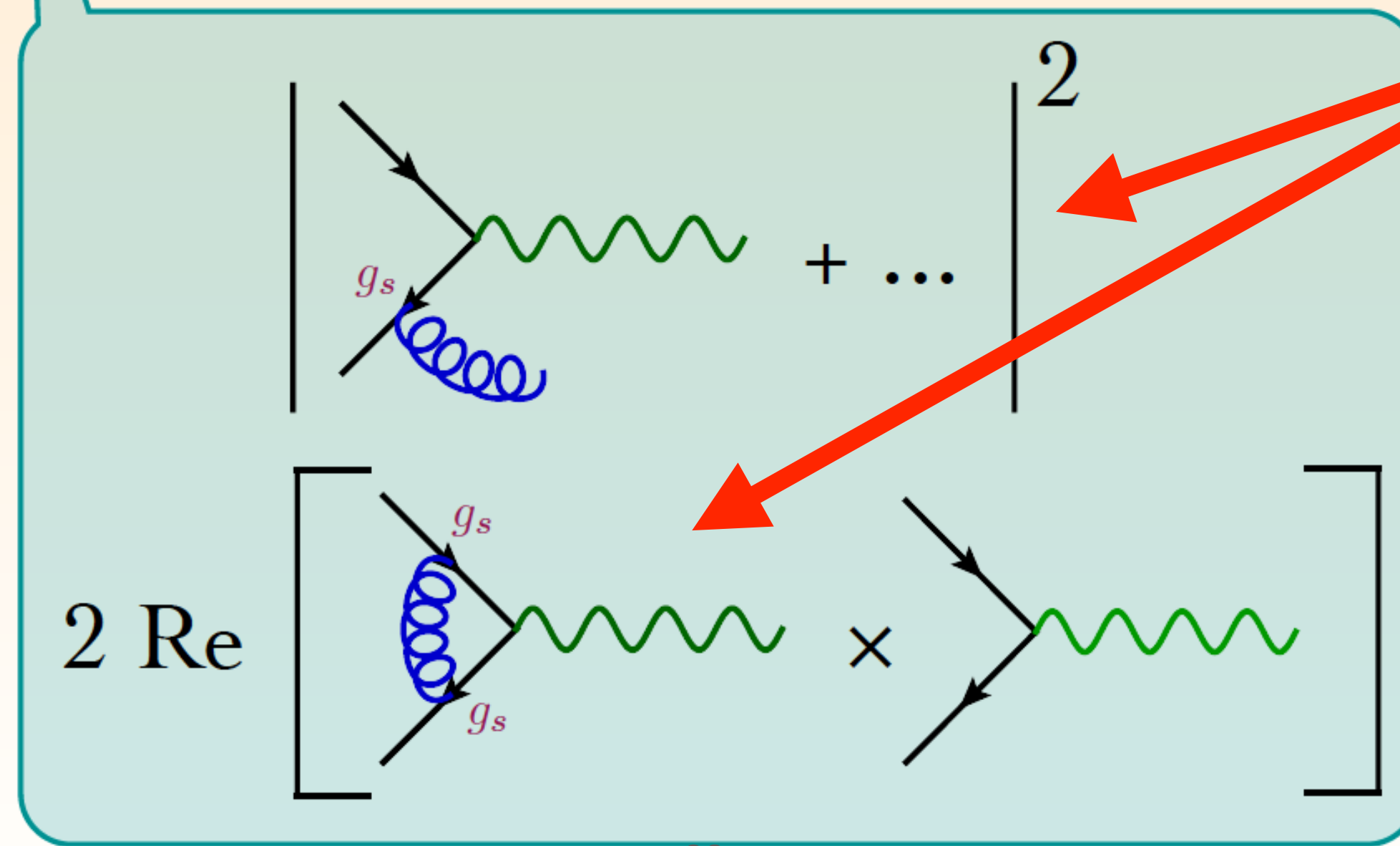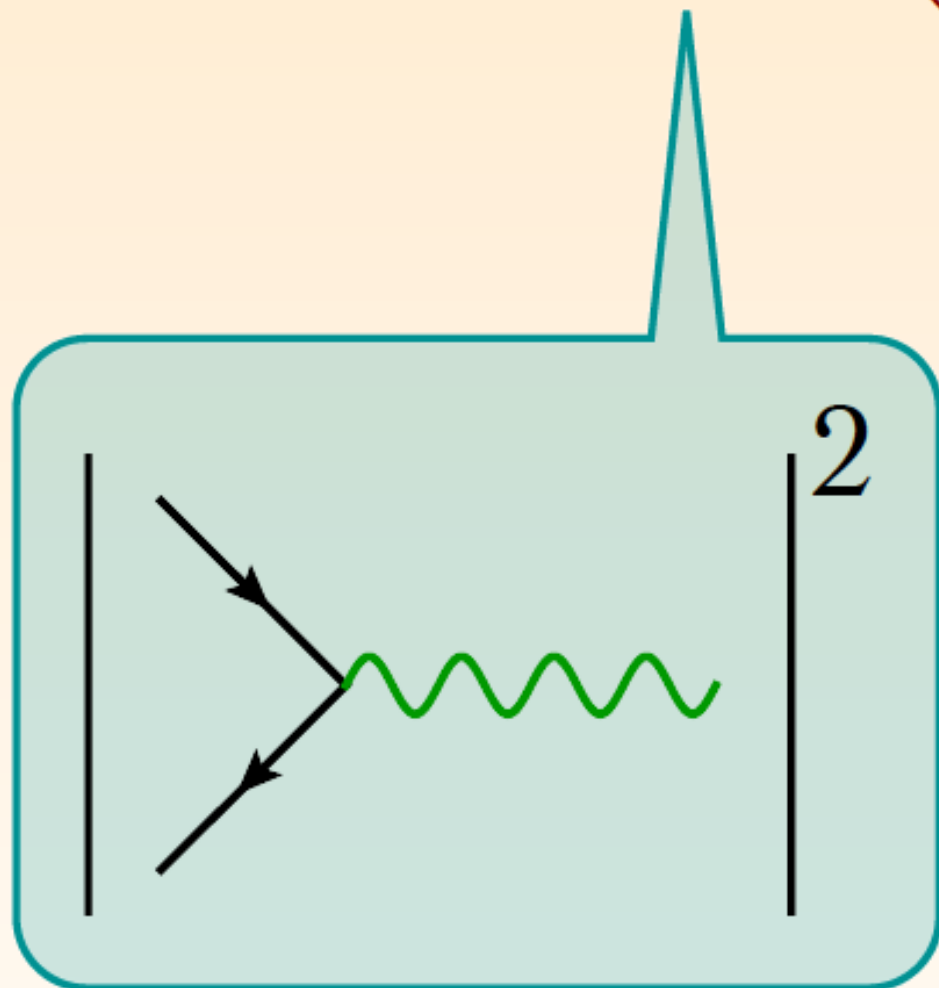
Predicting hadronic cross sections

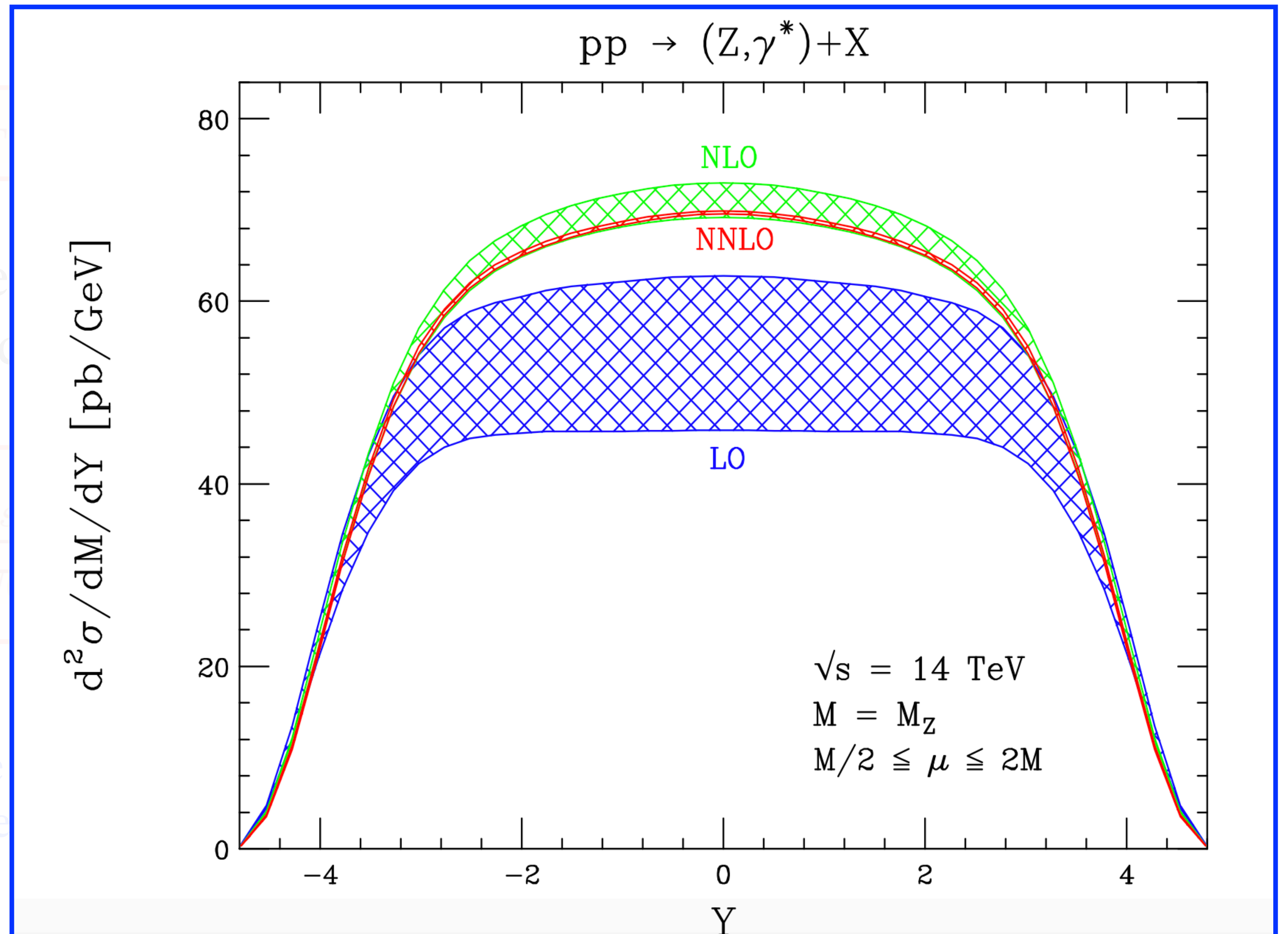$$\hat{\sigma}_{ab \to X}(\hat{s}, \mu_F, \mu_R) \quad \text{Parton-level cross section}$$

Computed perturbatively as an expansion in the coupling constant, for example the strong coupling:

$$\hat{\sigma} = \sigma^{\text{Born}}\left(1 + \frac{\alpha_s}{2\pi}\sigma^{(1)} + \left(\frac{\alpha_s}{2\pi}\right)^2 \sigma^{(2)} + \left(\frac{\alpha_s}{2\pi}\right)^3 \sigma^{(3)} + \dots\right)$$

known for up to W+5jets

known for most relevant $2 \to 2$ processes

known for inclusive Higgs and DY production

Predicting partonic cross sections

- Drell-Yan as an example:

$$\hat{\sigma} = \sigma^{\text{Born}} \left(1 + \frac{\alpha_s}{2\pi} \sigma^{(1)} + \ldots \right)$$

Both real and virtual corrections are needed to cancel all singularities arising from soft and collinear emissions

Predicting partonic cross sections

$$\hat{\sigma}_{ab \to X}(\hat{s}, \mu_F, \mu_R) \quad \text{Parton-level cross section}$$

Computed perturbatively as an expansion in the coupling constant, for example the strong coupling:

$$\hat{\sigma} = \sigma^{\text{Born}}\left(1 + \frac{\alpha_s}{2\pi}\sigma^{(1)} + \left(\frac{\alpha_s}{2\pi}\right)^2 \sigma^{(2)} + \left(\frac{\alpha_s}{2\pi}\right)^3 \sigma^{(3)} + \ldots\right)$$

Including higher orders in the perturbative expansion improves the accuracy of our prediction and reduces the dependence on non-physical parameters such as μ_F and μ_R.

Predicting partonic cross sections

Very large corrections from LO to NLO in QCD. The correction is smaller when going from NLO to NNLO
$\implies$ the perturbative expansion is converging and stable

$pp \to (Z, \gamma^*) + X$

$\sqrt{s} = 14$ TeV
$M = M_Z$
$M/2 \leqq \mu \leqq 2M$

Anastasiou, Dixon, Melnikov, Petriello (2004)

Predicting partonic cross sections

- LO tree level predictions are not sufficient to describe the data. NLO QCD corrections were the first quantitatively reliable prediction.

- ~50% increase in the cross section was observed for the rapidity distribution when going from LO → NLO

- NNLO QCD results available for the fully exclusive case (Melnikov, Petriello, 2006; Catani, Cieri, Ferrera, de Florian, Grazzini, 2009), as well as NLO electroweak and QED corrections (Baur, Keller, Wackeroth, 1999; Dittmaier, Kramer, 2007; Calame, Montagna, Nicrosini, Vicini, 2007).

- The state-of-the-art inclusive N3LO QCD corrections to DY due to a γ^*, Z exchange as well as a charged current are now available (Duhr, Dulat, Mistlberger, 2020; Duhr, Mistlberger, 2021)
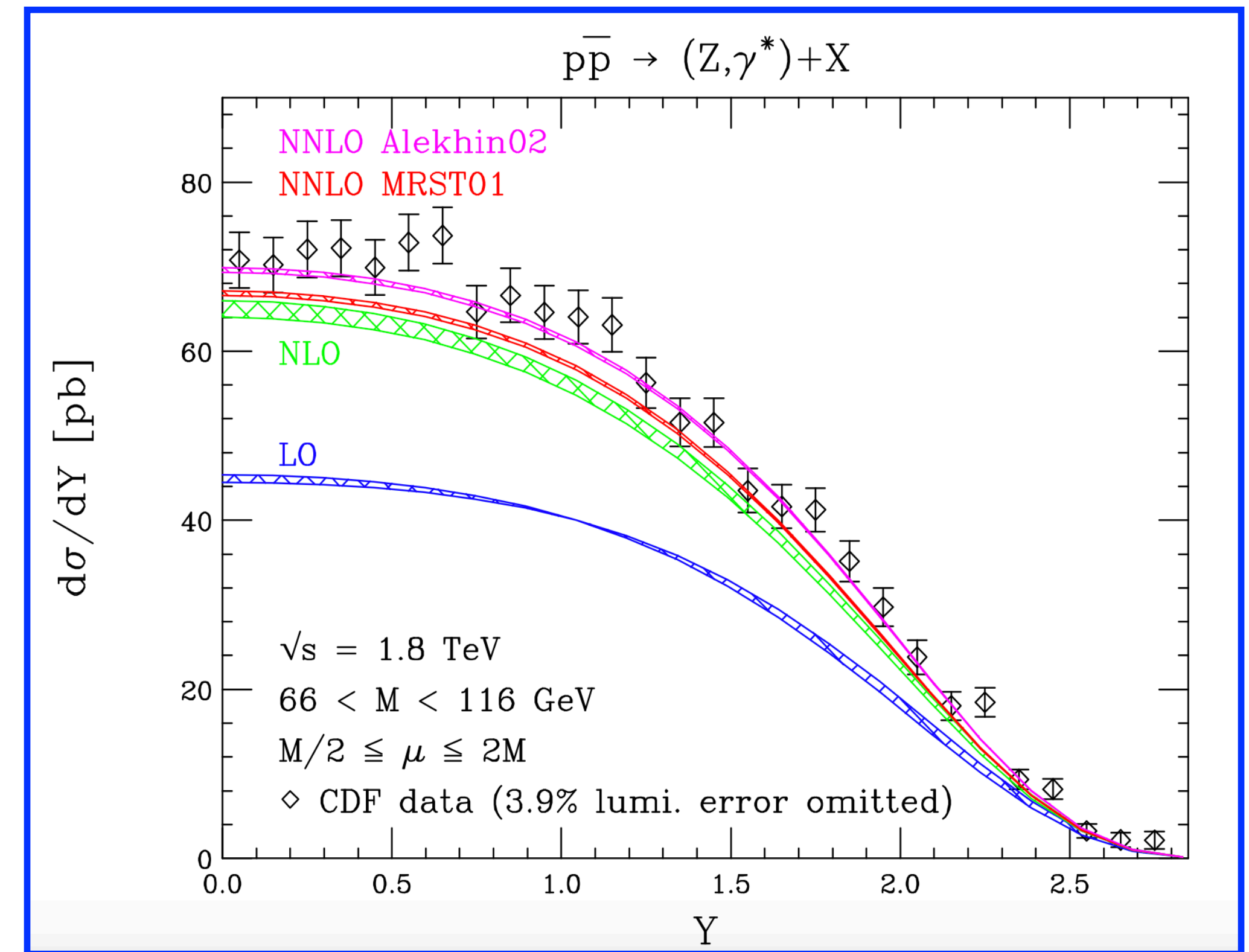
Anastasiou, Dixon, Melnikov, Petriello (2004)

$$Y = \frac{1}{2} \ln \left(\frac{E + p_z}{E - p_z} \right)$$

Drell-Yan at N3LO

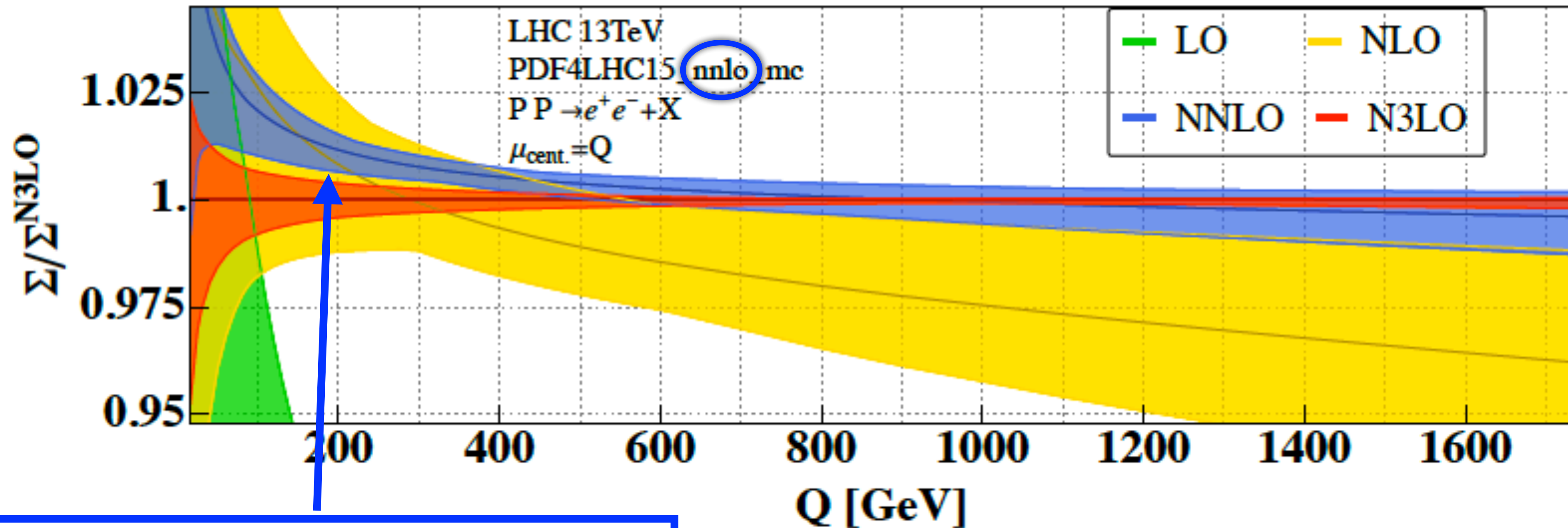- Neutral current cross section as an example (Duhr, Mistlberger, 2021):
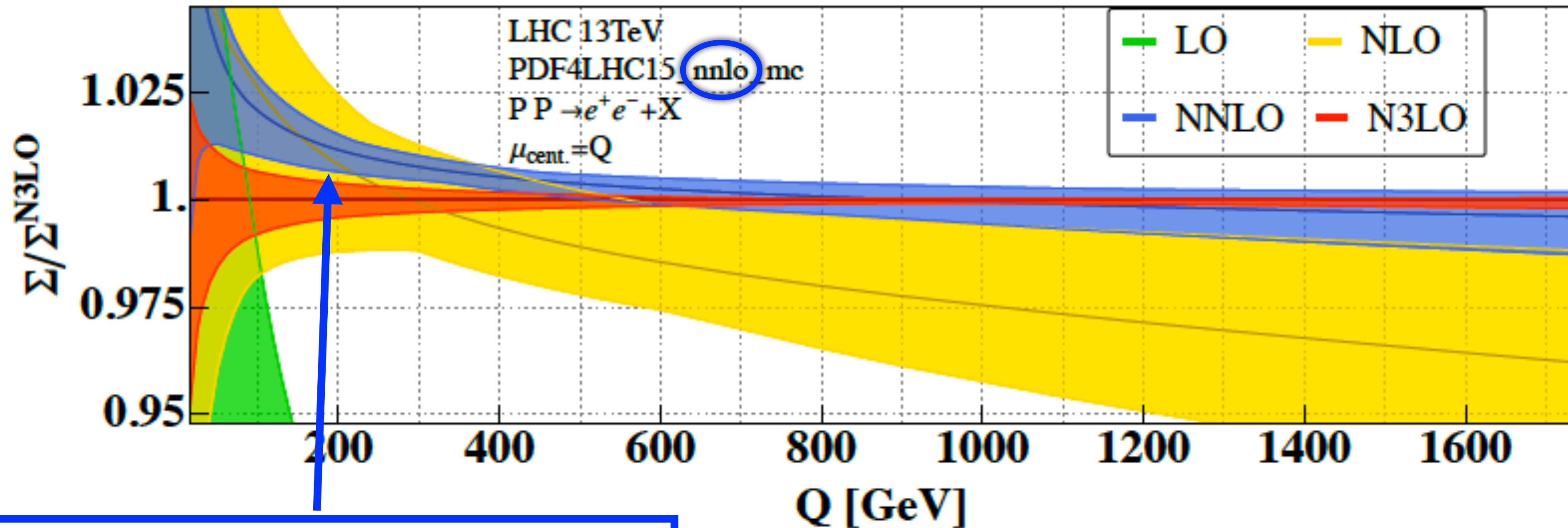
The ratio of lower-order results to N3LO reveals a slight non-overlap of scale variation bands for 40<Q<400 GeV

Central scale: $\mu_R=\mu_F=Q=m_{ll}$

$$\frac{1}{2} \leq \frac{\mu_R}{\mu_F} \leq 2$$

Drell-Yan at N3LO

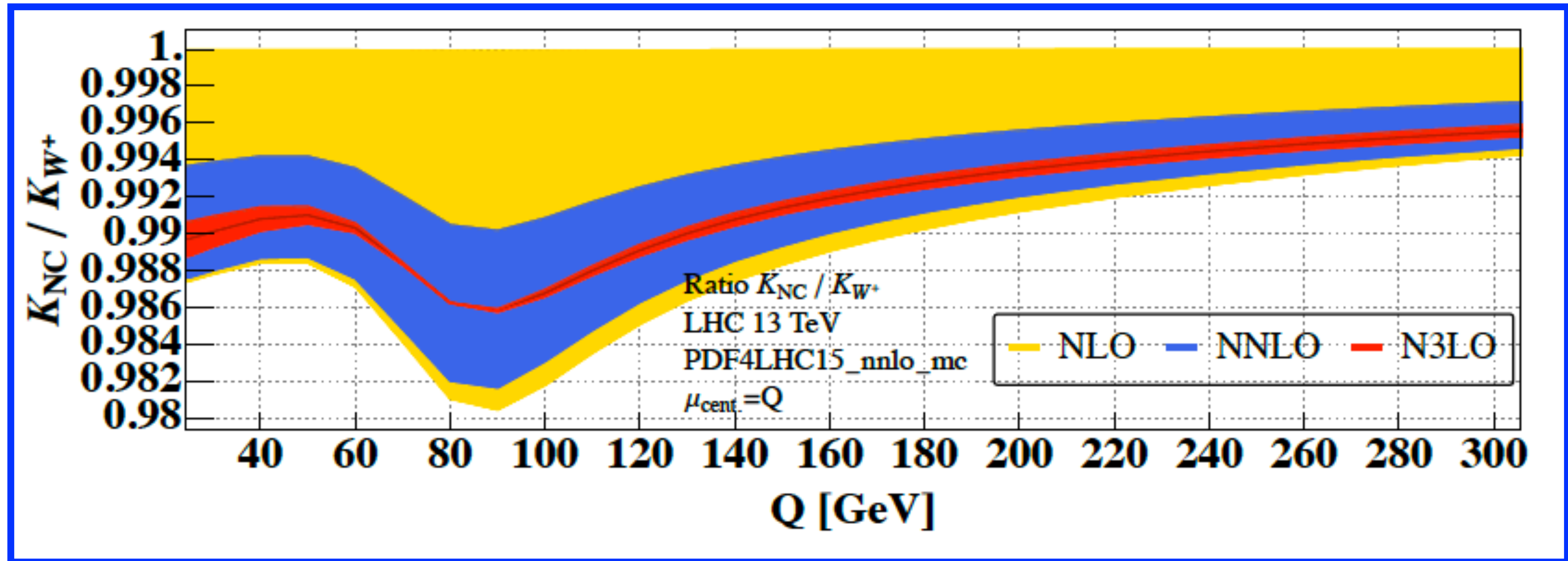- Neutral current cross section as an example (Duhr, Mistlberger, 2021):

LHC 13TeV
PDF4LHC15 nnlo mc
$PP \rightarrow e^+e^- + X$
$\mu_{cent.} = Q$

— LO	— NLO
— NNLO	— N3LO

The corrections show delicate cancellations between qg and qqbar partonic channel; this effect may be due to missing N3LO PDFs

Central scale: $\mu_R = \mu_F = Q = m_{ll}$

$$\frac{1}{2} \leq \frac{\mu_R}{\mu_F} \leq 2$$

Drell-Yan at N3LO

Ratio of neutral-current to charged-current K-factors extremely well-behaved in QCD perturbation theory; almost no residual scale dependence, overlap between NNLO and N3LO
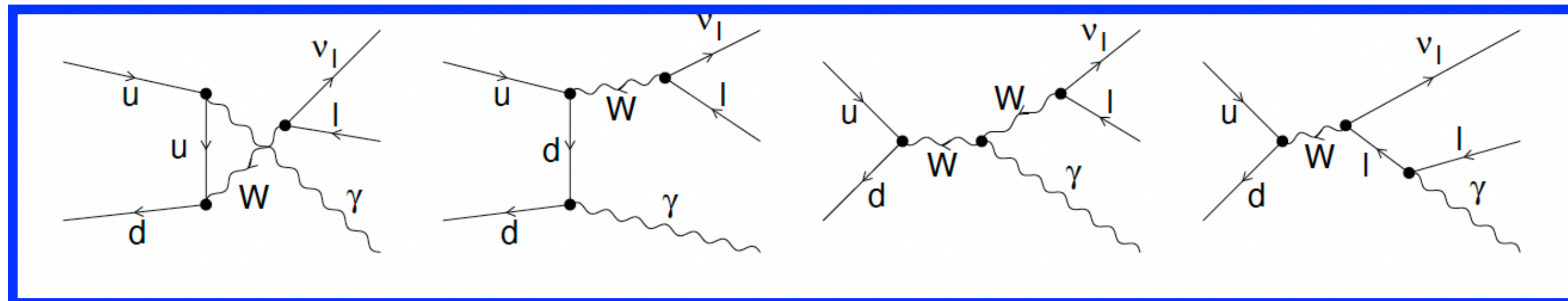
Electroweak and QED corrections

- Numerically we expect NNLO QCD corrections to be comparable to NLO QED and EW effects: $O(\alpha_s^2) \sim O(\alpha)$

- Virtual loops include photons, W and Z. For real radiation only photons are considered since the massive W and Z real radiation are reconstructed as di-boson event samples

- Example contributing diagrams to charged-current lepton pair production at NLO:
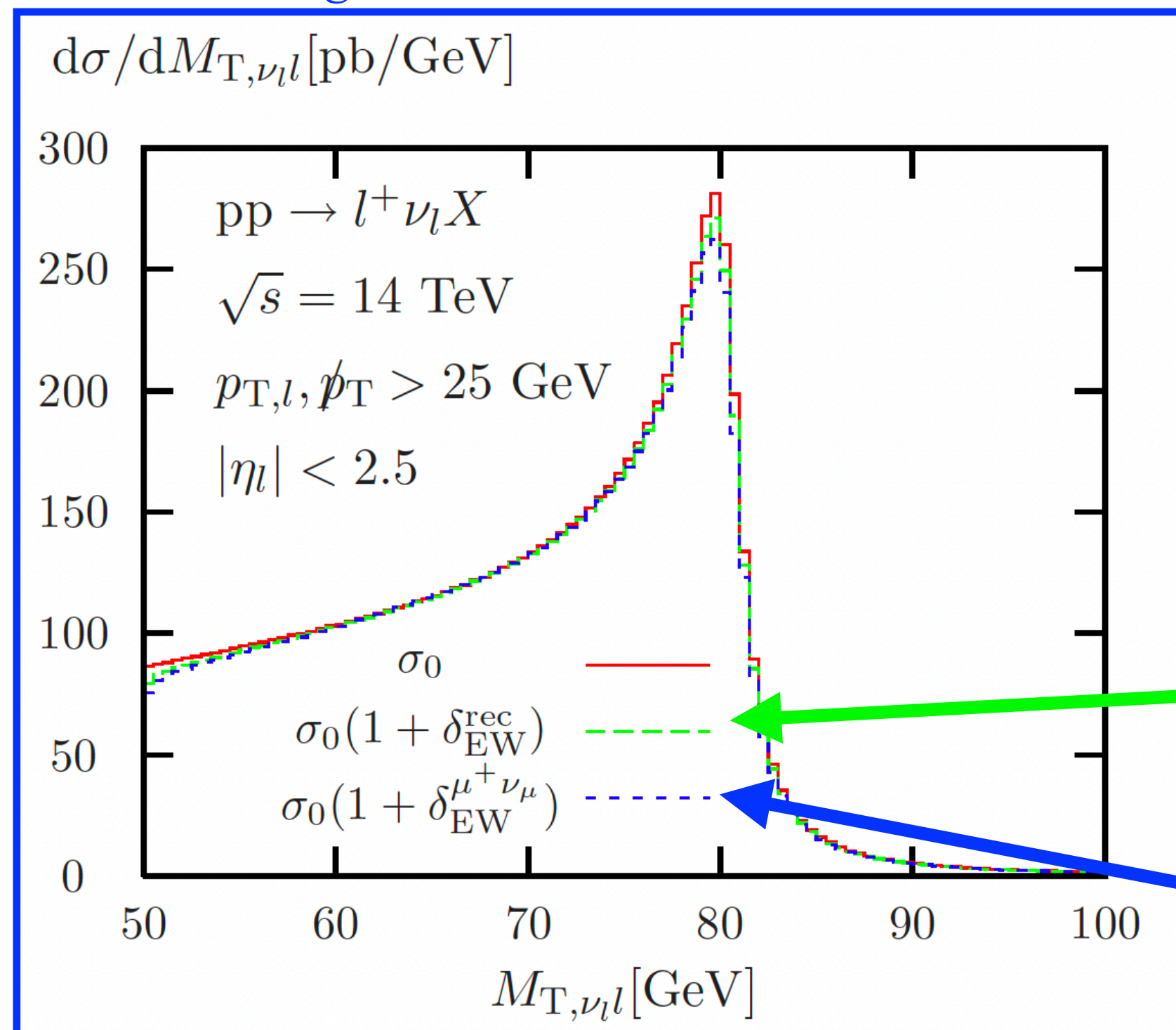
Virtual corrections:
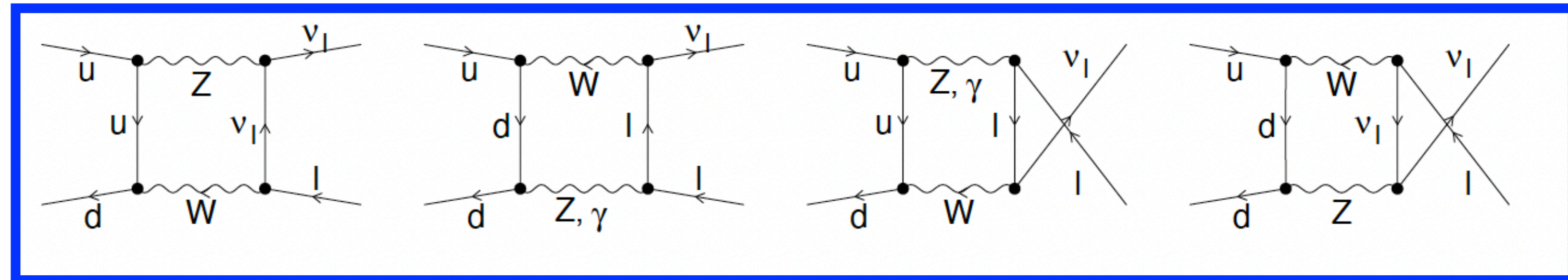
Real corrections:
(qγ/$\gamma\gamma$ processes are also present at higher orders)

Electroweak and QED corrections

- Numerically we expect NNLO QCD corrections to be comparable to NLO QED and EW effects:
  $O(\alpha_s^2) \sim O(\alpha)$

- Virtual loops include photons, W and Z. For real radiation only photons are considered since the massive W and Z real radiation is reconstructed as di-boson event samples.

- **Example:** corrections to the W-transverse mass distribution $M_{T,l\nu} = \sqrt{2 p_{Tl} \not{p}_T (1 - cos\phi_{\nu_l l})}$

Brensing, Dittmaier, Kraemer, Mueck, 2008

$d\sigma/dM_{T,\nu_l l}[\text{pb/GeV}]$

$pp \to l^+ \nu_l X$

$\sqrt{s} = 14$ TeV

$p_{T,l}, \not{p}_T > 25$ GeV

$|\eta_l| < 2.5$

σ_0

$\sigma_0(1 + \delta_{EW}^{rec})$

$\sigma_0(1 + \delta_{EW}^{\mu^+\nu_\mu})$

$M_{T,\nu_l l}[\text{GeV}]$

- QCD corrections (not shown) are ~ 20-30% but flat

- Shape distortion near the Jacobian peak. Leads to a shift in MW determination by ~ 100 (50) MeV for bare (dressed) leptons

- The peak at $M_{T,l\nu} \approx$ MW is used in the W-mass determination
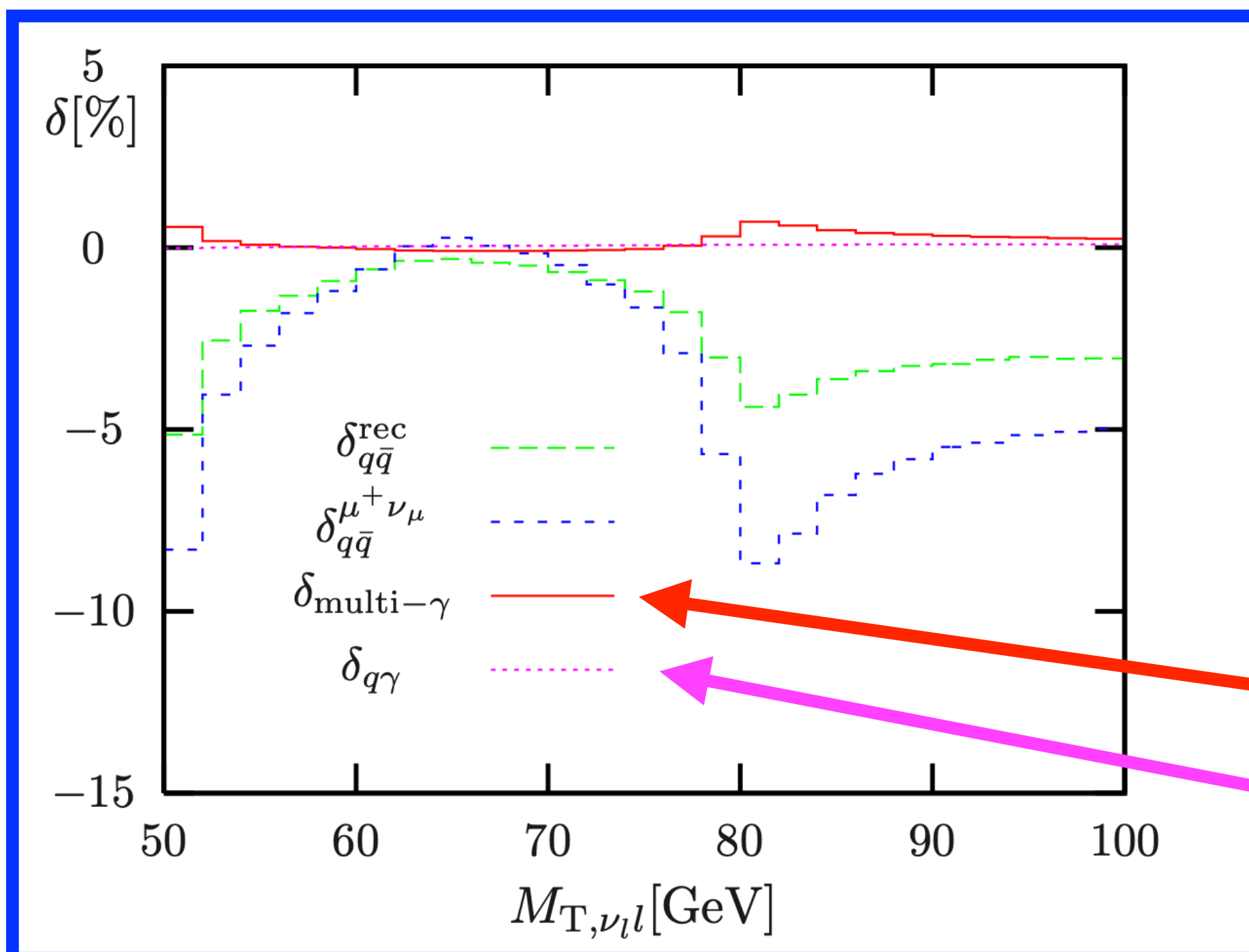
EW corrections with photon recombination, where leptons and sufficiently collinear photons are treated as one quasi particle

Bare final state muon, no photon recombination

30

Electroweak and QED corrections

- Numerically we expect NNLO QCD corrections to be comparable to NLO QED and EW effects: $O(\alpha_s^2) \sim O(\alpha)$

- Virtual loops include photons, W and Z. For real radiation only photons are considered since the massive W and Z real radiation is reconstructed as di-boson event samples.

- Example: corrections to the W-transverse $M_{T,l\nu}$ distribution $M_{T,l\nu} = \sqrt{2p_{Tl}\, \not{p}_T (1 - cos\phi_{\nu_l l})}$

Brensing, Dittmaier, Kraemer, Mueck, 2008

- Near the peak δ_{qqbar} reaches 10% for bare muons and 5% after photon recombination. Sensitivity to the definition of the lepton (bare vs dressed)

- Photon induced corrections are small near the resonance region

- Multi-photon emission reaches the percent near $M_{T,l\nu} \approx MW$ and induces a distortion that affects MW determination from the shape of the $M_{T,l\nu}$ distribution
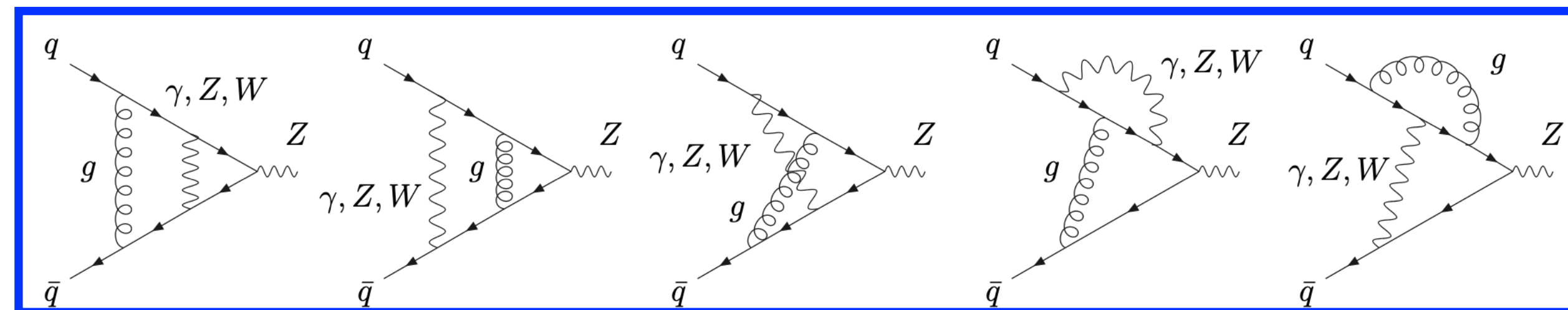
Multi-photon final state radiation

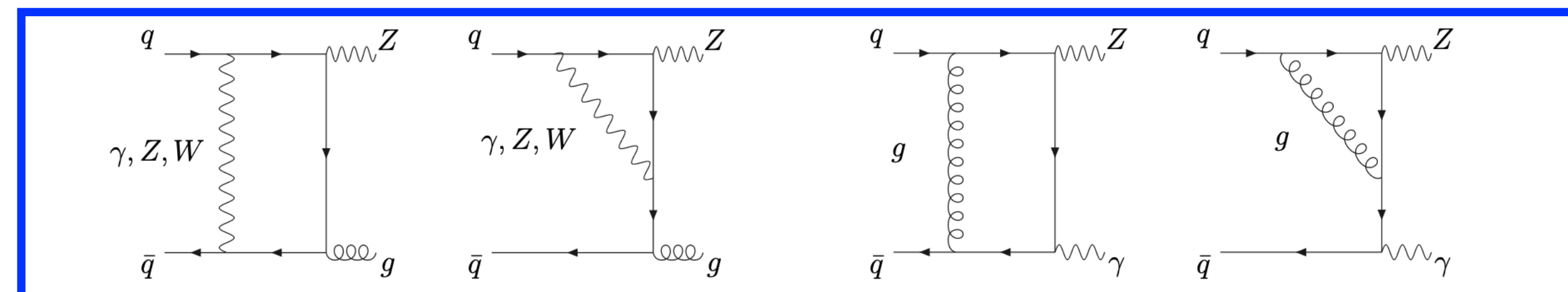Photon induced processes

31

Mixed QCD-EW corrections

- At this level of precision mixed QCD-EW corrections that go as $O(\alpha\alpha_s)$ must be considered. Can identify two categories of EW corrections: QED (includes a photon real radiation or loop), and purely weak (doesn't include a photon, loops only)

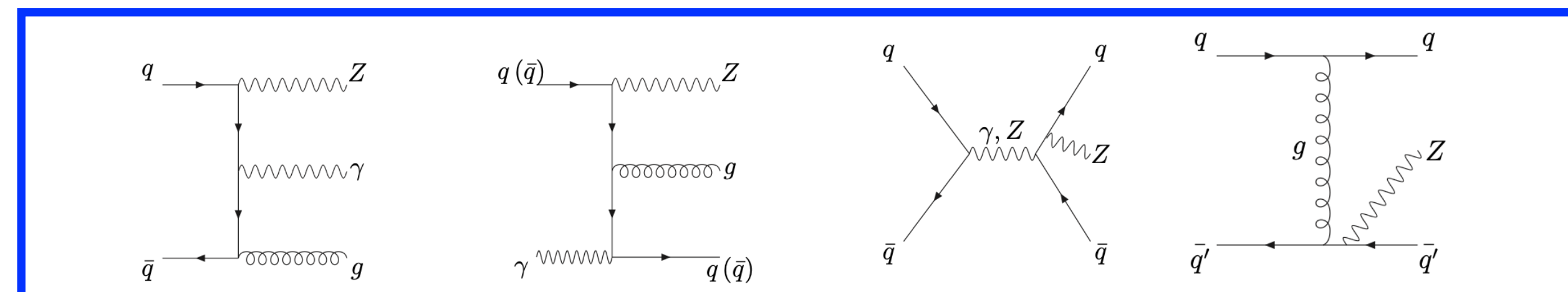- Example diagrams: $O(\alpha\alpha_s)$ corrections to Z-production
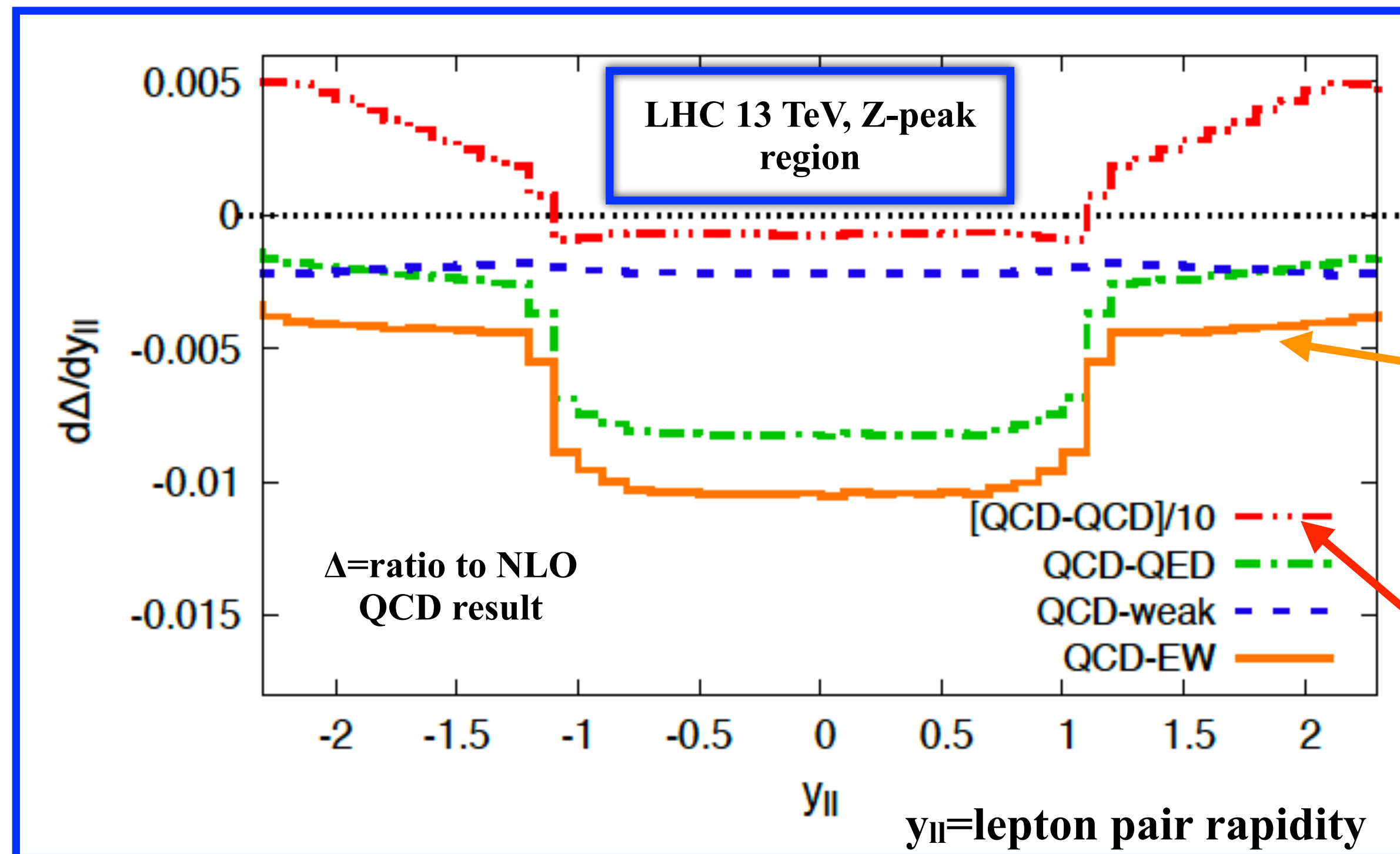
2-loop Virtual corrections:

Real-virtual corrections:

Double-real corrections:

From arXiv:2111.12694, Buccioni et al

Mixed QCD-EW corrections

- At this level of precision mixed QCD-EW corrections that go as $O(\alpha\alpha_s)$ must be considered. Can identify two categories of EW corrections: QED (includes a photon real radiation or loop), and purely weak (doesn't include a photon, loops only)

LHC 13 TeV, Z-peak region

Δ=ratio to NLO QCD result

[QCD-QCD]/10
QCD-QED
QCD-weak
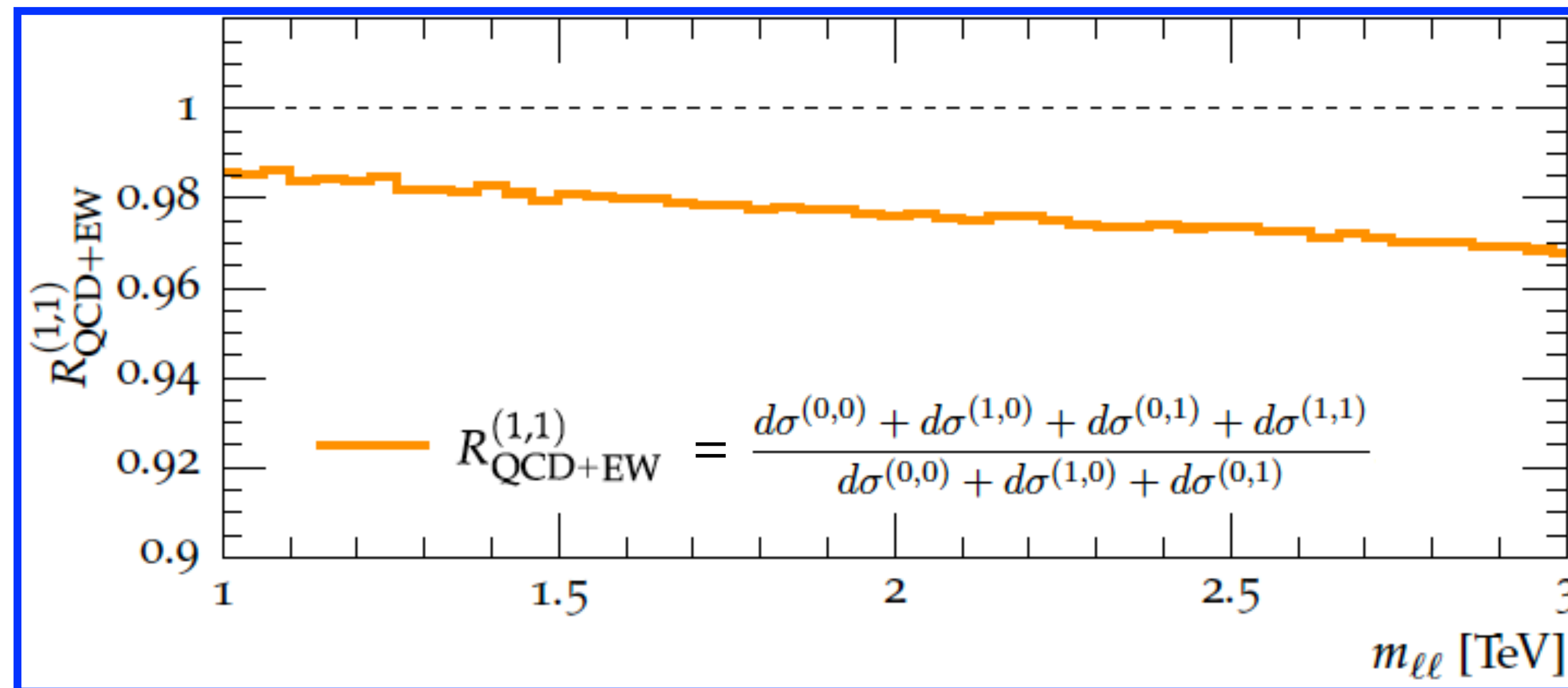QCD-EW

y_{ll}=lepton pair rapidity

NNLO QCD

- An example of mixed QCD-EW corrections to on-shell Z production at the LHC. Corrections applied to both production and decay in this plot

- Corrections are generically small, but dependent on kinematics

- Interplay between final-state cuts and real radiation leads to the structure observed in the corrections

Buccioni, Caola, Chowdhry, Delto, Jacquier, Melnikov, Rontsch, 2020

Mixed QCD-EW corrections

- Another phase-space region of interest is the high-invariant mass region, relevant for new physics searches at the LHC
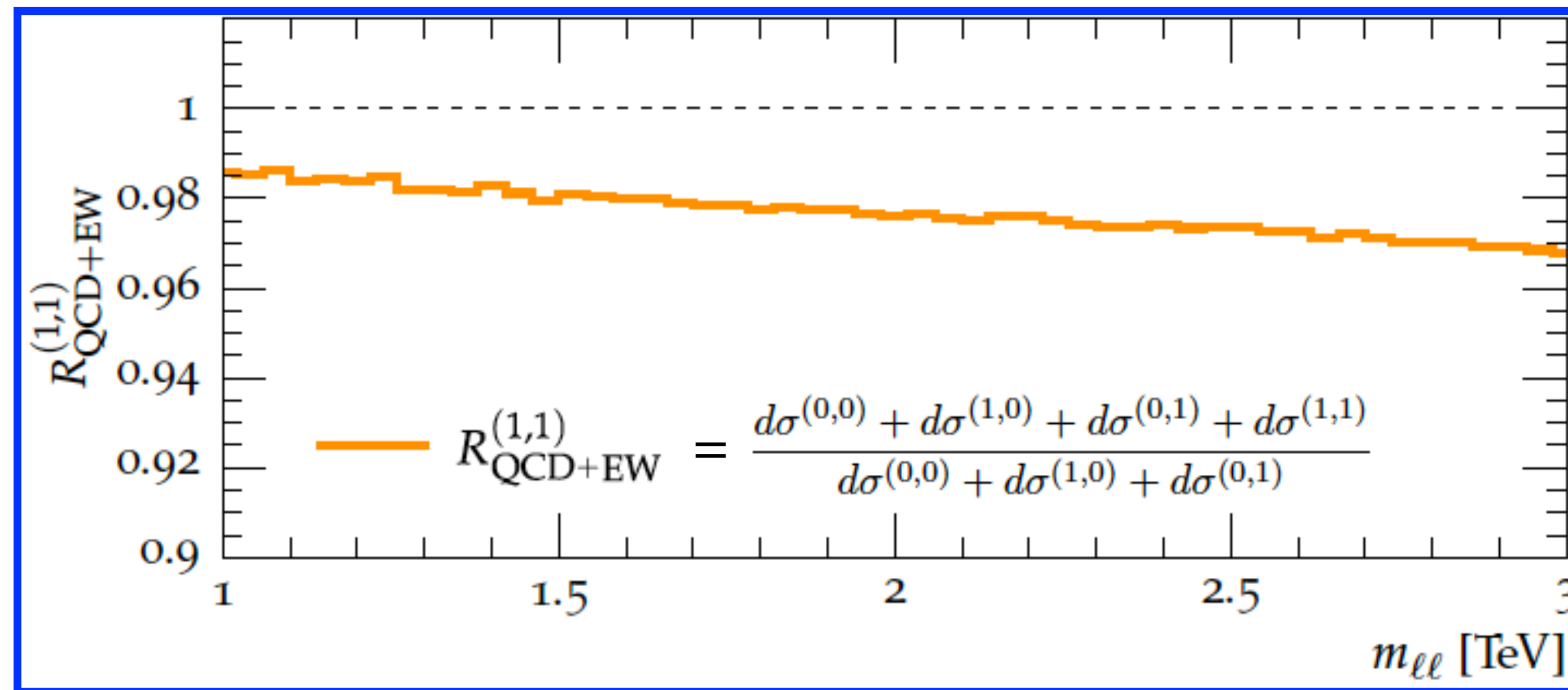

Buccioni, Caola, Chowdhry, Devoto, Heller, 2022

$$R_{\text{QCD+EW}}^{(1,1)} = \frac{d\sigma^{(0,0)} + d\sigma^{(1,0)} + d\sigma^{(0,1)} + d\sigma^{(1,1)}}{d\sigma^{(0,0)} + d\sigma^{(1,0)} + d\sigma^{(0,1)}}$$

Numerator includes mixed QCD-EW corrections; denominator only has NLO QCD and NLO EW separately. Mixed corrections result in a shift of 1-4%, which slowly increases with invariant mass.

Mixed QCD-EW corrections

- Another phase-space region of interest is the high-invariant mass region, relevant for new physics searches at the LHC


Buccioni, Caola, Chowdhry, Devoto, Heller, 2022

$$R^{(1,1)}_{\text{QCD+EW}} = \frac{d\sigma^{(0,0)} + d\sigma^{(1,0)} + d\sigma^{(0,1)} + d\sigma^{(1,1)}}{d\sigma^{(0,0)} + d\sigma^{(1,0)} + d\sigma^{(0,1)}}$$

A common approximation for mixed corrections: multiply NLO QCD with NLO EW corrections, i.e. $(1+\delta^{\text{NLO}}_{\text{QCD}})\times(1+\delta^{\text{NLO}}_{\text{EW}})$. This is found to reproduce the exact mixed QCD-EW corrections well for invariant masses above 1 TeV.

Modern applications

- The W-boson mass is an important observable in the global fit to electroweak precision data. The agreement between the direct M_W measurement and the indirect determination from fitting other data is a powerful constraint on Standard Model extensions.
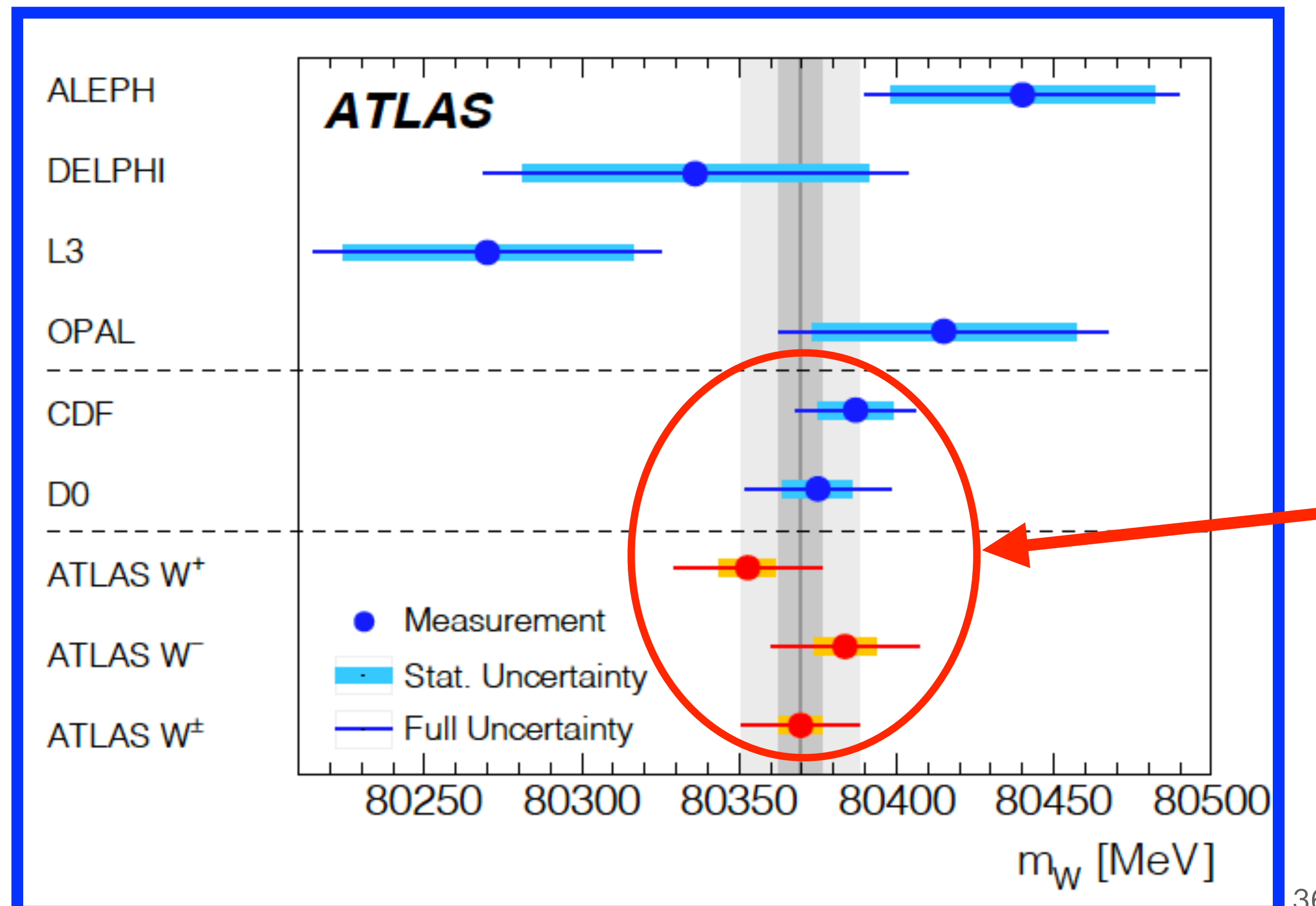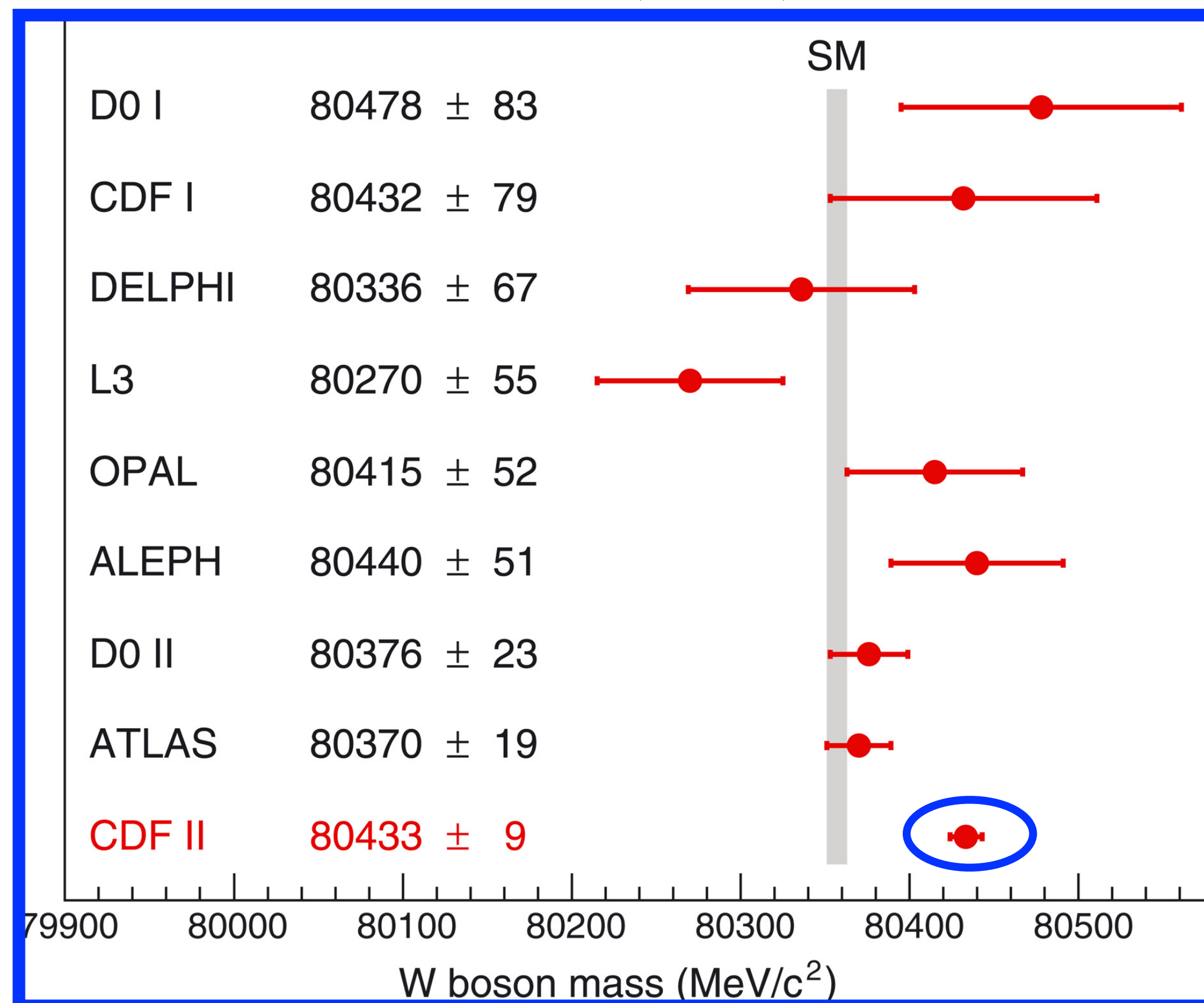

Direct measurement

Most precise determinations of M_W are from Drell-Yan production at the Tevatron and LHC

New W-mass result

- Note that there is a very recent measurement of the W-mass using 8.8 fb⁻¹ of integrated luminosity from CDF that differs from previous results by 7-sigma!

CDF, Science (2022) 376 170

D0 I	80478 ± 83	
CDF I	80432 ± 79	
DELPHI	80336 ± 67	
L3	80270 ± 55	
OPAL	80415 ± 52	
ALEPH	80440 ± 51	
D0 II	80376 ± 23	
ATLAS	80370 ± 19	
CDF II	80433 ± 9	

SM

W boson mass (MeV/c²)

79900 80000 80100 80200 80300 80400 80500

- There has been significant discussions whether this could be due to the QCD modeling used in the analysis; most detailed study argues this isn't the case Isaacson, Fu, Yuan 2205.02788

- Other SM explanations have been explored (Gao, Liu, Xie 2205.03942) but there is no conclusive result yet

Stay tuned!

Modern applications

- The W-boson mass is an important observable in the global fit to electroweak precision data. The agreement between the direct M_W measurement and the indirect determination from fitting other data is a powerful constraint on Standard Model extensions.
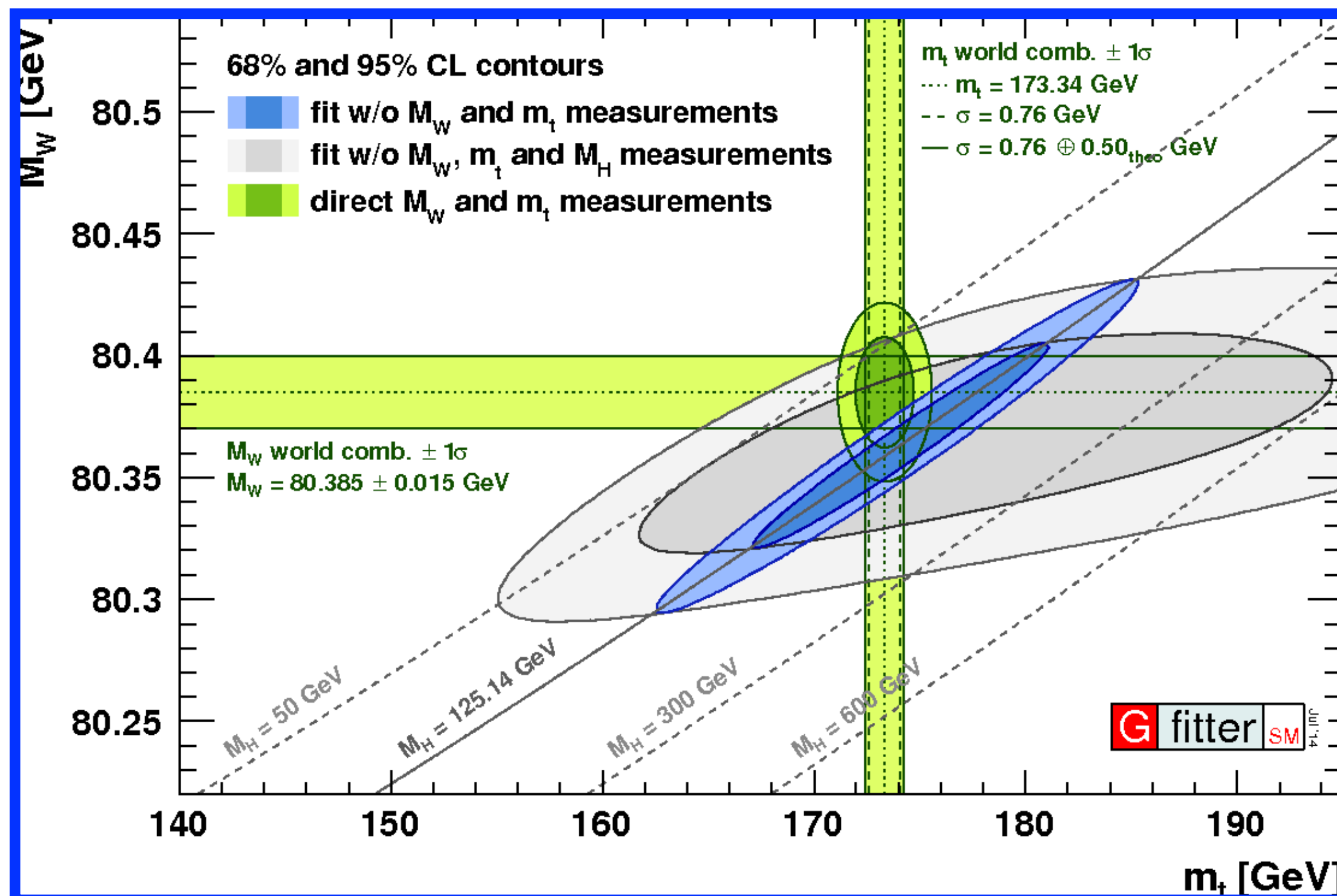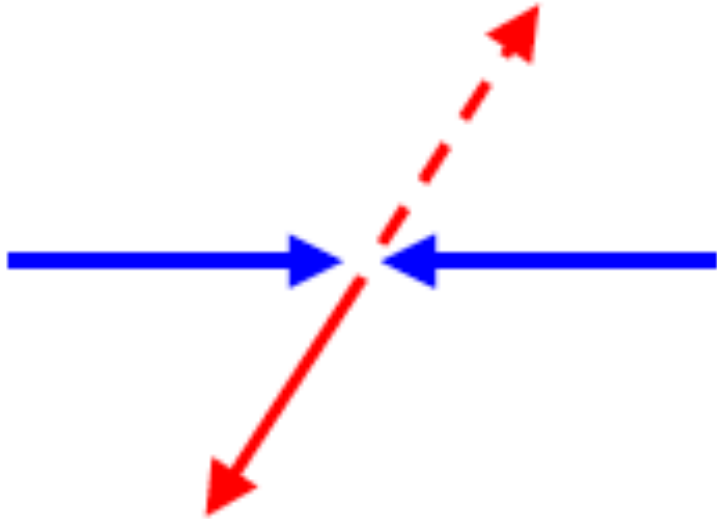

Indirect measurement

- All fits: use primarily LEP data (eg. forward-backward asymmetries in lepton pair production, total hadronic cross section, etc)

- Blue fit: uses in addition LHC Higgs mass measurement

- Grey fit: does not use LHC Higgs mass measurement

Good agreement between direct and indirect measurements

Measuring the W-mass

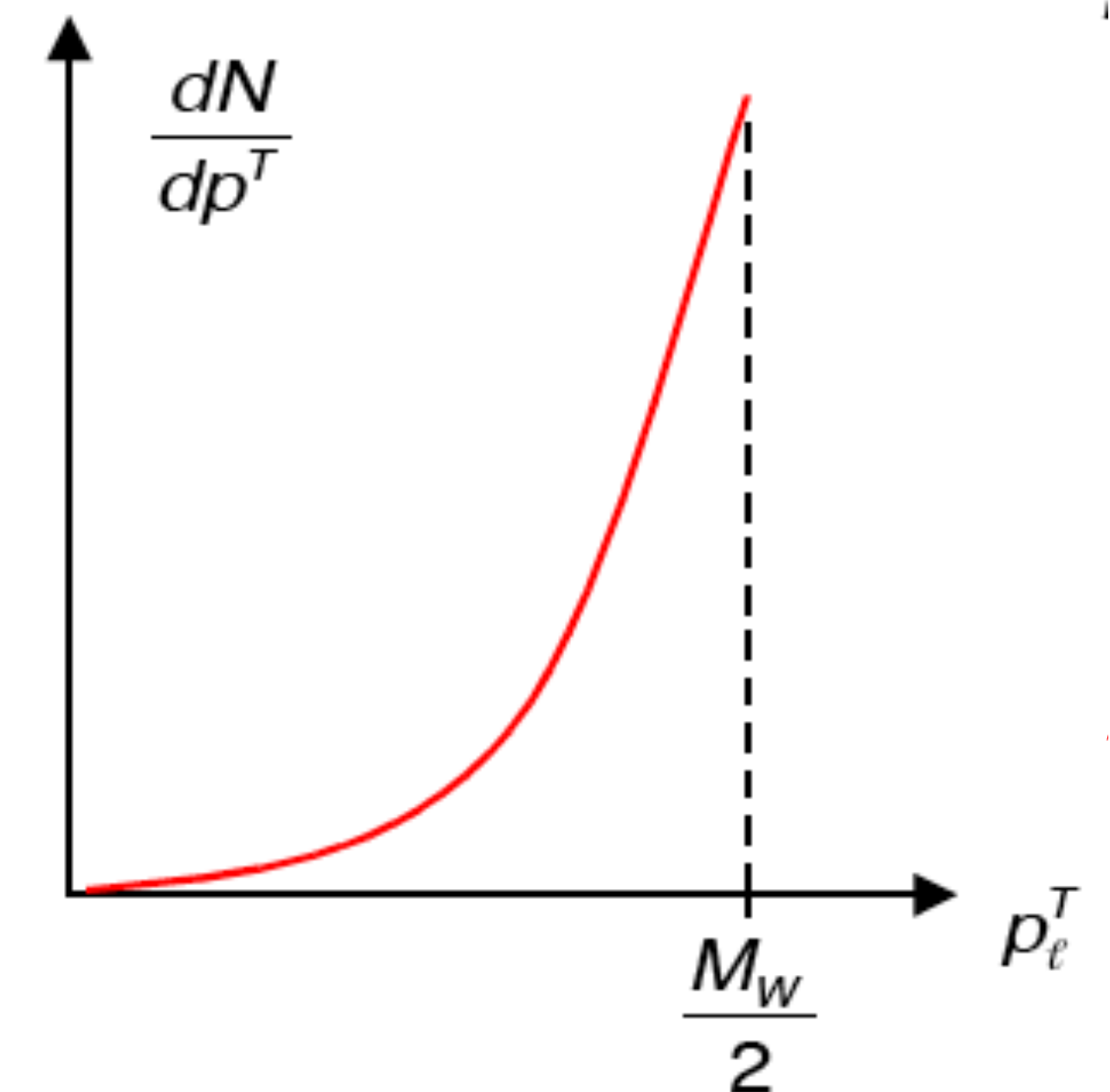- The W→lν contains final-state missing energy; cannot reconstruct the W mass peak

In the W rest frame:

- $\left|\vec{p_\ell}\right| = \left|\vec{p_\nu}\right| = \dfrac{M_W}{2}$

- $\left|p_\ell^T\right| \leq \dfrac{M_W}{2}$

$$\frac{d\sigma}{dp_T^e} = \underbrace{\left|\frac{d\cos\theta_*}{dp_T^e}\right|}_{\text{Jacobian}} \frac{d\sigma}{d\cos\theta_*} = \frac{1}{\sqrt{1 - \left(\frac{2p_T^e}{M_W}\right)^2}} \frac{4p_T^e}{M_W^2} \frac{d\sigma}{d\cos\theta_*}$$
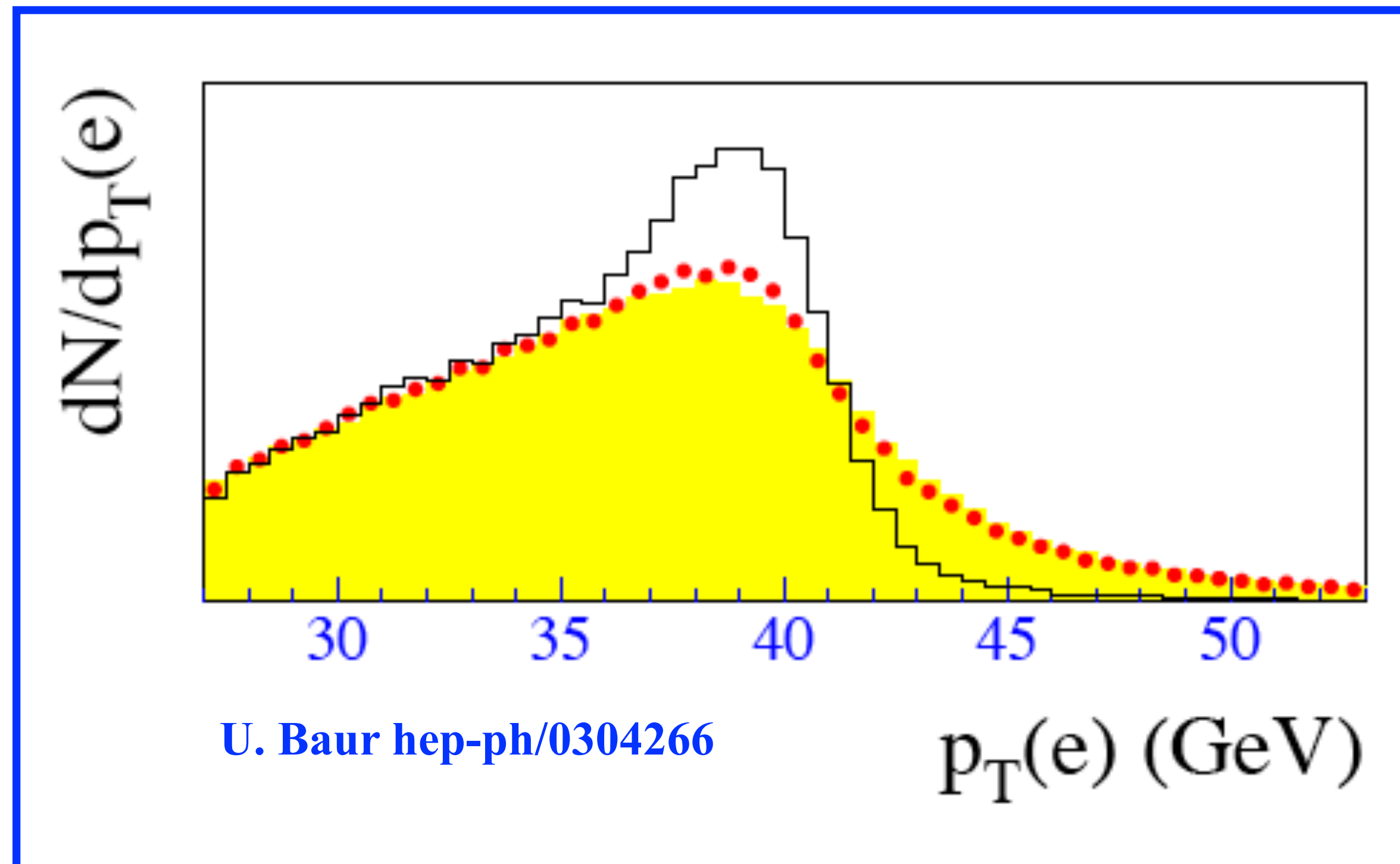
This is a smooth function (can write it in terms of spherical harmonics)

Predict a sharp drop at $M_W/2$; this distribution is sensitive to the W mass! Called a "Jacobian peak"

Measuring the W-mass

- Sensitivity to M_W reduced by several effects: width of the W boson, addition of finite p_{TW} (the previous derivation was valid for $p_{TW}=0$), detector smearing
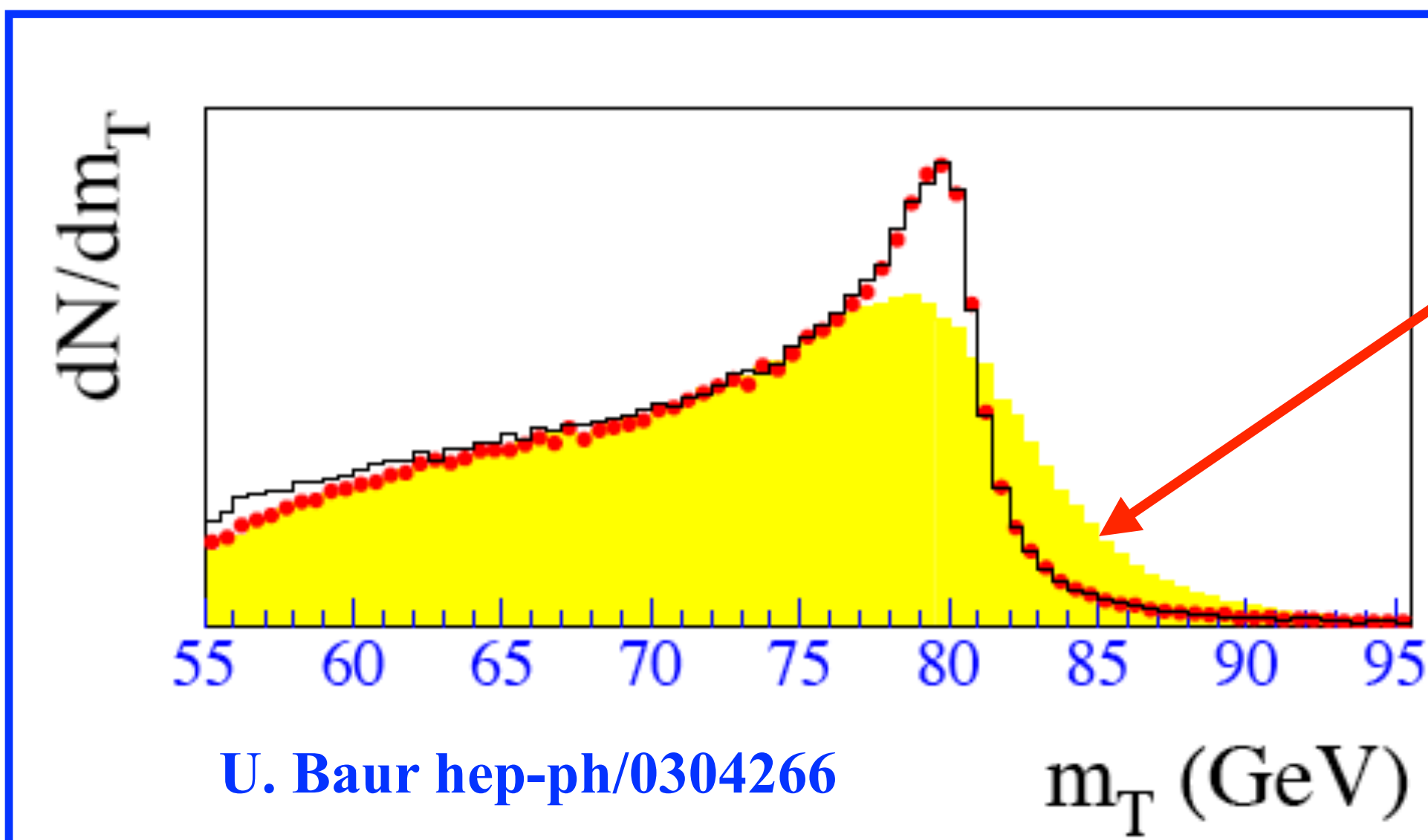

U. Baur hep-ph/0304266

- Black histogram: shows the effect of the width Γ_W

- Red dots: show the effect of a non-zero p_{TW} due to the hadronic radiation

- Yellow histogram: shows the effect of detector smearing

40

Measuring the W-mass

- Can construct the transverse mass, which is less sensitive to our theoretical understanding of p_{TW}

$$M_T = \sqrt{2p_T(\ell)p_T(\nu)(1 - \cos(\phi_{\ell,\nu}))}$$

U. Baur hep-ph/0304266

- Finite-p_{TW} corrections to the m_T distribution are suppressed by p_{TW}^2/M_W^2

- However, it is still sensitive to detector smearing

- In practice, m_T and p_T of both the electron and missing energy are used

Distribution	W-boson mass (MeV)	χ^2/dof
$m_T(e,\nu)$	$80\ 408 \pm 19_{\text{stat}} \pm 18_{\text{syst}}$	52/48
$p_T^\ell(e)$	$80\ 393 \pm 21_{\text{stat}} \pm 19_{\text{syst}}$	60/62
$p_T^\nu(e)$	$80\ 431 \pm 25_{\text{stat}} \pm 22_{\text{syst}}$	71/62

CDF, PRL 108 151803 (2012)
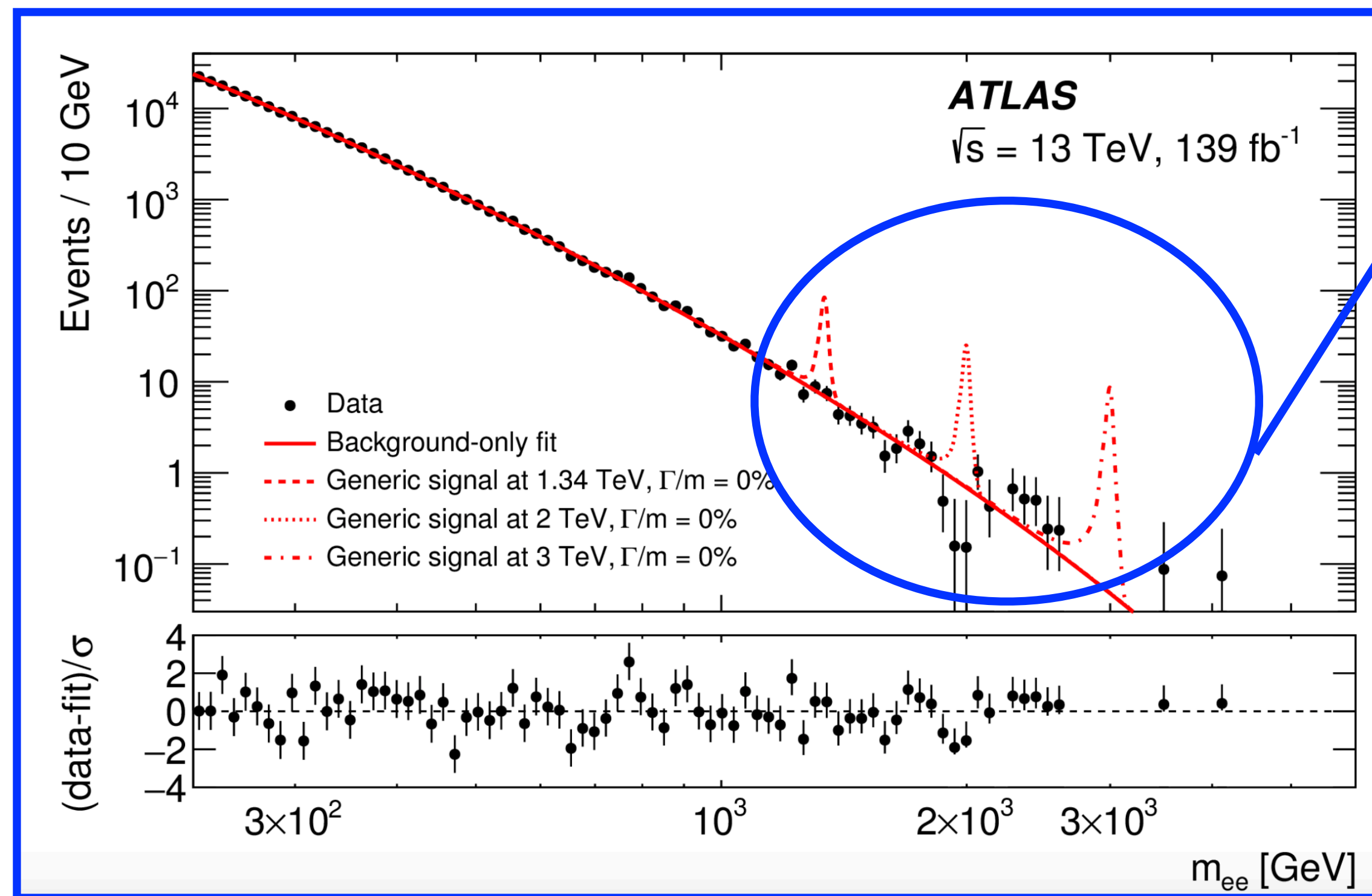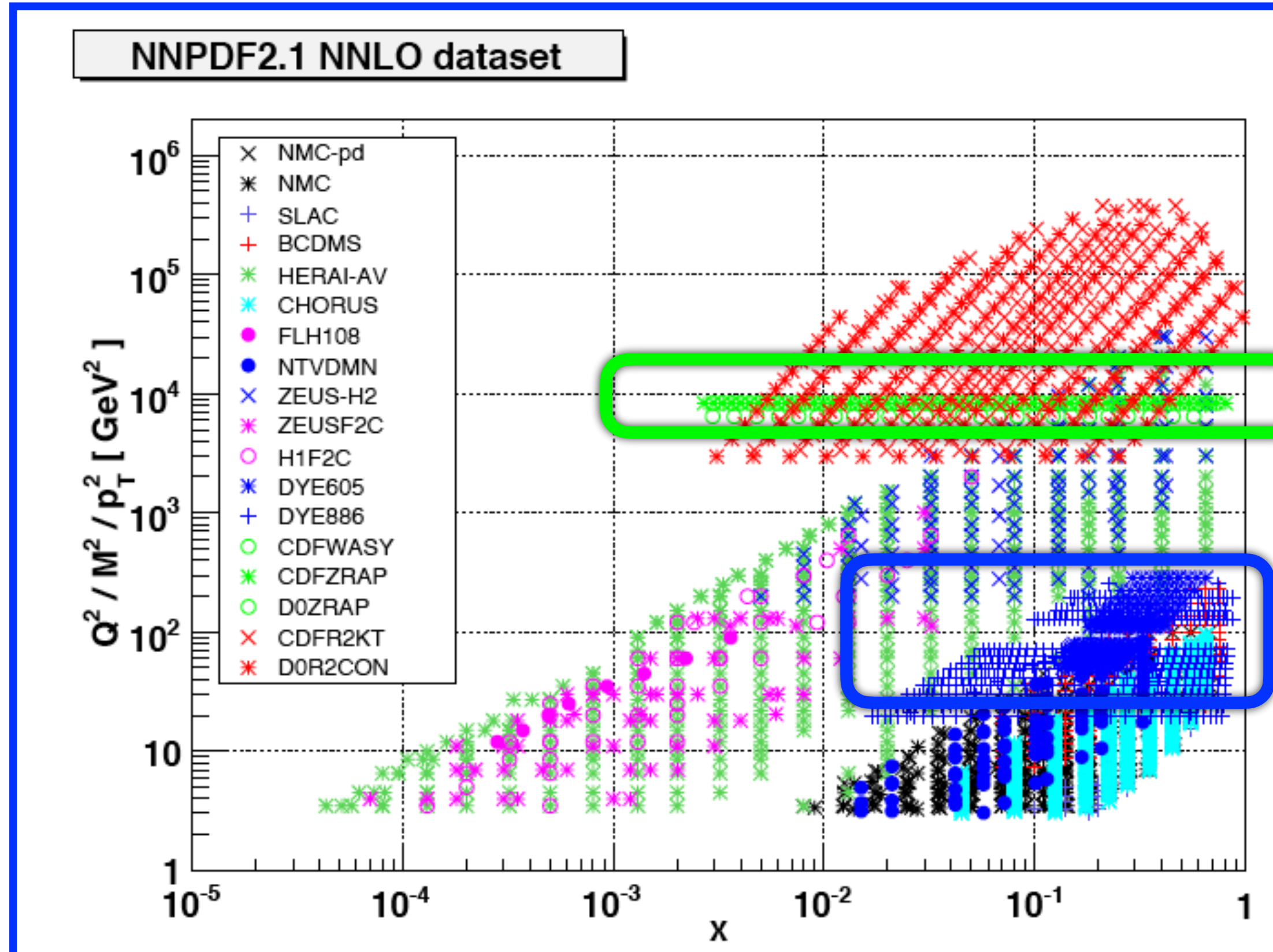
Modern applications

- Drell-Yan is the primary search mode for W' and Z' bosons that would signal an extension of the Standard Model gauge group
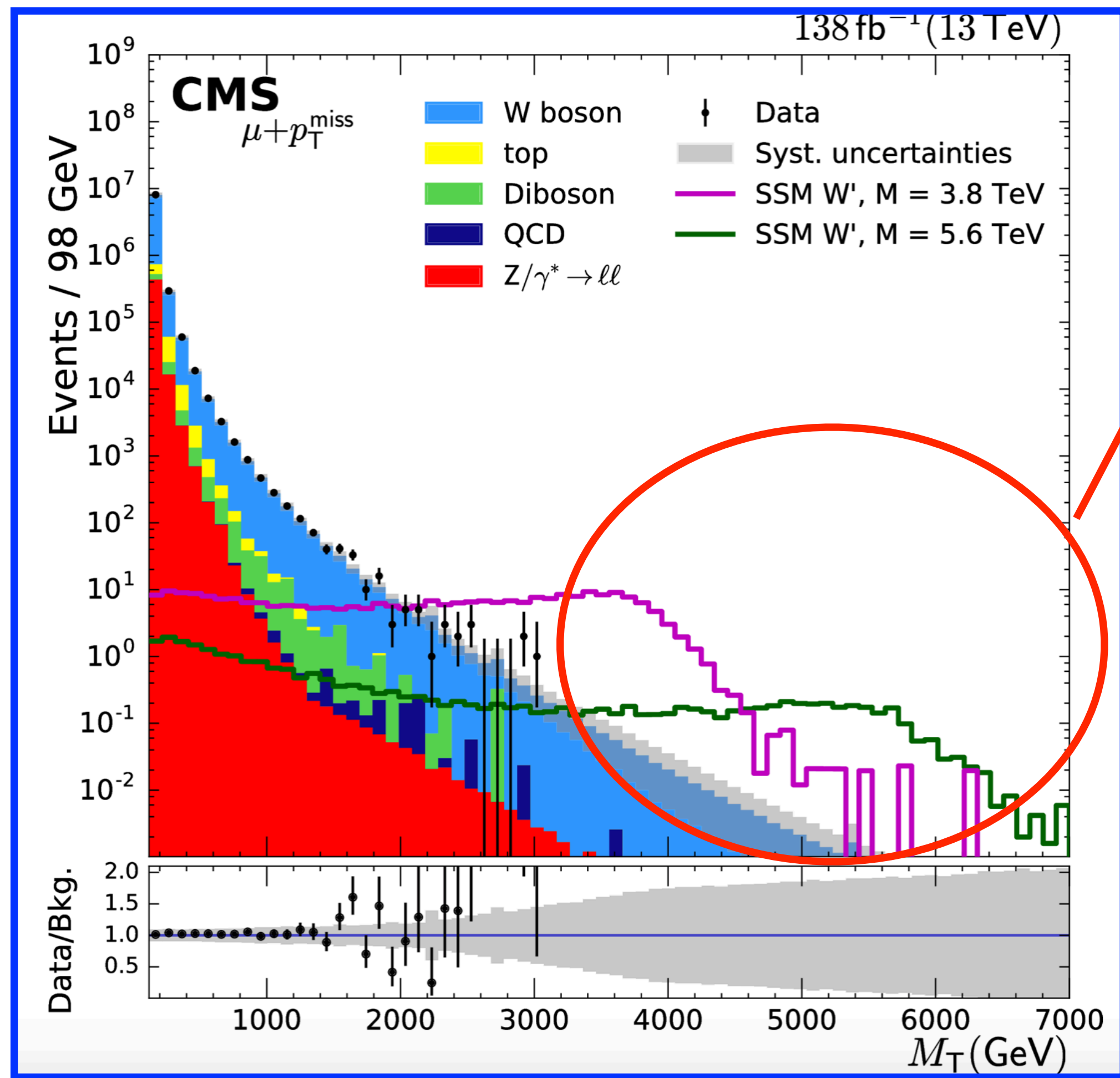
- Hypothetical signature of a W' boson with fermionic couplings identical to the Standard Model W couplings in the muon+missing transverse energy channel in CMS

- Probes extensions of the Standard Model to several TeV

- Note the Jacobian peak that appears for $M_T = M_{W'}$; same structure that appears for the Standard Model W

Modern applications

- Drell-Yan is the primary search mode for W' and Z' bosons that would signal an extension of the Standard Model gauge group

- Hypothetical signatures of an example Z' boson in the di-electron channel in ATLAS

- Probes extensions of the Standard Model to 4 TeV or beyond, depending on the exact model

- In this case the mass peak can be fully reconstructed

Modern applications (PDFs)

- Drell-Yan production, at both collider energies and fixed-target energies, provides invaluable information on PDFs

Tevatron W and Z production probe quark PDFs down to $x \sim 10^{-3}$ **(CDFWASY, CDFZRAP, DoZRAP)**

Important constraints on quark/anti-quark PDFs at higher-x from fixed-target Drell-Yan **(E605, E866)**

Modern applications (PDFs)

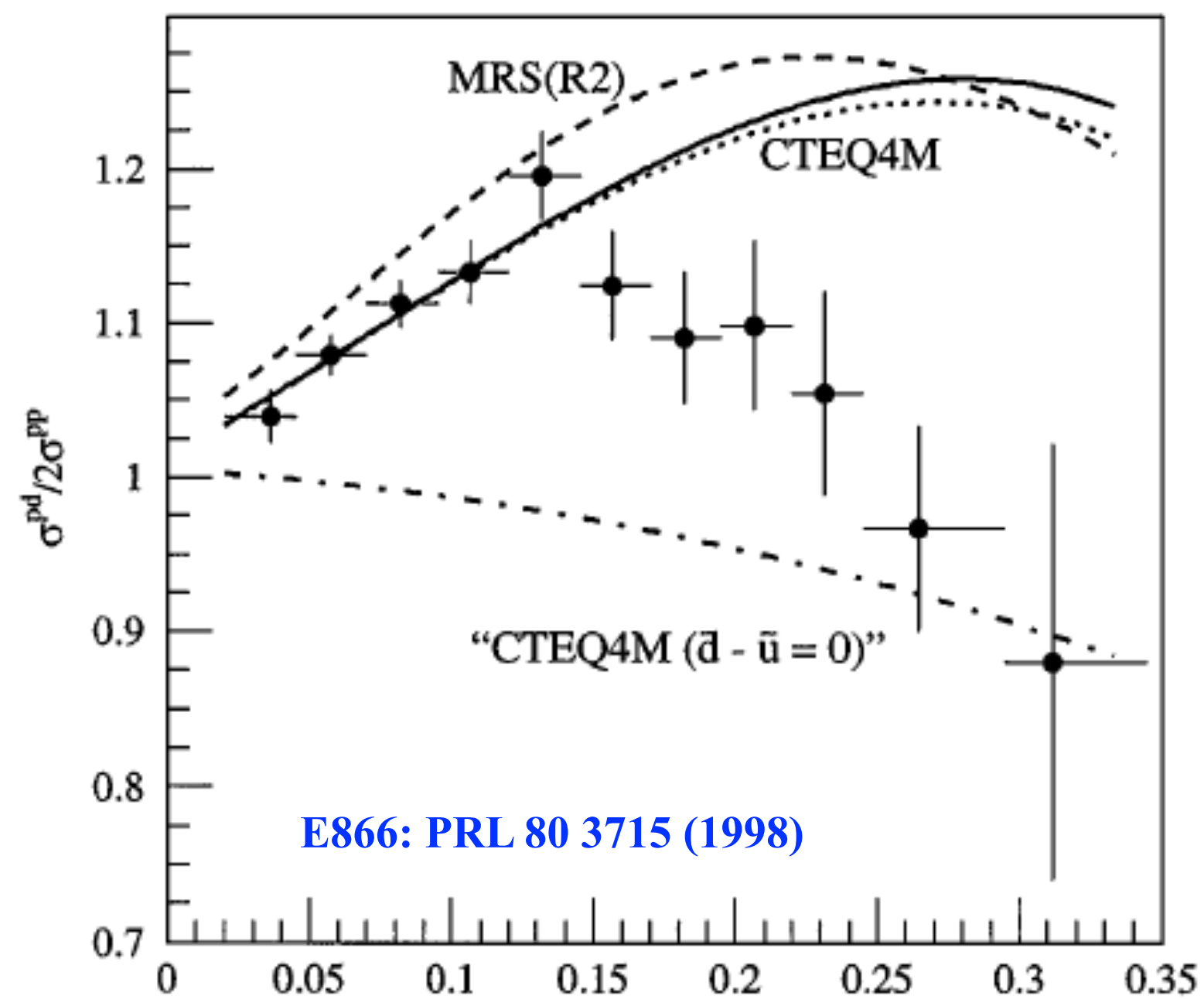- Drell-Yan production, at both collider energies and fixed-target energies, provides invaluable information on PDFs
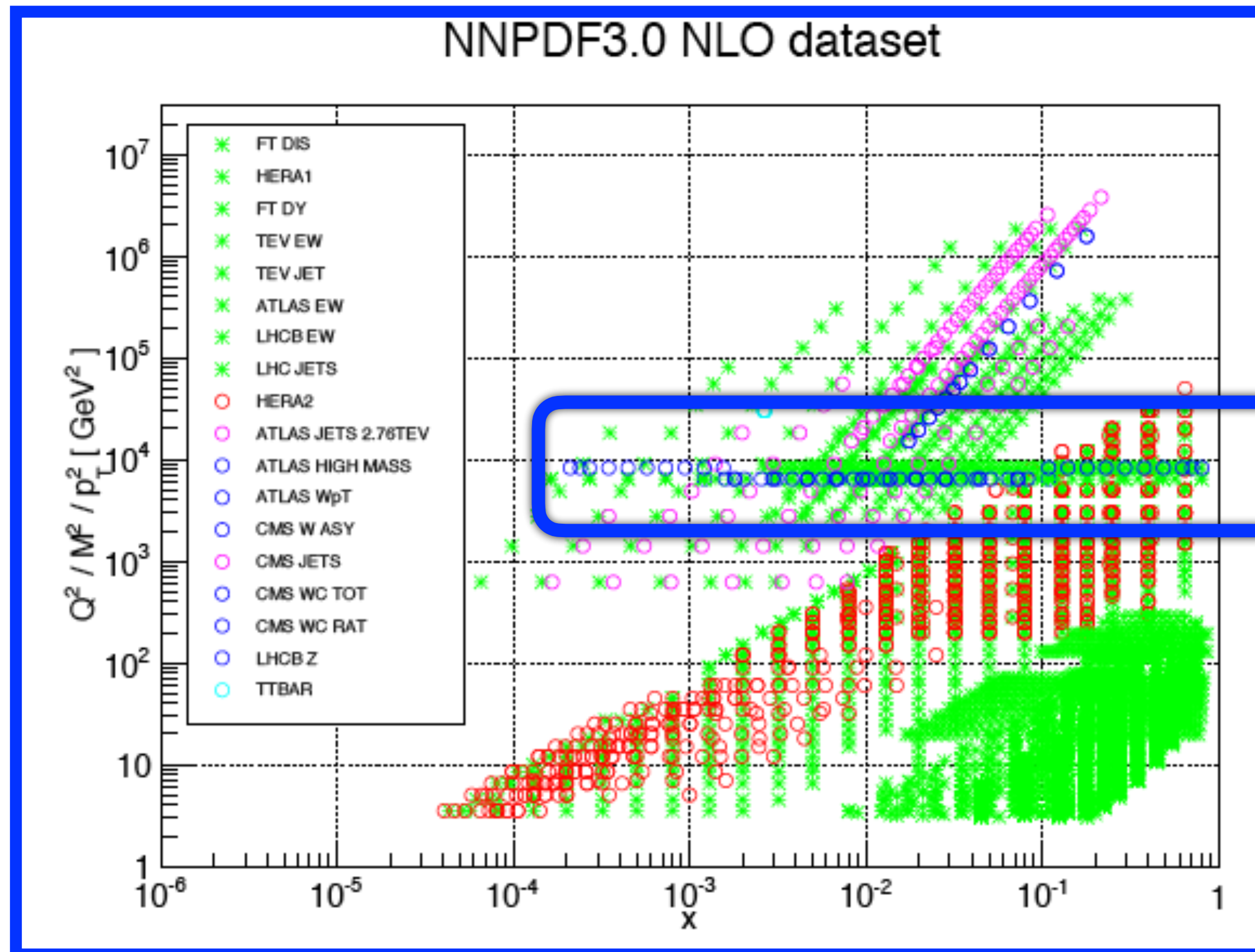
High-precision LHC data on W/Z production is critically an important element of modern PDF fits (eg. CMS W ASY)

Flavor separation of sea quarks

- Measuring Drell-Yan on a variety of nuclear targets probes differences in sea-quark PDFs

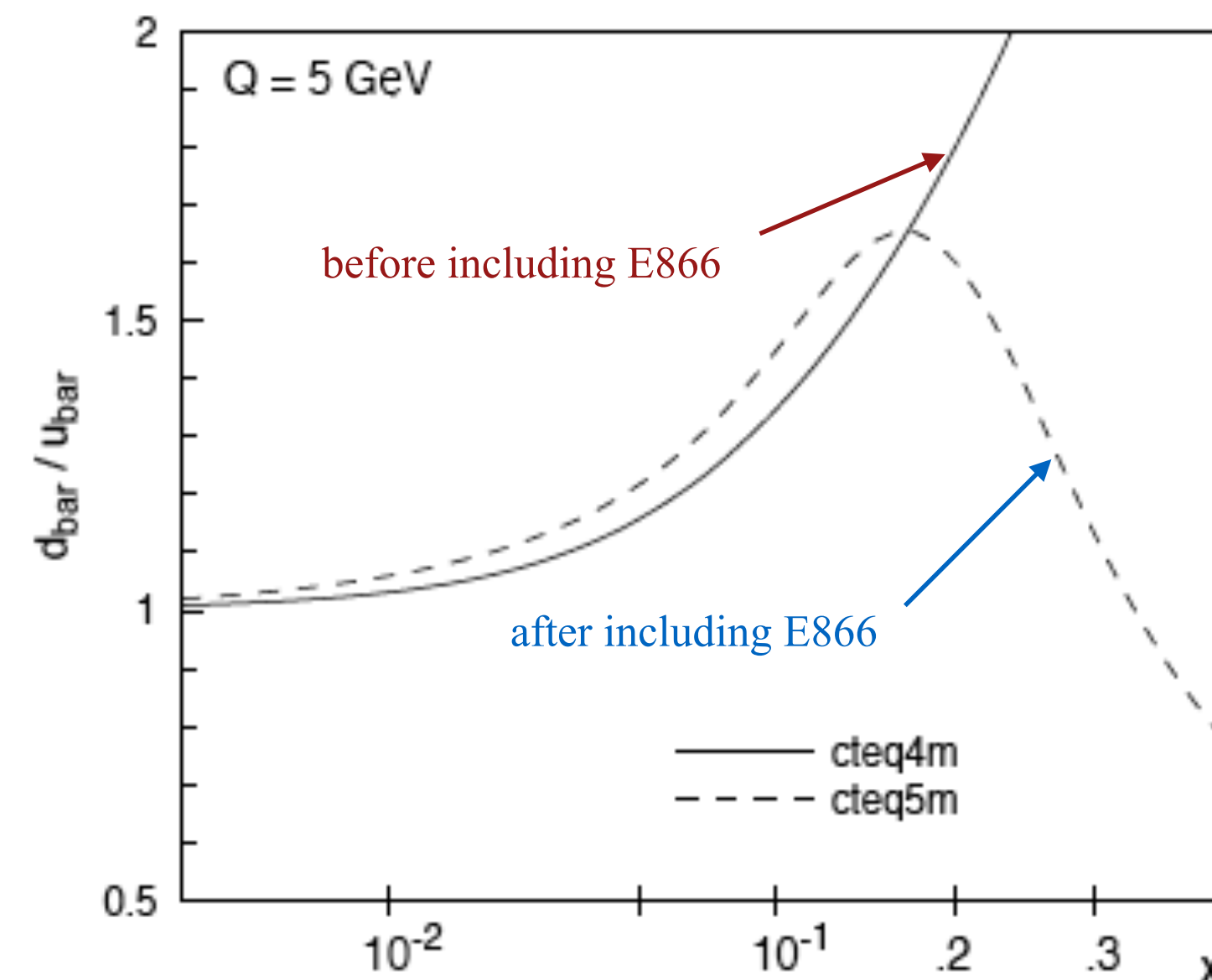**σ_{pd}: proton-deuterium xsection**

deuterium has 1 proton and 1 neutron

Historically important in ensuring an appropriate parameterization of the sea quarks in the high-x region

E866: lower energy DY measurement

E866: PRL 80 3715 (1998)

momentum fraction of the target quark

Accounting for E866 in CTEQ5:

before including E866

after including E866

Flavor separation of valence quarks

- Tevatron measurements of the W-boson charge asymmetry probes the flavor separation of the up/down valence quark ratio

$$A_{ch}(y_W) = \frac{\dfrac{d\sigma^{W^+}}{dy_W} - \dfrac{d\sigma^{W^-}}{dy_W}}{\dfrac{d\sigma^{W^+}}{dy_W} + \dfrac{d\sigma^{W^-}}{dy_W}} \approx \frac{\dfrac{u(x_A)}{d(x_A)}\dfrac{\bar{d}(x_B)}{\bar{u}(x_B)} - 1}{\dfrac{u(x_A)}{d(x_A)}\dfrac{\bar{d}(x_B)}{\bar{u}(x_B)} + 1}$$

$$x_A = \frac{M_W}{\sqrt{s}}e^{y_W}; \quad x_B = \frac{M_W}{\sqrt{s}}e^{-y_W}$$

Assuming born kinematics and valence quarks domination of the cross section

- As y_W goes to its maximum value (large rapidity), x_B becomes small (while $x_A \to 1$) and the ratio dbar/ubar $\to 1$ (see the plot on the previous slide for dbar(x)/ubar(x)). This allows us to constrain $u(x_A)/d(x_A)$.

Flavor separation of valence quarks

- Tevatron measurements of the W-boson charge asymmetry probes the flavor separation of the up/down valence quark ratio

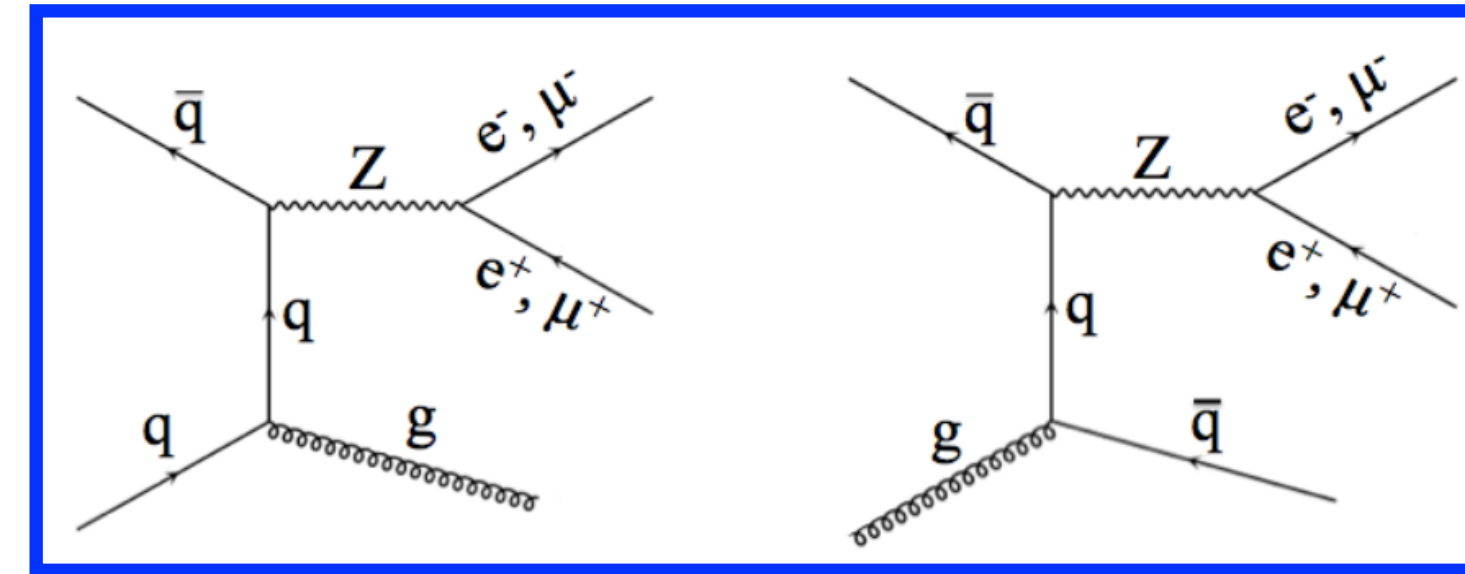electron charge asymmetry predicted using different codes and PDF sets

The intermediate rapidity range (y_w~1) shows differences between MSTW and NNPDF when using the same code **(MC@NLO)**

The charge asymmetry dataset is needed to better determine the proton structure
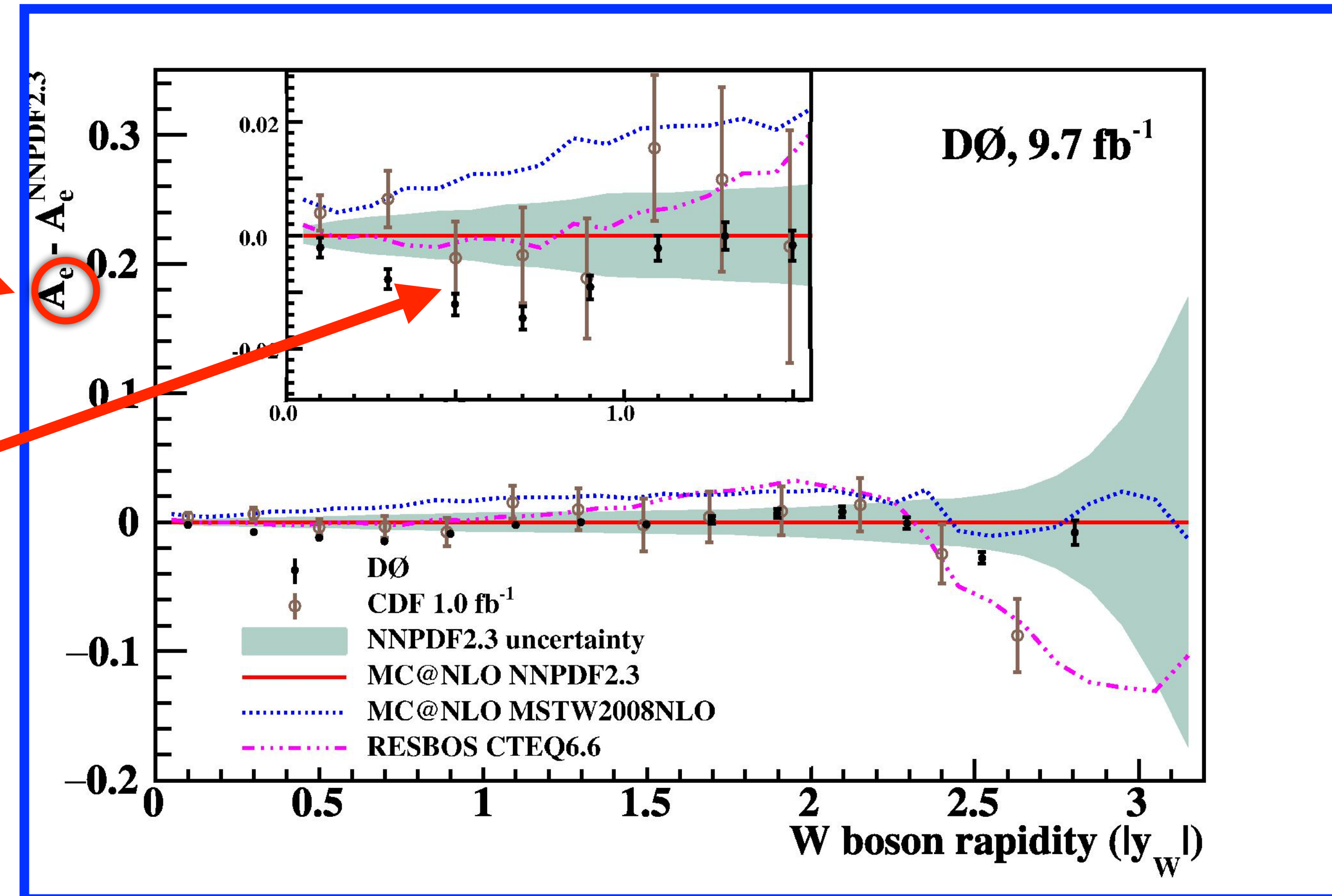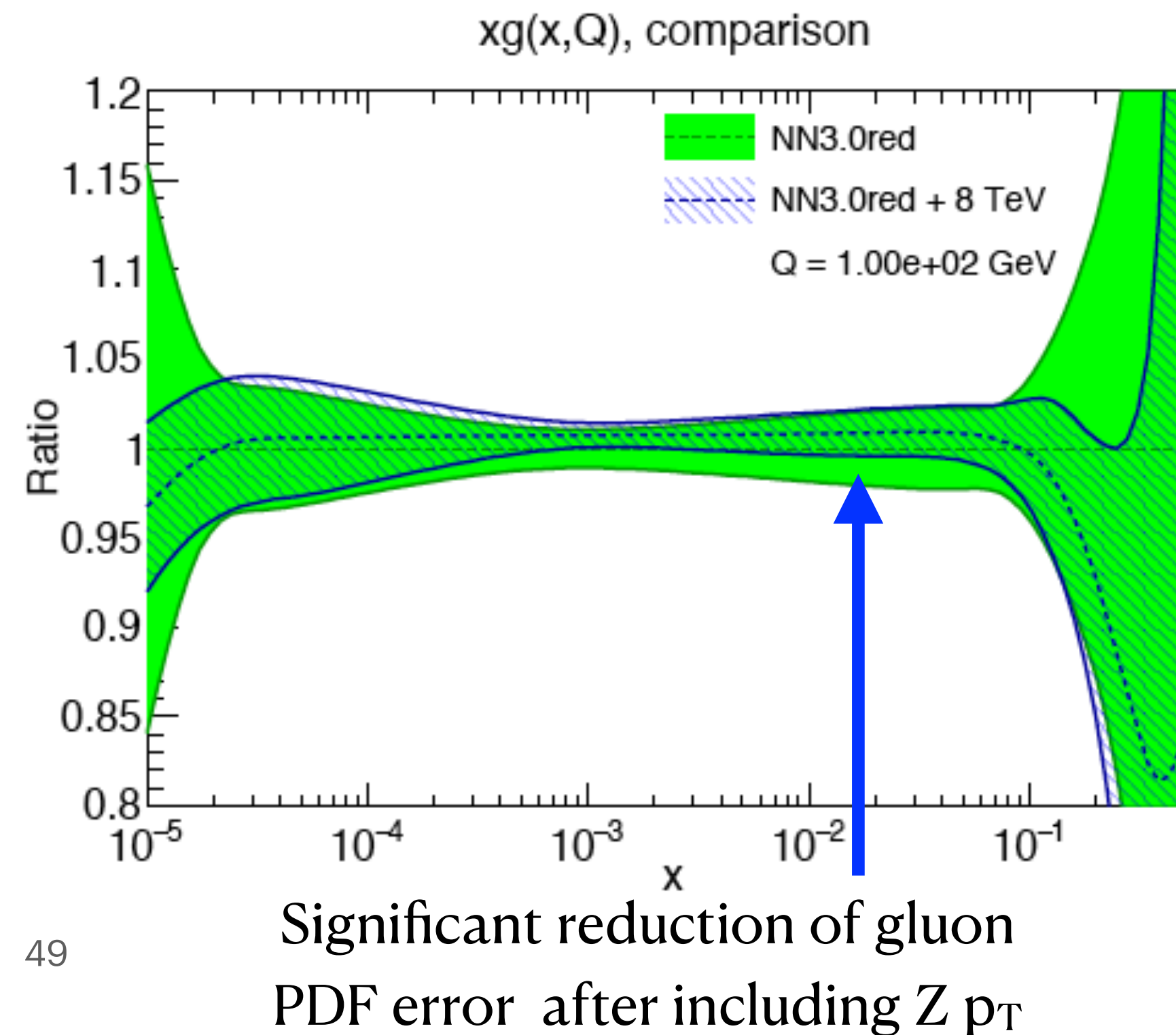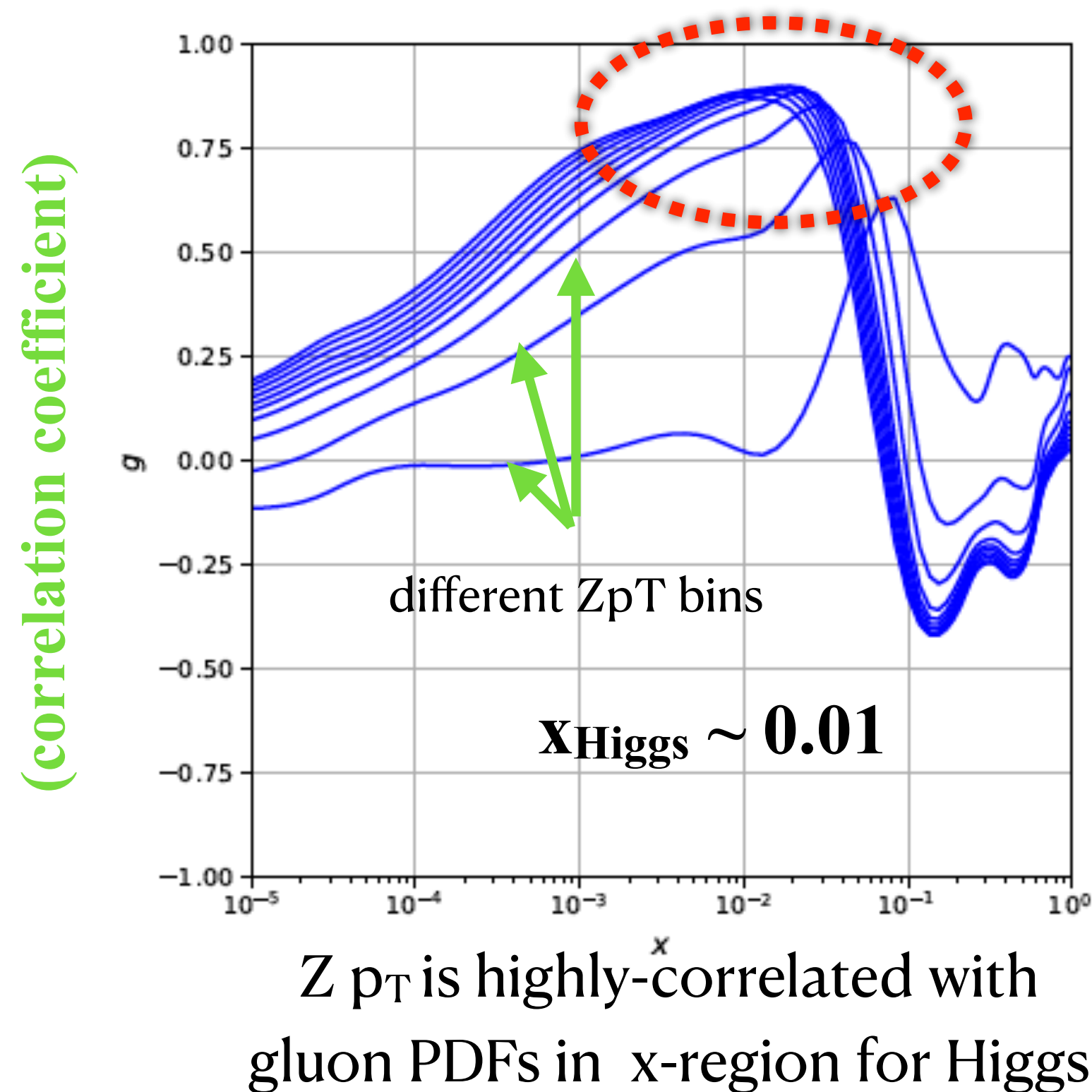
Gluon PDFs from the Z-boson p_T

- Can constrain the intermediate-x gluon PDFs relevant for Higgs production using the Z-boson p_T spectrum

RB, Guffanti, Petriello, Ubiali, 2017
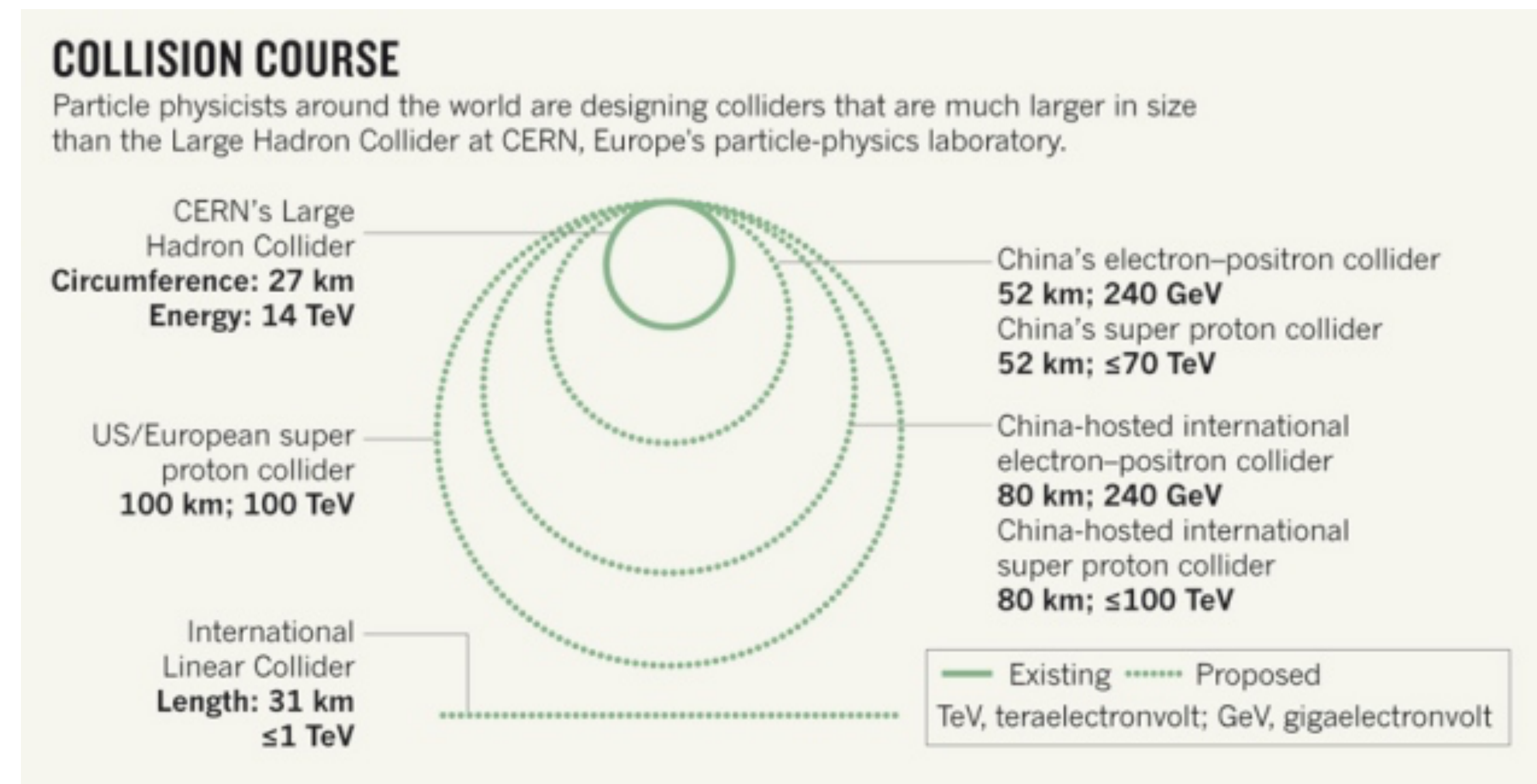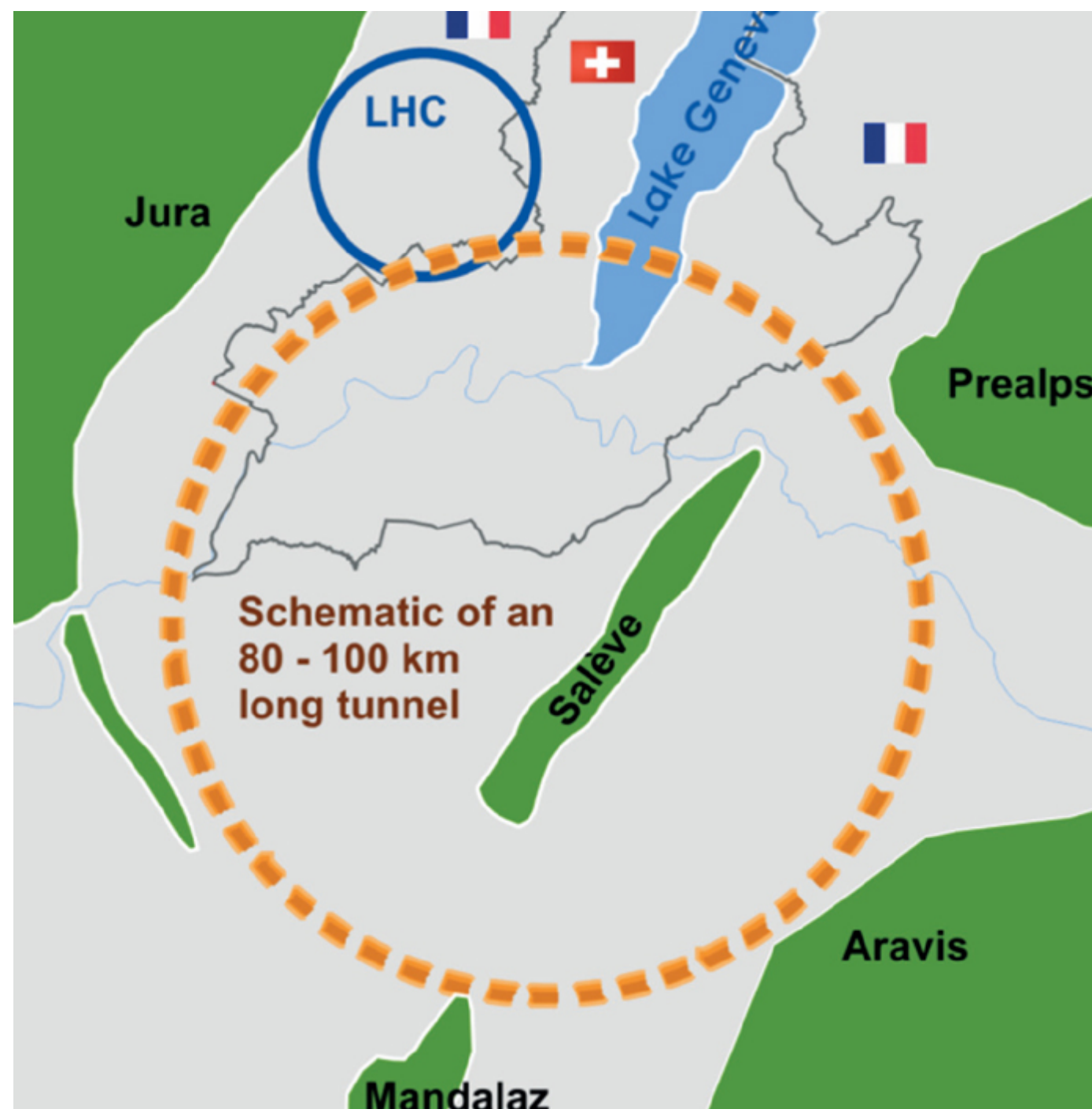
xg(x,Q), comparison

(correlation coefficient)

different ZpT bins

$x_{Higgs} \sim 0.01$

Z p_T is highly-correlated with gluon PDFs in x-region for Higgs

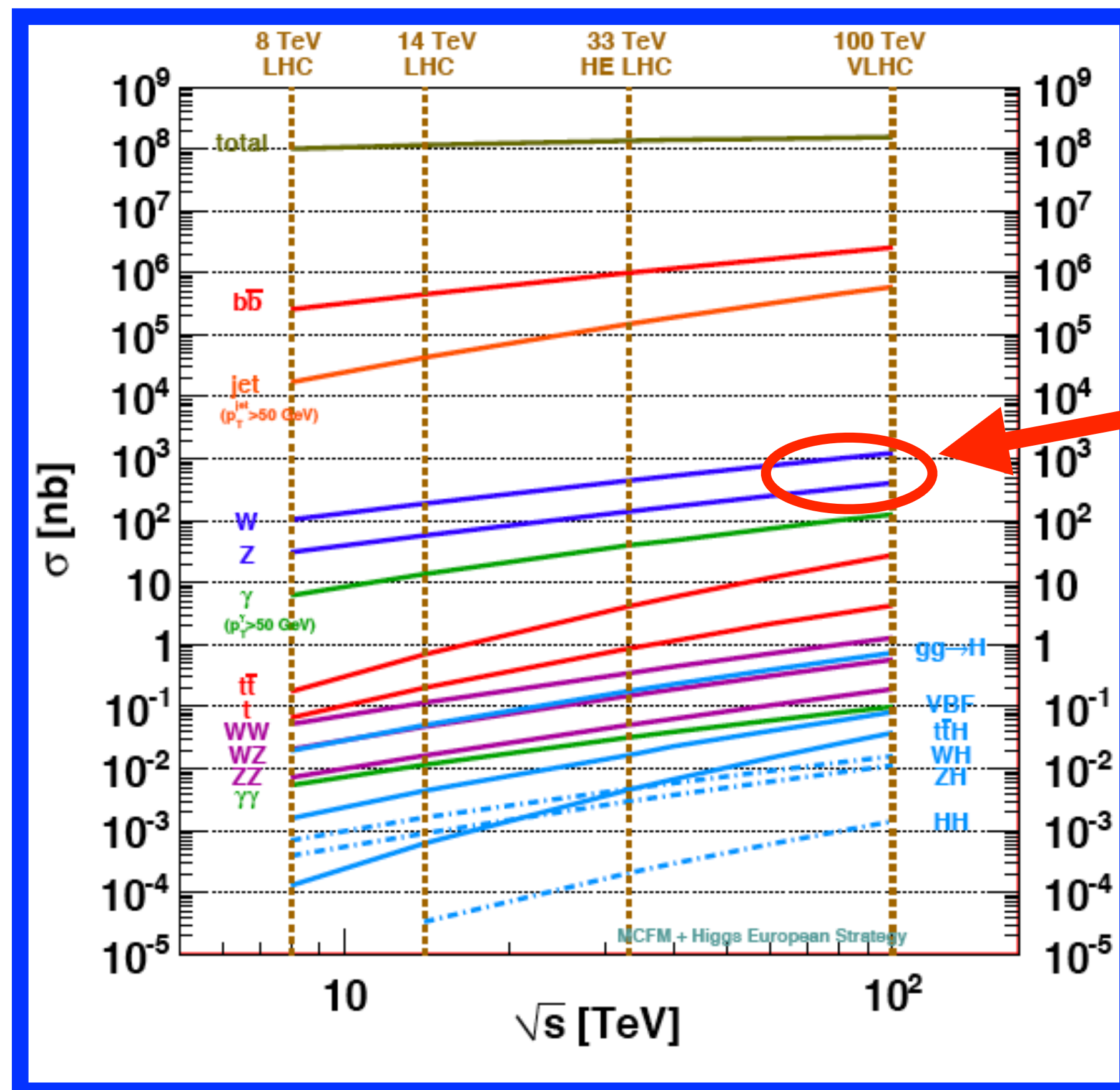Significant reduction of gluon PDF error after including Z p_T

Drell-Yan in the future

- There is growing interest in the HEP community to build a future high-energy pp machine with CM energy ~100 TeV

- Possible locations at CERN and China have been discussed. If at CERN this would possibly be after an e+e- Higgs factory is constructed.

LHC
Jura
Lake Geneva
Prealps
Schematic of an
80 - 100 km
long tunnel
Salève
Aravis
Mandalaz

COLLISION COURSE
Particle physicists around the world are designing colliders that are much larger in size than the Large Hadron Collider at CERN, Europe's particle-physics laboratory.

CERN's Large Hadron Collider
Circumference: 27 km
Energy: 14 TeV

China's electron–positron collider
52 km; 240 GeV
China's super proton collider
52 km; ≤70 TeV

US/European super proton collider
100 km; 100 TeV

China-hosted international electron–positron collider
80 km; 240 GeV
China-hosted international super proton collider
80 km; ≤100 TeV

International Linear Collider
Length: 31 km
≤1 TeV

Existing — Proposed ·····
TeV, teraelectronvolt; GeV, gigaelectronvolt

Drell-Yan in the future

- Drell-Yan will continue to play an integral role of the physics program at such future machines

Large production rates for W and Z boson production via Drell-Yan at 100 TeV; will remain an important background to any searches at high energies

Drell-Yan in the future

- Drell-Yan will continue to play an integral role of the physics program at such future machines
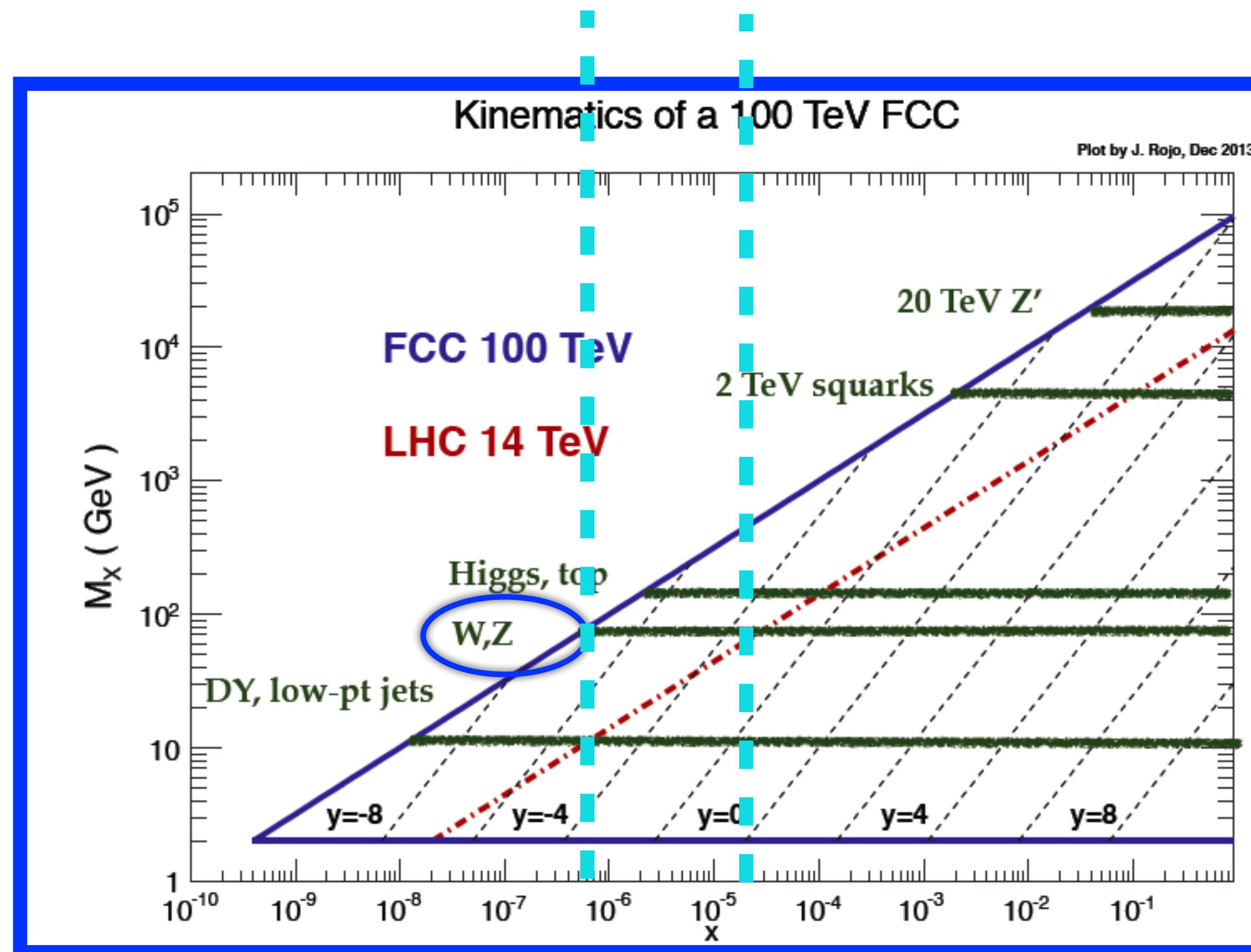
New kinematic regions probed; W/Z production down to Bjorken x~10^{-6}, more than an order of magnitude lower than LHC 14 TeV coverage

New gauge bosons at 100 TeV

- Unmatched reach for new gauge bosons which would indicate new forces of Nature beyond SU(3)xSU(2)xU(1)
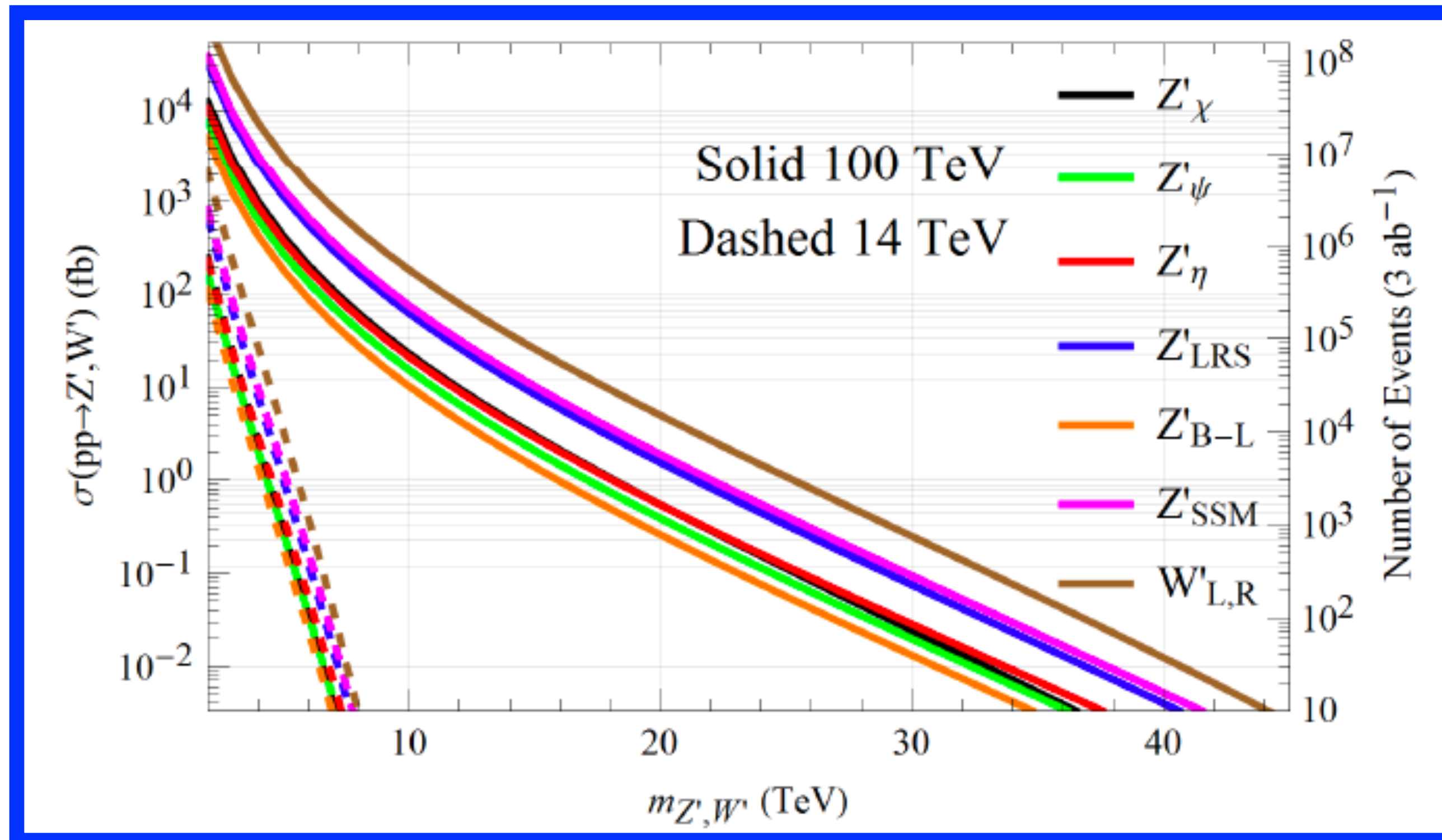
- Ultimate LHC reach in mass is ~7-8 TeV

- A 100 TeV machine extends this out to 35 TeV or beyond, depending on the model

Summary of lecture I

- What we covered in this lecture:

  - Overview of Drell-Yan basics and historical importance: relevance of higher-order corrections in resolving discrepancies with data over the years, discoveries, non-discoveries

  - State-of-the-art predictions including NNLO QCD, NLO EW, mixed QCD-EW effects

  - Modern applications of Drell-Yan processes: W-mass, flavor separation of sea quarks, valence quarks

  - Drell-Yan in the future: searches for BSM resonances